Electrospun nanofiber scaffolds and crosslinked protein membranes as scaffold materials in tissue engineering

By Zhengjun Lu

Supervisor: Professor Wen Wang

Submitted for the Degree of Doctor of Philosophy

School of Engineering and Materials Science

Queen Marry University of London

2015

I, Zhengjun Lu, confirm that the research included within this thesis is my own work or that where it has been carried out in collaboration with, or supported by others, that this is duly acknowledged below and my contribution indicated. Previously published material is also acknowledged below.

I attest that I have exercised reasonable care to ensure that the work is original, and does not to the best of my knowledge break any UK law, infringe any third party's copyright or other Intellectual Property Right, or contain any confidential material.

I accept that the College has the right to use plagiarism detection software to check the electronic version of the thesis.

I confirm that this thesis has not been previously submitted for the award of a degree from this or any other university.

Signature: Zhengjun Lu

Date: 18 February 2015

Acknowledgement

First of all, I would like to thank my supervisor, Professor Wen Wang, for giving me the opportunity to work on this PhD project. I thank him for his encouragement and support throughout my project，not only on study but also on my personal and healthcare issues. I thank Dr Jing Liu in the Regeneration Medicine Center of the First Affiliated Hospital of Dalian Medical University for her help and support in my research.

I would like to thank Dr. Hong Chang for the training and advice she gave me. I also thank Dr. Weiqi Li for his help in editing my thesis. I would like to thank all the colleagues in the group, Drs Xiaotian Yu, Lin Qiu, Devendra Deo, Ms Miao Lin and Mr Xia Chen. Thank you all for the warmth and professional environment in our laboratory.

I also want to thank the staffs and technicians in SEMS and First Affiliated Hospital of Dalian Medical University. Many thanks to Dr. Zofia Luklinska and Dr. Russell Bailey for their help on SEM and TEM imaging.

Finally，I want to thank my family, they always back me up whenever I needed. I couldn’t have done my Ph.D. without their support and understanding.

Abstract

Scaffold materials play an essential role in tissue engineering field due to its function of accommodate and guide cell proliferation. In this study, I investigated different types of crosslinked protein membranes that can be produced in microfluidic channels and a number of various types of PLGA electrospun composite nanofiber scaffold to examine their potentials as scaffold materials in tissue engineering. A simplified fabrication technique has been developed to produce a large surface area of crosslinked protein membranes to fulfill the purpose of cell culture experiments. Bovine serum albumin is used along with two acyl chloride crosslinkers, i.e. TCL and IDCL, respectively to accomplish the cross-linking. On the other hand, PLGA is dissolved in HFIP and enhanced with silk fibroin and carbon nanotubes to make composite electrospun materials. The morphology, physicochemical properties and biocompatibility of the membranes are studied. The biocompatibility of the membranes is investigated using cell proliferation of the PC12, ADSCs and neurons cultured on the membranes. Our results show that compared to crosslinked protein membranes, the electrospun materials are easier to prepare, less toxic and more suitable for mass production. Moreover, the electrospun materials are seen to have better biocompatibility in our cell culture study. Furthermore, the composite electrospun materials with high CNTs concentrations demonstrate positive effects on the proliferation of neurons.

Table of Contents

List of Symbols and Abbreviations

FDA	Food and Drug Administration (U S)
LOC	Lab-on-a-chip
ELISAs	Enzyme-linked immunosorbent assay
μTAS	Micro total analysis systems
BioMEMs	Biomedical microelectro mechanical systems
LFR	Laminar flow reactor
PDMS	Poly (dimethylsiloxane)
BSA	Bovine serum albumin
TCL	Terephthaloyl chloride
IDCL	Isophthaloyl chloride
PLGA	Poly (lactic-co-glycolic acid)
CNTs	Carbon nanotubes
MWCNTs	Multi-walled Carbon nanotubes
SWCNTs	Single-walled Carbon nanotubes
SF	Silk fibroin
HFIP	Hexafluoroisopropanol
PGA	Poly (glycolic acid)
PLLA	Poly (L-lactic acid)
PVA	Polyvinyl alcohol

CS	Chitosan
ALP	Alkaline phosphatase
PCL	Poly (caprolactone)
ABS	Acrylonitrile Butadiene Styrene
OD	Optical density
ECM	Extracellular matrix
SEM	Scanning electron microscope
TEM	Transmission electron microscope
UV	Ultraviolet
MSC	Marrow-derived mesenchymal stem cell
ADSCs	Adipose tissue-derived stem cells
NGF	Nerve growth factor
GABA	ɤ-Aminobutyric acid
GFAP	Glial fibrillary acidic protein
FITC	Fluorescein isothiocyanate
TRITC	Tetramethylrhodamine
DMSO	Dimethyl sulfoxide
PFA	Paraformaldehyde
CCK-8	Cell counting kit 8
WST-8	[2-(2-methoxy-4-nitrophenyl)-3-(4-nitrophenyl) -5-(2,4-disulfophenyl)-2H-tetrazoliu,monosodium salt]

List of Figures

List of Tables

1. Introduction

1.1 Background

Organ and tissue loss or failure caused by injuries and disease has been a critical problem since the beginning of human history. To solve this issue, people have devised many solutions, from the wheelchair to high-technology cybernetic artificial limbs. Currently, the most common and effective treatment for patients suffering in this way is tissue or organ transplantation. However, insufficient organ donation is a major problem that results in extremely long waiting lists for suitable organs. Other possible therapies, such as synthetic prostheses, surgical reconstruction, medication and medical devices, are not restricted by resources but have other problems. For example, people with synthetic prostheses or artificial structures or devices cannot fully regain the function of damaged organs or tissues, and this may also biocompatibility and maintenance issues. To counter the limitations of these therapies, tissue engineering has emerged as a promising alternative approach that can provide a biological replacement for failed organs or tissue loss resulting in better biocompatibility and the ability to regain more functionality.

Rapid developments in the field of tissue engineering have resulted in various tissue engineering replacement and implementation therapies. With the scientific progress of stem cell and biomimetic research, a unique opportunity to fabricate autologous tissues

has arisen. This technology consists of a platform that combines engineered extracellular matrices (scaffolds), cells and physical or chemical stimulations in order to manufacture autograft tissue. Using a patient's stem cells as base material, the engineered tissue has the advantages of autografts without the problem of long waiting lists caused by an insufficient organ supply. One of the major challenges that tissue engineering is currently facing is the need for more functional cells and the need for functional and biomechanical stability of laboratory-grown tissues intended for implantation.

To manufacture tissue using the patient's stem cells is the key to this project. However, it is not possible to gather enough stem cells from a biopsy. With a limited number of stem cells, the problem is how to maintain cell function and stability during the tissue engineering process while promoting cell proliferation to meet the clinical needs. The answer might be the use of scaffold material, an essential part of tissue engineering. Research indicates that scaffold material plays a significant role in stem cell proliferation, multiplication, differentiation and identification (Román A. Pérez 2013, Sabata Martino 2012).

Recently, a crosslinked protein membrane was produced in a microfluidic channel (Nair et al., 2006). The physicochemical properties of the membrane have already been researched (Chang, 2010), but the possibility of it serving as scaffold material still

needs to be studied. The very unique feature that can be formed in a microfluidic device could become a very useful advantage in cell co-culturing, micro bioreactors and many other applications (Ziaie et al., 2004, Wei Li, 2009). Electrospun Poly (lactic-co-glycolic acid) (PLGA) materials are some of the most popular materials used in tissue engineering and have already been used in many FDA-approved therapeutic devices (Greiner, 2007, Huang, 2003). Many PLGA composite materials have been proven to have some unique advantages in particular areas. For example, electrospun scaffolds of silk fibroin (SF) and PLGA material have been reported facilitate to endothelial cell growth (Wei Zhou, 2015). Research has also demonstrated that electrospun scaffolds of PLGA and multi-wall carbon nanotubes (MWCNTs) have advantages in promoting cell growth of bone marrow-derived mesenchymal stem cells (MSCs) and inducing the differentiation of MSCs into osteoblasts (Cuilin Lina and Shefang Yea, 2011).

1.2 Tissue engineering process

Tissue engineering is an interdisciplinary field that combines the use of cells and engineering and materials science with suitable biochemical and physicochemical methods to produce or improve functional tissue in developing clinical therapeutics to replace, repair and/or maintain tissue function.

Tissue engineering starts with cells harvested from biopsied tissue. Next, the cells are cultured on scaffolds so they can multiply to eventually form new tissue or a new organ for implantation. Regenerative medicine is a sub-field of tissue engineering, although the emphasis of regenerative medicine is on producing tissue using stem cells or progenitor cells.

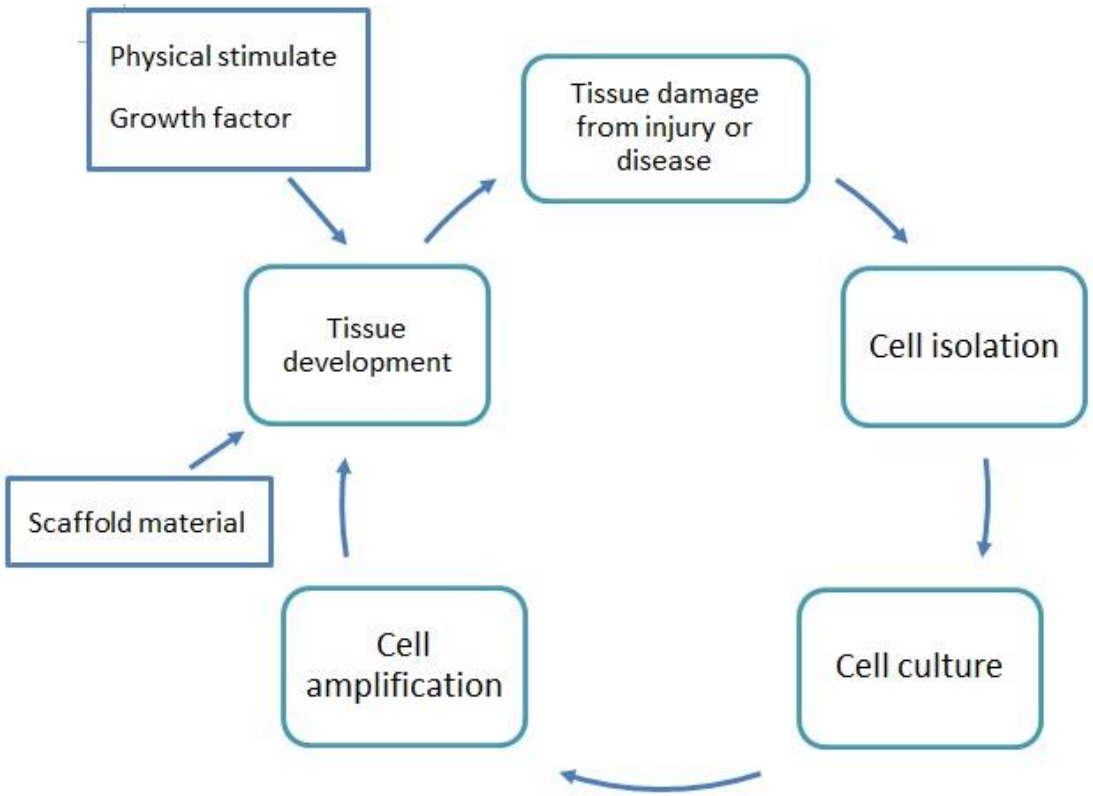

Figure 1-1 Schematic drawing of tissue engineering process

1.3 Crosslinked protein membrane

The crosslinking of polymers is a common way of producing membrane materials and is widely used in various industries and research applications. Crosslinking occurs as a result of polymerization between reagents. The crosslinking reaction happens between the molecules of the crosslink reagents. During the reaction, polymers re-establish new chemical bonds with crosslinkers and link one polymer chain to another. The crosslink reaction will create a new material with different physiochemical properties and functionalities. In many cases, the composite material becomes a better material for particular applications than the proteins or polymers alone. During the crosslinking process, the mechanical strength, chemical properties and biodegradability of the new material can be controlled (Arshady.R, 1999). Theoretically, there are infinite combinations of reagents to create new materials, which is a fascinating potential of this method.

1.3.1 Crosslinking reagent

Both synthetic polymers and natural polymers (such as proteins) can accomplish this kind of reaction. Proteins are well-known natural polymers that are ideal in fabricating crosslinked materials. Albumin is one typical naturally occurring protein that plays an important role in many different medical applications.

Bovine serum albumin

Bovine serum albumin (BSA) is a protein extract from cow's serum and is widely used in many experiments and applications, such as enzyme-linked immunosorbent assays (ELISAs), Western blot, restriction digests and immunohistochemistry for cancer diagnoses. BSA is also used as a nutrient substance in cell cultures. BSA is widely used because of its stability, and it shows inertness in many biochemical reactions. Because large amounts of BSA can be easily purified from bovine blood that is a graziery by-product, it is also relatively inexpensive.

BSA is a large spherical protein (66,000 Da) that consists of 585 amino acids in one polypeptide chain (Bernier G M and Putnam, 1964). BSA can be manufactured into many forms, such as membranes or nanospheres, because of the massive numbers of reactive functional groups on the polypeptide chain. There has been growing interest in BSA due to its ability to inhibit fibrinogen, platelet aggregation and adsorption, which makes BSA an ideal biomaterial that could be used to enhance blood compatibility (Nair Lakshmi S, 2006). The shape of BSA molecules is shown in Figure 1-2. BSA molecules consist of three homologous domains (I, II, III) that are divided into nine loops (L1–L9), as shown in Figure 1-3 (Brown, 1975).

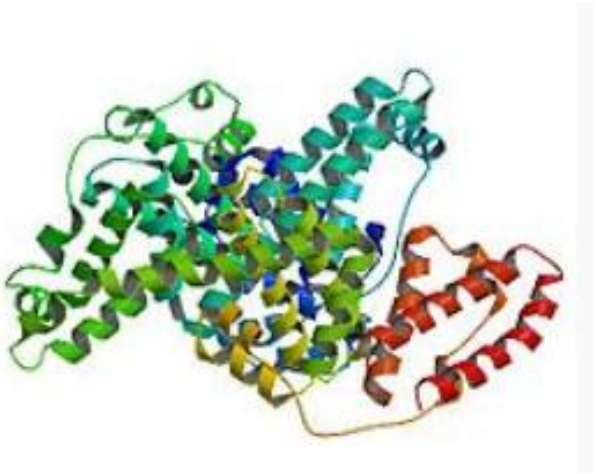

Figure 1-2 BSA molecule shape

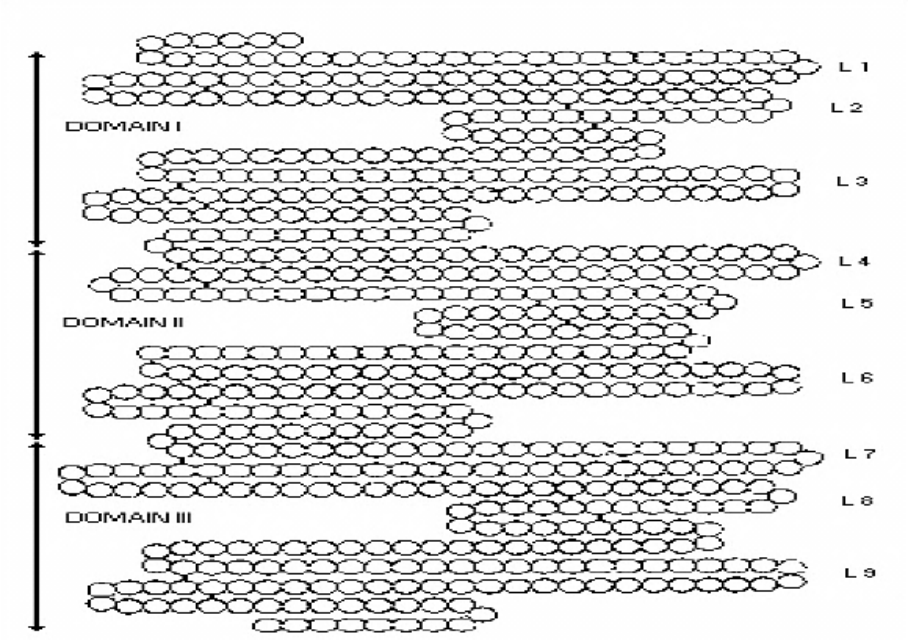

Figure 1-3 The molecule structure of bovine serum albumin

Crosslinking agents

Crosslink reaction is like building, there are polymers that act as the ‘blocks’ which form the main body of the building, and there are crosslinking agents that act as the ‘concrete’ which is the adhesive material. Different crosslinking agents have been used to create stable protein membranes. In this study, terephthaloyl chloride (TCL) and iso-phthaloyl chloride (IDCL) were used as crosslinking agents. TCL and IDCL are isomer acid chlorides with the same chemical formula of $C_8H_4Cl_2O_2$, but they have different chemical structures; acid chloride is very reactive with amino groups at room temperature. The structures of TCL and IDCL are shown in Figure 1-4. They are white crystalline at room temperature that is soluble in many organic solvents. The polymers that are crosslinked by TCL and IDCL can provide excellent chemical resistance and temperature stability, and they are lightweight and usually very strong (William R. Berti, 2006). After formation, they are expected to have different membrane morphology structure.The reaction scheme for amino-based protein crosslinking with TCL is shown in Figure 1-5. The crosslinking reaction involves a nucleophilic substitution between protein and acid chloride, which includes a nucleophilic attack by the lone-pair electrons of the amino groups on the protein on the polarized carbon atom of acid chloride. The outcome is C=O double bond re-formation, chloride ion removal and the subtraction of hydrogen from nitrogen, with hydrochloric acid as the product (Chang, 2010).

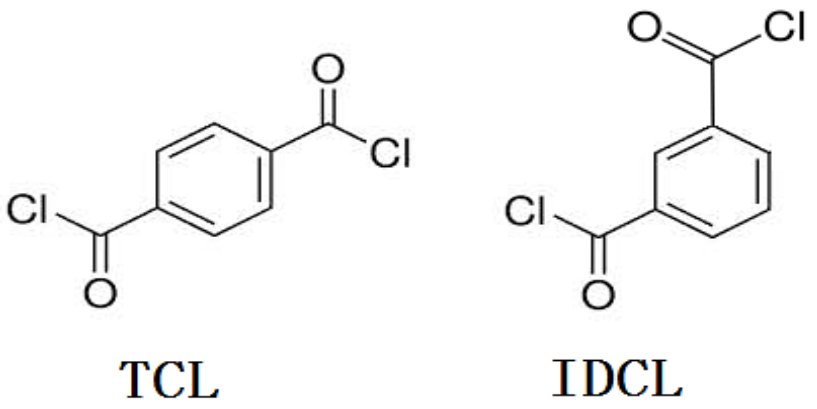

Figure 1-4 The structures of TCL and IDCL

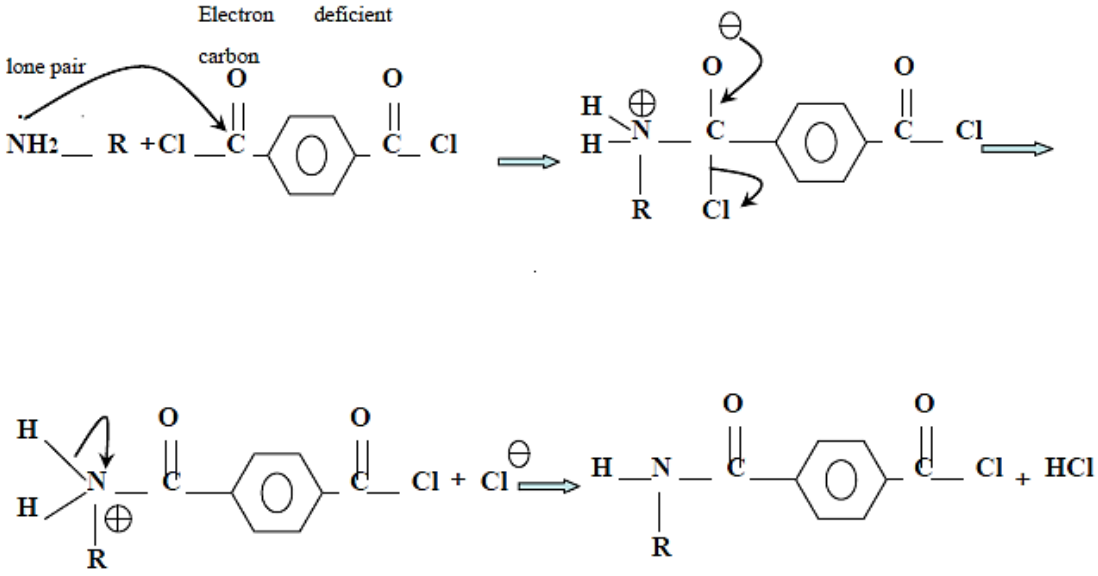

Figure 1-5 Scheme for amino-based protein crosslinking with terephthaloyl chloride

1.3.2 Microfluidics

Microfluidics is an interdisciplinary field that includes engineering, physics, chemistry, biochemistry, nanotechnology and biotechnology. It consists of systems or devices that manipulate tiny amounts of fluid in microchannels that offer precise control and includes various tests of the fluids' characteristics and behaviour. The scale of microfluidics is usually very small; the diameter of the microchannel is normally less than one millimetre. Microfluidics technology offers the ability to carry out various tests with tiny sample volumes and can also provide as an integrated chips due to its miniaturization size. Typical applications include inkjet spray heads, DNA chips, lab-on-a-chip (LOC) technology and micro-propulsion. The applications of microfluidic devices can be divided into four main categories: diminutive analysis systems, biomedical devices, chemistry and biochemistry test equipment and systems for fundamental physical research (Beebe D J, 2002).

The first microfluidic device was built in the 1970s (Erickson D and D, 2004). It was a miniaturized gas chromatography (GC) system and was not developed further. With the advance of molecular biology, especially genomics, microfluidic systems have been found to be very helpful in analysing complex compounds, particularly DNA and proteins. The typical achievements of this field are (LOC) and micro total analysis system (μTAS). Apart from the applications that focused on the mechanical and microfabrication technologies, the devices that focus on biological applications are

called biomedical microelectromechanical systems (BioMEMs). Since the 1990s, BioMEMs have not only been used in the academic area but also in commercial products. For example, an MEMs-based DNA sequencer has been widely used in post offices for the bio-agent detection of anthrax and other deadly pathogens. The sequencer device can analyse the different complementary DNA sequences in samples to detect the existence of possible harmful biomolecules and pathogens (Smart CyclerR). The US Postal Service has installed similar devices at 283 mail-processing centres in order to have heavy-duty biohazard detection system units across the country. Bio-MEMS drug delivery systems are also used by many hospitals and research facilities. Bio-MEMS drug delivery systems can provide controlled drug delivery by integrating silicon chips and electroactive polymer technology (Shawgo G M, 2002).

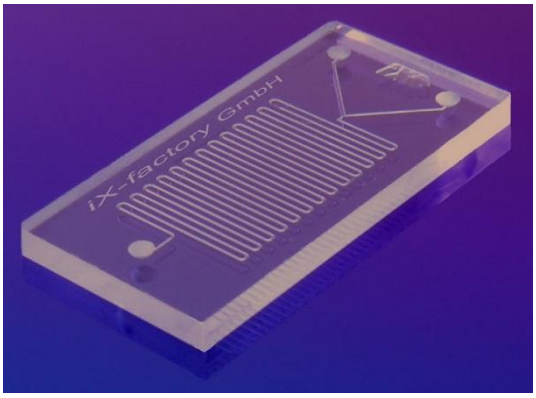

Figure 1-6 microfluidic chip fabricated in Glass (Tombrink, 2014)

Fabrication of microfluidics

The choice of materials used in microfluidics is varied. Most of the early microfluidics systems were fabricated with silicon and glass. The original purpose of these systems was to analyse aqueous solutions (Wu Z, 2009). Glass has the advantage of optical transparency. Silicon is more expensive than glass and also blocks UV light in the visible zone of the optical spectrum, so silicon is unsuitable for devices that need optical analysis.

Both silicon and glass can be used easily to manufacture microfluidics with the etch method, which only requires a dust-free environment. However, many biomedical devices are required to be made from soft materials that are pliable with smooth, non-linear surfaces such as skin or clothes. Patients may prefer these soft materials due to their comfort and pliability. Many polymer materials fit this requirement, such as silicone rubber, isobornyl acrylate and polyimide (McDonald J C, 2000). In addition, the physical properties of polymer materials can be controlled; they can be manipulated to become robust, hard material or soft, elastic material. Furthermore, most polymers are relatively inexpensive. However, they also have disadvantages. For example, some polymers react with or dissolve in some organic solvents and are sensitive to temperature. Recently, microfluidics systems made of poly (dimethylsiloxane) (PDMS) (Kirill Efimenko, 2002) have been reported. PDMS is an excellent material for fabricating microchannel systems. PDMS is a polymeric

organosilicon compounds which is vastly used in joint mixture, lubricant, contact lenses and many other industrial applications. PDMS has everything that a microfluidics needed it is non-toxic, non-flammable, can be hardened at low temperatures, has excellent optical transparency and stable in most organic solvents.

Laminar flow

Laminar flow is a unique flow feature in a low-velocity flow condition. When laminar flow occurs, the liquid flow in the channel appears in parallel layers that do not interfere with each other as shown in Figure 1-7. In this condition, two or more different fluid streams moving in the same channel will not have any turbulence. The only interaction between the individual flow streams is by diffusion (Beebe D J, 2002).

There are two types of flow conditions, laminar flow and turbulent flow. Determining flow type in a channel is important. The Reynolds number is an important figure that describes whether the flow condition is laminar or turbulent. The Reynolds number is defined as the ratio of inertial forces to viscous forces. When the flow velocity is low, the viscous force predominates over the inertial force and will reduce the turbulence in the flow; therefore, the flow condition tends to be stable. When the flow velocity is high, the inertial force takes control and as a result, the flow condition will be more changeable. Normally, in a standard flow condition (straight channel) with a Reynolds

number below 2100, the flow condition will definitely be laminar, whereas when the Reynolds number is greater than 4000, the flow will be turbulent.

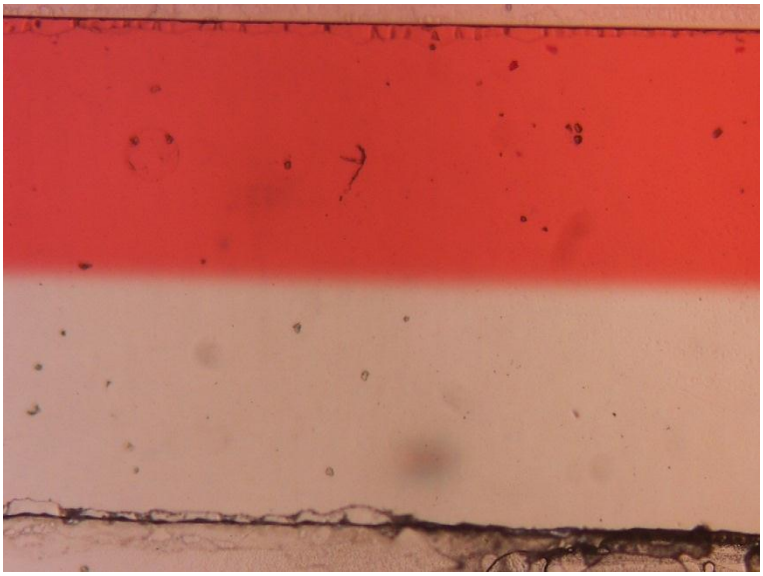

Figure 1-7 Laminar flow in self-made PDMS microfluidic channel (red: ponceau S solution, white: PBS) at a flow of 300 µl/min

The flow condition in microfluidics is almost always laminar because of the small size of channels. Laminar flow in microchannels has been utilized in many applications, including diffusion-based separation and detection, solvent extraction, mixing and hydrodynamic focusing (J. Gargiulia, 2006, Nair G, 2006 , Peterson D S 2005 , Jong J, 2006). Controlled laminar flow in microfluidic devices has been applied in numerous applications. For example, laminar airflow is used to separate volumes of air or exclude airborne contaminants. Laminar flow hoods are used to prevent contaminants

in sensitive processes in science, electronics and medicine. Laminar flow reactor (LFR) uses laminar flow to study chemical reactions and process mechanisms. In recent years, microfluidics have been refined and used in new scientific applications, such as micro bioreactors for tissue engineering and drug delivery or release studies at capillary conditions (Shawgo G M, 2002). The potential for the broad use of microfluidic systems is shown in Table 1-1.

Area	Application
Small amount sample analysis	Detection of single molecules
Small-scale organic synthesis	Combinatorial synthesis (Konrad R, 1998)
Studying the flow of fluids	To study laminar flow in small channels, to study diffusion (Brody J P, 1996)
Biomimetic systems	Development of mimic biological functions (Shawgo G M, 2002)
Sample preparation	Purification of biological specimens (Paul C. H. Li, 1997)
Biomedical devices	Drug delivery (Shawgo G M, 2002)
Miniaturized analytical systems	Analysis blood or interstitial fluids
Genomics and proteomics	Rapid, high-density sequencing (Woolley A T 1995 , Liu S, 1999), combinatorial analysis, forensics
Clinical analysis	Rapid analysis of blood or interstitial fluids, immunological diagnostics (Chiem N and J, 1997 , Colyer C L, 1997),enzymatic assays (Hadd A G, 1997)
Environmental testing	In situ analysis of environmental contamination (Van den Bery A, 1993)

Table 1-1 Application of microfluidic systems

1.3.3 Fabrication membranes in microfluidics

Substances fabricated using microfluidics appears to have applications in reagent and solvent handling, especially in chemical processes such as mixing and separation (Beebe D J, 2002 , Wu Z, 2009 , Erickson D, 2004). In 1999, Kenis et al. (Huang C J, 2006) published a method of microfabrication within capillary channels using the diffusive transport of reactive reagents to the interface to form structures with feature sizes of less than 5 mm. The management of the complex solid–liquid interface between living systems and synthetic materials also occurs in tissue engineering, drug delivery and implantable biomaterials applications (Babak Ziaie, 2004). The laminar flow condition in microfluidics allows the precise control of fluid flow which provides the opportunity to fabricate a crosslinked membrane along the interface of laminar flow in the microfluidic channel. To form a crosslinked membrane in a microfluidic channel, two streams of crosslinking reagents are introduced simultaneously. Because of the laminar flow condition in the microfluidic channel, the two crosslinking reagents will react by stable diffusion and start to form membranes based on the interface of the two flow streams. The membranes formed in microfluidics can be utilized in many applications, such as barrier films to protect sensors that allow electrochemical detection for biological recognition, scaffold material for cell amplification or cell co-culturing, transduction and electronic signal processing (McDonald J C, 2000).

There are usually four different ways to fabricate structures in microfluidics.

Direct incorporation of membranes

This is the most straightforward way to fabricate a membrane in a microchannel. The whole system can be directly built just by clamping or gluing the prepared membrane into the channel (Liu Changchun, 2011). The advantages of this method are that it is a simple process and there is a wide choice of membrane types. The membrane can be purchased from a commercial supplier. However, the major problem with direct incorporation of membranes is sealing. When attaching the membrane to the channel, the glue can get sucked into the channel due to the capillary force and block the whole system.

Pre-installing a membrane in a chip during the fabrication process

This method can be achieved in several ways, such as producing sieves with well-defined pores by etching (Baldi A, 2006), preparing polymeric membranes by casting (Liu Changchun, 2006), creating pores using ion track technology and photopolymerization of ion-permeable hydrogels (Khaled Al-Aribe, 2006). The membranes fabricated using this method normally have excellent sealing because the membrane is built in before fabricate the microfluidics. The disadvantages of this method are the complex manufacturing process that requires professional instruments and the high cost.

Building the membrane as part of the chip

This method is quite similar to the previous one, but instead of installing the membrane on the chip, the membrane is built as part of the chip. The method is simple as no additional fabrication steps are required; just build the chip using material that can serve as membrane material. Typically, such materials are polymers. When a polymer solution is phase-separated from a microstructure mould, a membrane is formed by an inverse replication of the mould features (Moorthy J 2003). The disadvantage of this technology is the limited choice of materials; only a few polymers can be used, such as polyimides and PDMS. In addition, it is hard to change the properties of the membrane because the properties of the chip will have to be changed as well, which greatly limits the application of this method.

Crosslinked membranes in microfluidics

This is a more advanced method of forming polymer membranes in microfluidics. This method uses the unique feature of laminar flow in microfluidics, providing an environment for fabricating crosslinked membranes at the interface of two laminar flow streams by diffusion. Recently, Hisamoto et al. (Hisamoto H, 2003) successfully demonstrated that highly efficient molecular transport between two phases for analytical and synthetic applications was achievable using aqueous/organic multilayer flows. Based on these ideas, a Y-shaped microfluidic channel was fabricated first, and then two crosslinking reagent solutions were simultaneously injected into the

microchannel with a syringe pump. In the laminar flow condition, a liquid–liquid interface is formed within a short time. Using this method, a thin membrane is formed along the interface of the flow. The crosslink reaction is rapid, and different membranes can be formed simply by using different crosslink solutions.

1.4 Electrospinning technology

Electrospinning uses an electrical charge to draw very fine (typically on the micro or nano scale) fibers from a liquid. Electrospinning shares characteristics of both electrospraying and the conventional solution dry spinning of fibers (Ziabicki A, 1976). This method does not need to use any chemical reactions or high temperatures to produce nanoscale fibers from solutions. This makes the process particularly suitable for the production of fibers using materials that have complex large molecules or that are heat sensitive. Another benefit of this method derives from the use of highly evaporative solvents; it is guaranteed that no solvent will be carried over into the final product.

Electrospinning is a simple and efficient method to produce nanoscale porous scaffolds. It is very convenient to form fibers with a broad range of materials, including both natural and synthetic polymers. Additionally, the parameters of the scaffolds, such as the morphology, fiber diameter and porosity, can be changed by altering the electrospinning parameters, including the solution concentration, injecting viscosity,

applied voltage and the distance between the spinneret and the collecting target. Due to the versatility of the electrospinning technique, electrospun scaffolds have been widely used in tissue engineering as scaffold material in stem cell, cardiovascular and musculoskeletal tissue engineering. Electrospinning technology has attracted considerable attention and has been widely used because of three advantages. First, electrospinning provides a more powerful, rapid and low-cost integrated process to produce continuous nanofibers compared to other multi-step traditional fiber manufacturing methods. In addition, the technique can also be used for mass production without significantly increasing production costs. Second, electrospinning has flexibility in manoeuvring physical parameters and structures by adjusting the use of different polymer composites. Controlling parameters offers the capability of designing nanofiber scaffolds that can meet the demands of numerous applications. Third, an electrospun nanofiber provides a biomimetic cellular environment that resembles the extracellular matrix (ECM). The electrospun nanofiber scaffold has a structure similar to collagen fibers in natural, native tissues and is thus able to interact with cells.

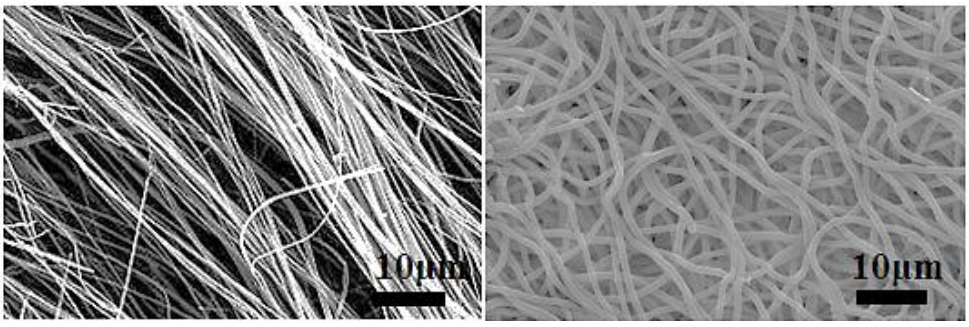

Figure 1-8 Electrospun PLGA nanofibers (left: aligned fibers, right: random fibers)

Electrospinning process

The electrospinning process is shown in Figure 1-9. When an appropriate high voltage is applied to a drop of liquid, it becomes charged. The electrostatic repulsion force then overcomes the surface tension of the liquid drop and stretches it into a triangle shape called the Taylor cone. With the constant supply of liquid, a stream of liquid material is drawn out under the electrostatic field and is then randomly addressed on the collector surface. The highly evaporative solvent dries out during the flight, leaving the nanofiber on the collector. To achieve electrospinning, the molecular cohesion must be high enough to maintain the integrity of the molecule group under the electrostatic repulsion force; otherwise, the drop will be spread evenly, as in electrospraying. As the jet dries in flight, the mode of current flow changes from ohmic to convective as the charge migrates to the surface of the fiber. The jet is then elongated by a whipping process caused by electrostatic repulsion initiated at small bends in the fiber until it is finally deposited on the grounded collector. The elongation and thinning of the fiber resulting from this bending instability leads to the formation of uniform fibers with nanometre-scale diameters (Dan Li, 2004).

Controlling parameters of the electrospinning process

Changing the controlling parameters of the electrospinning could lead to a change in the appearance of the electrospun nanofiber material. For example, decreasing the distance between the needle and collector will cause insufficient evaporation of the solvent, which will make the nanofiber stick together. Using a unique rotation collector could result in the manufacture of aligned nanofiber material as shown in Figure 1-8.

The parameters involved in the electrospinning process are listed below.

Controlling parameters
Molecular weight, structure and distribution of the polymer in the electrospun solution (branched, linear, etc.).
Flow rate of the solution
Physicochemical properties of the electrospun solution (viscosity, conductivity and surface tension)
Distance between the jet needle and the collector surface
Environment parameters (temperature, humidity and air velocity in the chamber)
Characteristics of the collector (rotation, size, shape)
Needle size

Table 1-2 List of controlling parameters in the electrospinning process

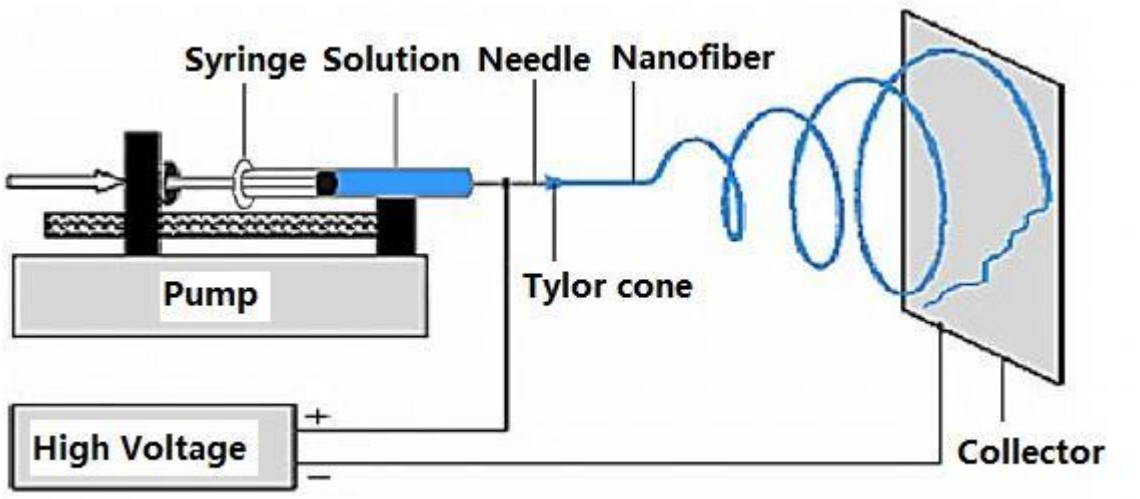

Figure 1-9 Schematic drawing of the electrospinning process

1.4.1 Electrospinning materials

Material choice is crucial for electrospinning in different applications. The ideal materials for neural tissue engineering should be biocompatible and should have appropriate chemical and physical properties to facilitate the required support and guidance of axon regeneration (Cao, 2009). Many synthetic and natural materials have been used to provide nanofibrous scaffolds for neural tissue engineering, such as poly(caprolactone) (PCL), poly(glycolic acid) (PGA), poly(L-lactic acid) (PLLA), Poly(lactic-co-glycolic acid) (PLGA), collagen, SF, and gelatin (Patel, 2008, Yang F., 2005, Wang G, 2011, Chunmei Li, 2006, Yang F, 2004, Bini et al., 2006). The combination of synthetic and natural material has the advantage of providing scaffolds that are more suitable for neural tissue engineering that have enhanced mechanical properties and improved biocompatibility over scaffolds made of a single material.

Regarding the polymers used for electrospinning, PLGA is one of the most popular and

has already been used in many Food and Drug Administration (FDA)-approved therapeutic devices. PLGA becomes an outstanding biodegradable polymer because it undergoes hydrolysis in the body and produces original monomers, lactic acid and glycolic acid. These two monomers are common by-products of various metabolic pathways in the body under normal physiological conditions. Since the body effectively deals with the two monomers, the cytotoxicity associated with using PLGA is minimal. In addition, the possibility of adjusting the polymer degradation time by altering the ratio of the monomers used during synthesis has made PLGA a common choice in the production of a variety of biomedical devices, such as grafts, sutures, implants, prosthetic devices and micro and nanoparticles. The aligned PLGA nanofibrous scaffolds have been shown to be appropriate for the adhering, growth and differentiation of C17.2 nerve stem cells (Bini et al., 2006). A study of electrospun PLLA-aligned fibers indicates that the same material could also improve neural stem cell differentiation (Yang F., 2005, Yang F, 2004).

Carbon nanotubes

Carbon nanotubes (CNTs), which have unique mechanical, electrical and surface properties, have been wildly applied in biomedical engineering, including in biosensors, cell delivery agents and tissue engineering scaffolds. Electrospun nanofibers based on CNT composites are very attractive materials because they combine the remarkable properties of CNTs, which could significantly improve the product's mechanical and

electrical properties (Huang, 2003, Qiao, 2011). CNT composite scaffolds have been used to promote neuronal differentiation efficiency in human embryonic stem cells (HESCs) (Chen, 2012).

CNTs have a seamless hollow cylindrical structure that is 1–2 nanometres in diameter and consist of a hexagonal network of carbon atoms, with one or both ends of the nanotubes being capped with a hemispherical fullerene molecule. There are two forms of CNTs, single-walled nanotubes (SWNTs) and multi-walled nanotubes (MWNTs), as shown in Figure 1-10. SWNTs have single cylindrical layers of this carbon atom network while MWNTs have several coaxial cylindrical layers. In this study, we use MWNTs as filler to enhance PLGA material.

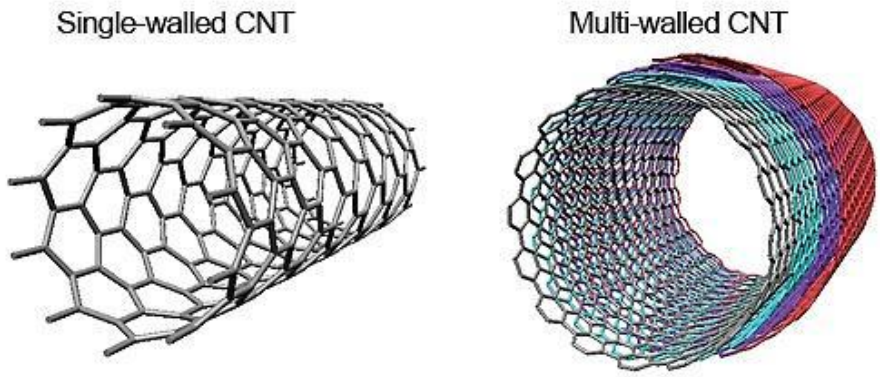

Figure 1-10 Structure of a single-walled CNT and a multi-walled CNT(DoldvariGroup)

Silk fibroin

Protein, as a typical natural material, is a rational choice for tissue engineering applications. Structural proteins, such as collagen, elastin, elastin-like peptides, albumin and fibrin, are often used as sutures, scaffolds and hemostatic and drug delivery agents (L.S. Nair, 2007). SF collected from silkworms is one commonly used natural protein material and has a long list of applications in human history. Currently, silk sutures are used in lips, eyes, oral surgeries and in the treatment of skin wounds (F.G. Omenetto and Kaplan, 2010). Recently, the use of SF has been increasingly developed in the biomedical area with the new discovery of its properties, including mechanical strength, biocompatibility and controllable biodegradability (F.G. Omenetto and Kaplan, 2010). These properties of SF are especially useful in tissue engineering. Recent studies indicate that silk can also be used in applications like real-time physiological and functional recording and optical systems for diagnosis and treatment (F.G. Omenetto and Kaplan, 2008, M.K. Hota, 2012). Silk is also an excellent material for applications in optics and photonic biosensors due to its remarkable (ca. 95%) optical transparency in-between the visible spectrum and its fantastic surface smoothness (M.K. Hota, 2012, H. Tao, 2012). Several reports have studied the fabrication, structure and application of silk-based implantable biomaterials that have the necessary functionality and sensitivity required for further potential applications (B. Kundu and S.C. Kundu, 2010, F.G. Omenetto and Kaplan, 2010, G.H. Altman, 2003, N. Kasoju, 2012).

1.4.2 Electrospun PLGA composite membranes

Despite PLGA being one of the most popular materials used in electrospinning due to its many advantages, there are still some issues with electrospun PLGA composite materials. The hydrophobicity of electrospun PLGA nanofibers negatively impact cell attachment, which greatly limits its use as a tissue engineering scaffold material. In tissue engineering applications, the requirements for the materials are complicated and varied. These requirements include features such as biocompatibility and biodegradability and other important functional properties, such as mechanical strength, hydrophilicity and morphology. Unfortunately, PLGA products often have low mechanical durability, which is not desirable for many practical biomedical applications. In addition, during PLGA degradation, the acidic products build up and decrease the local PH in the surrounding tissue; breaking the acid-base equilibrium could trigger inflammatory and foreign body reactions in vivo. Upon clinical application, these reactions lead to obvious symptoms, such as suddenly emerging pain, swollen tissues and even persistent fistulas (Huang et al., 2003, Yoon Sun Jung, 2008).

To overcome these limitations, it is common to enhance PLGA with other materials. Consequently, the outstanding physical properties of CNTs make them a perfect choice as fillers in polymer composites to produce enhanced nanofibers with better physical properties. Many successful applications of enhanced composite materials have been reported; multi-walled carbon nanotube (MWCNT)-incorporated electrospun polyvinyl

alcohol (PVA)/chitosan (CS) nanofibers have been proven beneficial in mouse fibroblast (L929) proliferation (Liao, 2011). There is also research that shows that incorporation of carboxylation MWCNTs with biodegradable PLGA exhibited better adhesion and viability of rat bone marrow-derived MSCs and also improved alkaline phosphatase (ALP) production significantly (Cuilin Lin, 2011). An electrospun PLGA MWCNT knitted scaffold was fabricated and reportedly can support cell growth of NR6 mouse fibroblast cells (Sharon L. Edwards, 2009). Similar to CNTs, silk material has become a very popular choice of support material in tissue engineering due to its outstanding biocompatibility, hydrophilicity and degradablility. PLGA nanofiber-coated silk composite scaffolds have been reported to have the potential to become a suitable material in connective tissue engineering. Also, electrospun PLGA-SF-collagen composite material has been verified to have better biocompatibility than pure PLGA material for Schwann cells (Guanglin Wang, 2010, Wei Zhou, 2015).

In this study, CNTs and SF were added into the polymer in order to change the properties of electrospun nanofibers. However, they also changed the parameters of the polymer, such as its viscosity and conductivity. Therefore, the electrospinning parameters may need substantial optimization to obtain satisfactory nanofiber materials that meet the requirements of tissue engineering applications. With the rapid development of CNTs in the biomedical area, there is increasing concern about the

toxicity and metabolism of CNTs (Bellucci, 2009). Many researches have been carried out to study the mechanism of the CNT's cytotoxicity and also try to reduce it, include in vivo toxicity and metabolism experiment and introduce surface modification on CNTs (Sheng-Tao Yang, 2012).

1.5 Neural tissue engineering

Nervous system damage is very common in trauma, congenital malformation and clinical practice and may lead to chronic disability. The repair of the nervous system brings great challenges for clinicians and researchers. Although nerve autografts are regarded as the 'gold standard', the shortage of donor sites limits its application (Beris, 2007, Cao, 2009). Tissue engineering provides an alternative approach to fabricating implantable scaffolds for neural regeneration. A three-dimensional scaffold that made of nanofiber materials can mimic the topography of a natural extracellular matrix (ECM). It provides an environment conducive to the adhesion, migration and proliferation of cells (Travis J. Sill, 2008, Zhang Y. Z, 2007). Meanwhile, the high porosity property expedites the delivery of drugs through the fibers. Therefore, nanofibrous scaffolds are also employed as potential drug carriers for chemical therapy.

1.5.1 PC12 cell line

PC12 is a cell line derived from a pheochromocytoma of the rat adrenal medulla and is a commonly used neural cell line that is capable of differentiating to neuron-like cells in the presence of nerve growth factor (NGF). This cell line was first cultured by Greene and Tischler in 1976 (Greene LA, 1976). It was developed in parallel with the adrenal chromaffin cell model because of its excellent adaptability in pharmacological controlled differentiation, ease of culture and the vast amount of information on its proliferation and differentiation (R.H.S. Westerink, 2008). PC12 cells can be easily differentiated to neuron-like cells because the pheochromocytoma is derived from neuroblastic cells that are precursors of neurons. 'Neuron-like' means the shape of the cell resembles neurons and they release similar secretion by vesicles. These characteristics provide a great advantage despite the relatively small size of the cells, which can hold only an average of 1.9×10^{-19} moles of neurotransmitter released by vesicles (R.H.S. Westerink, 2008). The vesicles contain catecholamines, mostly dopamine but also a small amount of norepinephrine. The PC12 cell line has helped in learning about the function of proteins underlying vesicle fusion and the role of synaptotagmin in vesicle fusion, in which increases in calcium concentrations displace synaptotagmin and catalyse membrane fusion. PC12 cells have the unique ability in that they can undergo chemically manipulated differentiation. This makes PC12 cells a powerful tool for neuronal differentiation and neurosecretion research. The PC12 cell line has been used to obtain more information about diseases of the brain. It has been

used in research about hypoxia, where acute hypoxia induces exocytosis and prolonged hypoxia induces excessive exocytosis. PC12 cells were used to find which prion protein fragments cause neuronal dysfunction (R.H.S. Westerink, 2008). PC12 has also been used in studying some forms of Parkinson's disease; the findings support the idea that there is interference after vesicle docking and prior to vesicle release.

1.5.2 Adipose tissue-derived stem cells

Stem cells are undifferentiated biological cells that can differentiate into specialized cells and can divide (through mitosis) to produce more stem cells. They are found in multicellular organisms. In mammals, there are two main types of stem cells: embryonic stem cells that are isolated from the inner cell mass of blastocysts and adult stem cells that are found in various tissues. In adult organisms, stem cells and progenitor cells act as repair systems for the body by replenishing adult tissues. In a developing embryo, stem cells can differentiate into all the specialized cells, including ectoderm, endoderm and mesoderm cells but also maintain the function of regenerative substances and organs, such as blood, skin or intestinal tissues.

There are three ways to access the autologous adult stem cells in humans:

Source	Treatments
Bone marrow	Needs penetrate extraction which requires drilling into bone (typically the femur or iliac crest)
Adipose tissue	Requires liposuction surgery
Blood	Requires extraction with pheresis, blood is drawn from the patient and passed through filter equipment which collect the stem cells and returns the remaining blood to the donor.

Table 1-3 Human stem cell source

Stem cells can also be taken from umbilical cord blood just after birth. Of all types of stem cell harvesting, the harvesting of autologous cells involves the least risk. By definition, autologous cells are obtained from one's own body, just as one may bank his or her own blood for elective surgical procedures. Adult stem cells are frequently used in medical therapies, for example, in bone marrow transplantation. Stem cells can now be artificially grown and transformed (differentiated) into specialized cell types with characteristics consistent with cells of various tissues, such as muscles or nerves. Embryonic cell lines and autologous embryonic stem cells generated through somatic cell nuclear transfer or dedifferentiation have been proposed as promising candidates for future therapies (Tuch BE, 2006).

Adipose tissue-derived stem cells are also referred to as adipose-derived stem/stromal cells (ASCs), adipose-derived adult stem (ADAS) cells, adipose-derived adult stromal cells, adipose-derived stromal cells (ADSCs), adipose stromal cells (ASCs), adipose mesenchymal stem cells (AdMSCs) and lipoblast, pericyte, preadipocyte and processed lipoaspirate (PLA) cells. To prevent confusion, the International Fat Applied Technology Society reached a consensus to adopt the term 'adipose-derived stem cells' (ADSCs) to identify the isolated, plastic-adherent, multipotent cell population (Gimble J. M., 2007). Adipose tissue derives from the mesodermal layer of the embryo and develops both prenatally and postnatally (Kakudo.N., 2008, Gonda. K, 2008). The reason why adipose tissue contains a stem cell population is not still clear. There is some discussion whether the cells are a subpopulation of fibroblasts that reside within the fat tissue or are perhaps mesenchymal or peripheral blood stem cells passing through the fat tissue (Crisan, 2008 , Dellavalle, 2007).

The ASCs represent a readily available source for the isolation of potentially useful stem cells (Aris Sterodimas, 2010). In cultures, they have been shown to have an impressive developmental plasticity, including the ability to undergo multilineage differentiation and self-renewal (Liu, 2009). When ADSCs are compared with BM-MSCs, further similarities have been demonstrated in regards to their growth kinetics, cell senescence, gene transduction efficiency (De Ugarte, 2003), CD surface marker expression and gene transcription (Katz, 2005). Compared to bone marrow

MSCs, ASCs have potential advantages for tissue engineering applications because of the tissue accessibility, multipotency and ease of isolation without painful procedures or donor site injury.

1.5.3 Rat primary cortical neurons and neuroglia

Cortical neurons are the cells of the brain's largest region, the two hemispheres of the cerebral cortex. These neurons are packed into the cortex, also called the grey matter, which is up to 4 mm thick along both cerebral hemispheres. Most of the complex activity of the brain enabling thought, perception and voluntary movement is connected to the activity of these neurons. The brain has more than a dozen types of cortical neurons, broadly classified according to whether they activate or inhibit neural activity. It is important to note that while many psychophysical phenomena seem to depend on the cerebral cortex, no single region or individual neuron can account for complex mental activity, which is often spread among many different networks of millions of neurons working together. These nerve cells communicate with each other through chemical and electrical signalling and often use molecules called neurotransmitters to send messages to junctions called synapses located at hundreds of sites on the outer surface of any given cell. At a synaptic site, two cell membranes come into proximity, and both of them have lots of molecular structures called receptors that enable them to receive messages from each other. Electrical synapses

convey signals between neurons in the form of a current called an action potential, while chemical synapses rely on neurotransmitters released by one cell and then bind to the other cell in the synapse.

The surface of the cerebral cortex is folded into many grooves of various depths, called sulci, enabling a large number of neurons to fit into the relatively small area of the hemispheres. Here, neurons are arranged in six layers. Different types of cortical neurons populate these layers, from I to VI, which are identified by laboratory staining techniques and by their different sizes and shapes. Some types of neurons stimulate electrical firing and are called excitatory neurons; others stop or slow electrical activity and are called inhibitory neurons. A third category, interneurons, facilitates communication between the different types of neurons. Major excitatory cortical neuron types include pyramidal cells and spiny stellate cells. The former were named for their triangular cell bodies and have extensive connections with other neurons in the cortex and beyond. Inhibitory neurons come in many varieties, including basket and chandelier cells and the smooth, spineless stellate cells named for their lack of spiny projections to other nerves. Both groups of cortical neurons use chemical signalling to interact with adjacent cells, relying on specialized chemicals called neurotransmitters for this purpose. Excitatory neurons often use the neurotransmitter glutamate, while inhibitory cells predominantly signal through the compound γ—aminobutyric acid (GABA).

1.6 Aims and objectives

As stated previously, the potential of the crosslink protein membranes as scaffold material has still not been well researched. This PhD project seeks to investigate the biocompatibility of these crosslinked protein membranes along with a number of different types of PLGA electrospun composite nanofiber membranes in order to examine their potential as scaffold materials in tissue engineering.

The objectives of this project are as follows.

- Develop a method to manufacture the crosslinked protein membranes that can be used in cell culture experiments.

  A dropping method was used to produce the crosslinked protein membranes for cell culture experiments, and 3D printed ABS rings were used to immobilize the membranes in culture plates.

- Explore the biocompatibility of the crosslinked membranes.

  Because the two sides of the crosslinked membranes have different morphology, both sides of two types of crosslink membranes were tested (BSA crosslink with TCL and IDCL). The morphology of the membranes was examined with SEM. PC12, ADSCs and neurons were cultured on the membranes. The biocompatibility of the membranes was researched using CCK-8 to reflect the living cell numbers.

- Research the properties of the electrospun composite nanofiber materials.

  Four kinds of different electrospun materials were used (PLGA, PLGA+SF, PLGA+CNTs and PLGA+SF+CNTs). PC12, ADSCs and neurons were cultured on the electrospun materials. The biocompatibilities of the materials were tested using CCK-8. Specially designed spring-shaped clips were used to prevent the shape-shifting of electrospun materials and to immobilize the samples in culture plates. The morphology of the materials was tested with SEM. The mechanical properties of the materials were tested with a tensile tester, and the hydrophilicity of the materials was also tested.

- Study the effect of different CNT concentrations in electrospun materials on neuron cultures.

  Neurons from neonatal Sprague Dawley rat (SD rat) were cultured on electrospun PLGA materials with different CNT concentrations. Three trackers, tubulin 3, glial fibrillary acidic protein antibody (GFAP antibody) and Hoechst 33342 were used to label neuron and glia cells. Images were taken with a laser scanning confocal microscope to calculate the neuron and glial cell numbers. The CNT formation in electrospun nanofibers was tested with Transmission electron microscope (TEM). The morphology, physicochemical and mechanical properties of the materials were also tested.

2. Materials and methods

2.1 Materials

2.1.1 Materials for crosslink membranes

BSA (Fraction V, initial fraction by heat shock treatment), TCL, IDCL, distilled xylene, and hydrogen peroxide were purchased from Sigma-Aldrich (Sigma, Dorset, UK). The phosphate buffer saline (PBS) consisted of 52.8 mM Na2HPO4 (BDH, Dorset, UK), 15.6 mM NaH2PO4 (BDH, Dorset, UK) and 5.1 mM NaCl (Sigma, Dorset, UK).

2.1.2 Materials for electrospun membranes

PLGA（PLGA:85/15 M=1x10_5）was purchased from Jinan Daigang Biomaterial Co., Ltd. (Jinan, China). 1, 1, 1, 3, 3, 3-hexafluoroisopropanol (HFIP) was purchased from Chengdu Xiya Reagent Co. Ltd. (Chengdu, China). MWCNTs were purchased from Chengdu Organic Chemicals Co. Ltd. (Chengdu, China). SF was purchased from Huzhou Xintiansi Bio-tech Co., Ltd. (Huzhou, China).

2.1.3 Materials for cell culture

Cell Counting Kit-8, PBS, calcein, propidium iodide, Hoechst 33342, β-tublin 3, rabbit anti-rat antibody and FITC-labelled goat anti-rabbit antibody were purchased from Sigma-Aldrich. GFAP antibody, mouse anti-rat antibody and TRITC-labelled goat anti-mouse antibody were purchased from Chemicon. Cell culture-treated flasks, cell culture-treated 24-well plates and cell culture-treated 96-well plates were purchased from Thermo Scientific. Coverslips and centrifuge tubes were purchased from VWR. The PC12 cell line was purchased from Invitrogen.

ADSCs were provided by the Regeneration Medicine Center at the First Affiliated Hospital of Dalian Medical University. All the adipose tissue was legally obtained via liposuction surgery from anonymous donors. Primary cortical neurons and neuroglia cells were dissected from neonate SD rats purchased from Dalian Medical University Test Animal Center.

The neuron seeding medium contains 77% Neurobasal medium (Gibco, US), 2% B27 supplement (Gibco), 10% FBS (Gibco), 10% horse serum (Gibco) and 1% l-glutamine (Gibco). The neuron maintenance medium contains 96% Neurobasal medium (Gibco), 2% B27 supplement (Gibco), 1% l-glutamine (Gibco) and 1% penicillin/streptomycin (Gibco).

2.2 Manufacture of crosslink membranes

2.2.1 Crosslinked membranes in PDMS microfluidic channel

The original microfluidic channel was made of glass and was sealed. To examine the biocompatibility of membranes, the membranes have to be suitable for cell culture and have to be examined using many instruments. Thus, a microfluidic channel made with PDMS is necessary so the channel can be opened to allow the membranes to be taken out for examination. A Y-shaped plastic mould was cut from a 0.5 mm thick plastic plate and stuck on a glass slip and placed at the bottom of a Petri dish. PDMS and a hardener were mixed and then dropped into the Petri dish. The mould was heated in the oven at 80 ℃ until the PDMS hardened. Next, the PDMS in the Y channel was cut from the Petri dish and penetrated with two number 9 needles. The two needle tips were cut off and fixed in the PDMS channel, and the whole thing was stuck on a piece of glass.

A KD Scientific 200 syringe pump (Royem Scientific Ltd., UK) was coupled with a microfluidic channel with Tygon tubing (1.6 mm ID, 3.2 mm OD). BSA solution and a crosslinker solution were pumped into microfluidic channels simultaneously at flow rate of 300 µl/minute to create laminar flow to form crosslink membranes in the microfluidic channel.

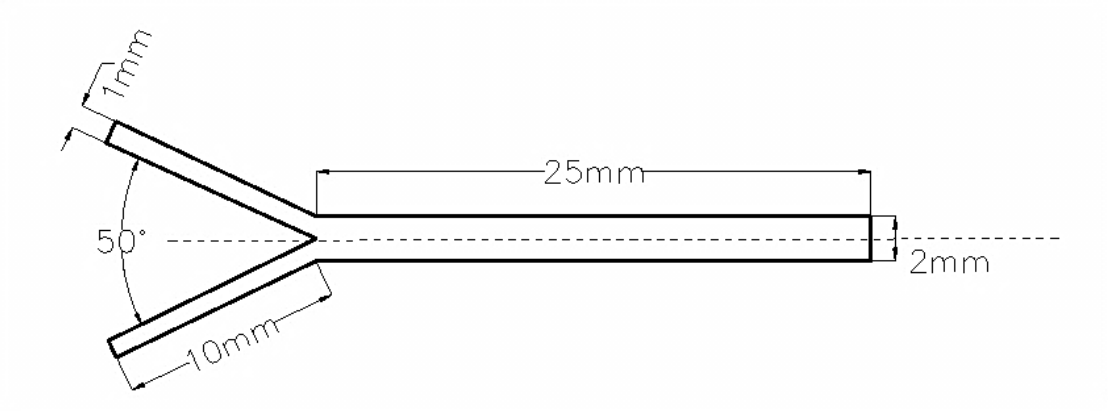

Figure 2-1 Schematic drawing of Y-shaped mould for PDMS channel

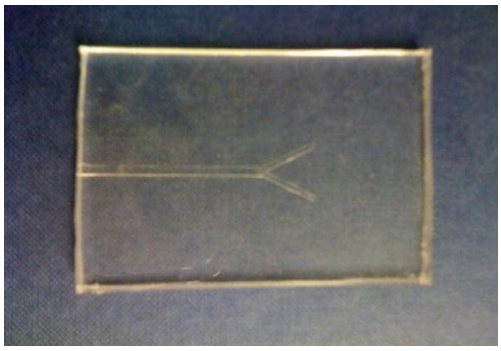

Figure 2-2 PDMS channel

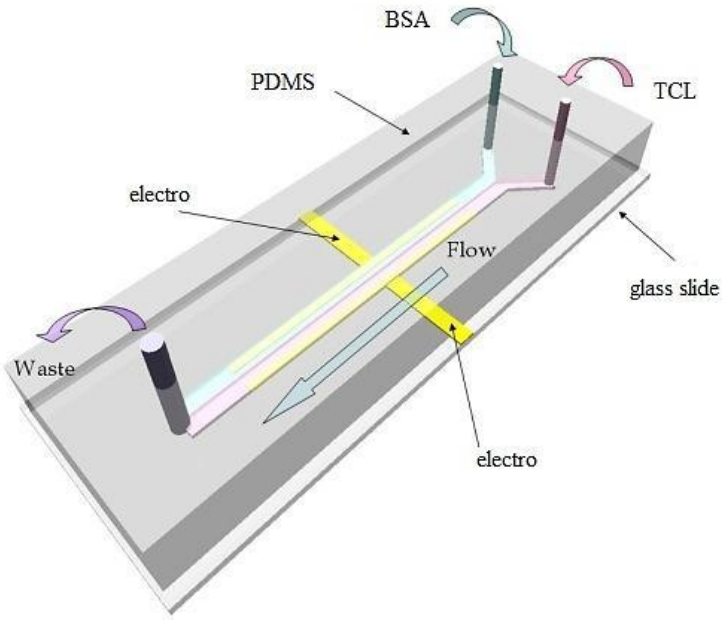

Figure 2-3 Schematic drawing of PDMS microfluidic with electro

2.2.2 Preparation of crosslink membranes for cell culture

The crosslinked membranes formed in microfluidics channels are not suitable for cell culturing due to the difficulty of sterilization and visualization. Therefore, an alternative method was used to make large area membranes to create the crosslink membranes outside the microfluidic channel (Chang, 2010).

Next, 1.25 g BSA was dissolved in 5 ml PBS to make an albumin solution. Then, 0.1 g TCl and 0.1 g IDCL were dissolved in 10 ml xylene to become a crosslink reagent. BSA solution in the amount of 1 ml was then added to a weighing bottle, and a micropipette was used to remove any bubbles to provide a flat surface for the crosslink reaction. Next, 1 ml of TCL or IDCL solution was carefully added on top of the BSA

solution. The membranes formed within 10 minutes but required 24 hours to become thick enough to take out, as shown in Figure 2-4.

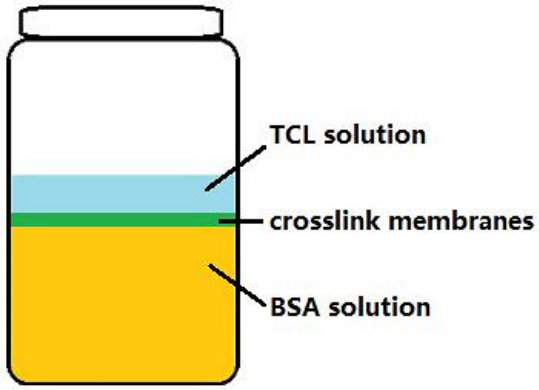

Figure 2-4 Schematic drawing of the manufacturing method for large surface membranes. TCL solution (blue) reacted with BSA solution (yellow) to form crosslink membranes (green) at the interface.

After 24 hours of crosslinking, the TCL solution was drained, and the membranes were cut from the wall of the bottle with a surgical knife (blade number 13). The bottle was positioned at an angle in order to remove the membranes from the solution from below using a flat-tipped metal stick. Then the membranes were cleaned with PBS several times and stored in a PBS solution at 4 ℃.

However, this method has a very high membrane damage rate, wastes a lot of material and is very time-consuming. Therefore, a simplified manufacturing method was developed to make the membranes faster and to better fulfil the requirements of cell culture experiments.

In the next method, 50 µl BSA solution was dropped on a 13 mm diameter round coverslip and flatted by a 10 mm diameter metal bar. This was the protein base for the membranes. TCL or IDCL solution was continually dropped on the bases for 8 hours. After 8 hours of the crosslink reaction, the membranes were washed with xylene in order to eliminate residual crosslinkers and were then washed several times with PBS. The membranes were stored in PBS solution at 4 ℃ after washing. The diameter of the membranes was approximately 12 mm with a thickness of approximately 70 µm. As shown in Figure 2-5, Figure 2-6.

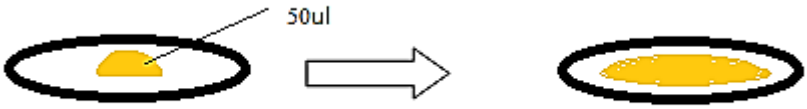

Figure 2-5 Schematic drawing of the simplified manufacturing method for crosslink membranes

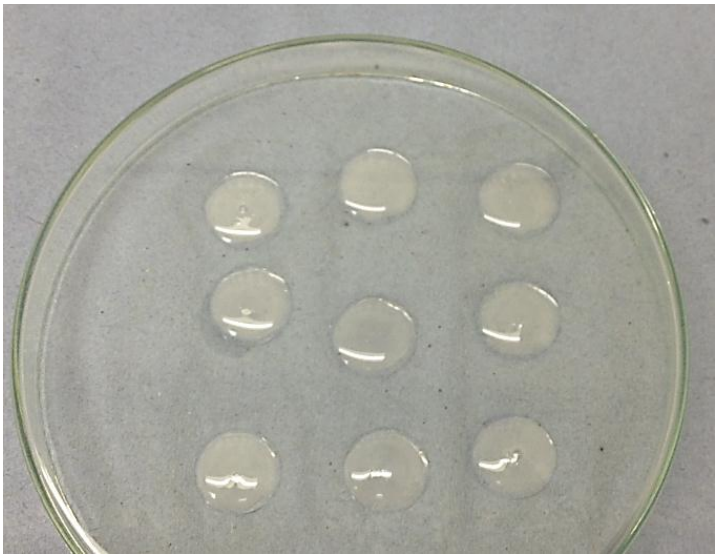

Figure 2-6 Membranes in progress

2.3 Fabrication of electrospun materials

2.3.1 Fabrication of composite electrospun materials

PLGA powder was dissolved in HFIP and left overnight in a 37 ℃ water bath to become a PLGA solution. CNTs were added and sonicated for 2 hours and then mixed with the PLGA solution to make a CNT-PLGA composite solution. This was then magnetically stirred for 1 hour at room temperature. SF was dissolved in HFIP and magnetically stirred for 2 hours to become SF solution. Then the SF solution was mixed with the PLGA solution and was stirred for 1 hour for electrospinning. The CNT-PLGA composite solution with 0.15 g/ml PLGA and 0.002 g/ml CNTs was electrospun at a voltage of 15 KV, a distance of 10 cm and a flow rate of 1 ml/hour. Fibres were collected on an aluminium foil-covered metallic plate after 2 hours of electrospinning.

The PLGA-SF solution with 0.15 g/ml PLGA and 0.1 g/ml SF and the PLGA-CNT-SF solution with 0.15 g/ml PLGA, 0.1 g/ml silk and 0.002 g/ml CNTs were electrospun using the same method under the same conditions.

PLGA powder was dissolved in HFIP to become PLGA solution. Different amounts of CNTs were added into the HFIP sonicated for 2 hours and then mixed with PLGA solution to make a CNT-PLGA composite solution. This was magnetically stirred for 1 hour at room temperature to become an electrospinning solution.

The CNT-PLGA composite solutions with different amounts of CNTs (0.001 g/ml, 0.003 g/ml, 0.005 g/ml, 0.007 g/ml and 0.01 g/ml) were electrospun at a voltage of 15 KV, a distance of 10 cm and a flow rate of 1 ml/hour. Fibres were collected from an aluminium foil-covered metallic plate after 2 hours of electrospinning.

2.3.2 Preparation of electrospun materials for cell culture

The electrospun materials were cut into 5 mm ×5 mm squares and ultraviolet sterilized on each side for 1 hour. The samples were then tightened onto specially designed spring clips. After that, the clips were put into 96-well plates and left in PBS overnight. In the neuron culture experiment, the scaffolds were immersed in Neurobasal medium for 24 hours and were coated with 0.001% poly-L-lysine and incubated overnight. The membrane preparation process is shown in Figure 2-7.

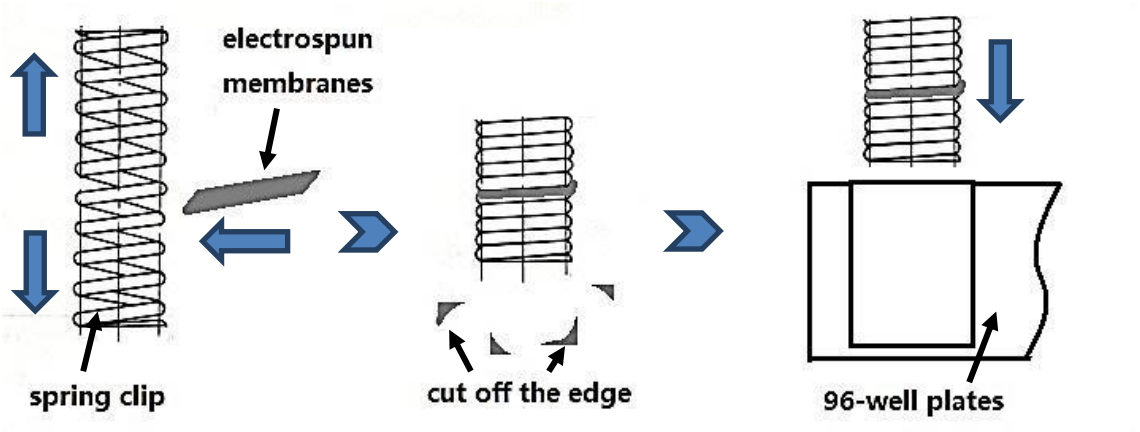

Figure 2-7 Schematic drawing of electrospun membrane preparation for cell culture

2.4 Cell culture

2.4.1 Cell culture on crosslink membranes

Membranes were prepared using the simplified method and placed into a 24-well plate. A 3D printed ABS ring (makerbot replicator) was carefully put in the 24-well plate to immobilize the membrane at the bottom of the well. ADSCs and PC12 at a density of 1 $\times 10^4$ cells/well were seeded on four different kinds of membranes and cultured for 8 days. Empty 24-well plates were used as control groups.

CCK-8 was used to indicate the viability of the cells on the membranes. Next, 20 μl CCK-8 (Sigma) was added to each well and the plate was incubated for 4 hours. Next, the Optical density (OD) values of the supernatant were measured at 490 nm using a microplate reader. High glucose DMEM culture medium was used in ADSC culture. RPMI 1640 culture medium was used in PC12 culture.

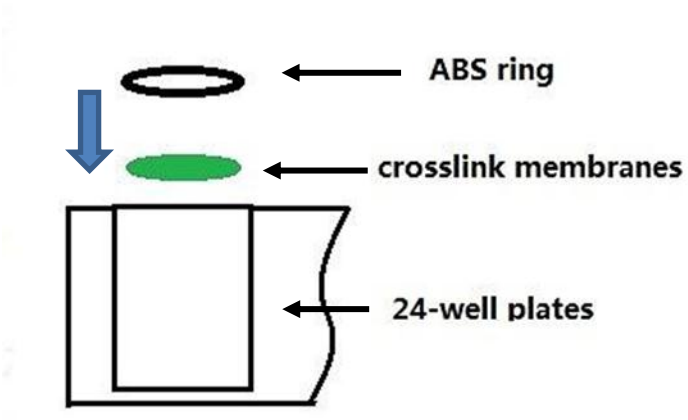

Figure 2-8 Schematic drawing of experiment procedure

2.4.2 Cell culture on electrospun membranes

The electrospun membranes were cut into 0.5 mm x 0.5 mm pieces and were ultraviolet sterilized for 1 hour per side. The samples were then tightened between the spring clips. After that, the clips were put into 96-well plates and left in PBS overnight. When culturing ADSCs, the samples were immersed in ADSC culture medium overnight instead. Before seeding, PBS was drained from the 96-well plates and the PC12 or ADSCs were seeded on four different kinds of electrospun membranes (PLGA, PLGA+SF, PLGA+CNTs, PLGA+SF+CNTs) and cultured for 8 days. OD values were tested every day to measure cell viability.

Primary cortical neurons and neuroglia cells were dissected from the superficial layers of the brain cortexs of neonatal SD rats (within 24 hours) (from the Dalian Medical University Test Animal Center). A neurons and neuroglia (95%/5%) cell mixture was dissociated in a seeding medium. The cell density and viability were assessed using a Trypan Blue dye exclusion assay, and the seeding density was adjusted to 5×10^4 cells/ml. Next, 100 μl of the neuron and neuroglia cell mixture were seeded on scaffolds fixed in 96-wells plates. The samples were cultured in seeding medium for 4 hours and then washed twice with culture medium and switched to a maintenance medium. Afterwards, all samples were cultured under standard conditions (37 ℃, 5% CO2).

2.4.3 Biocompatibility tests

A Cell Counting Kit-8 was used to indicate the cell viability of the membranes. Where 96-well plates were used, 10 μl CCK-8 solution was added to each well. For 24-well plates, 20 μl CCK-8 was used in each well. This amount was increased to 30 μl as the number of cells increased. The plate was incubated for 4 hours and then the supernatant of the culture medium was removed to new 24 or 96 well-plates. The OD values of the samples were measured at 490 nm using a microplate reader.

Cell Counting Kit-8 (CCK-8) allows very convenient assays by utilizing the highly water-soluble tetrazolium salt WST-8 produces a water-soluble formazan dye upon reduction in the presence of an electron carrier. WST-8 is reduced by dehydrogenases in cells to give a yellow colour product (formazan), which is soluble in the cell culture medium. The amount of the formazan dye generated by the activity of dehydrogenases in cells is directly proportional to the number of living cells. The detection sensitivity of CCK-8 is higher than other tetrazolium salts such as MTT, XTT, MTS or WST-1 (Sigma-Aldrich).

2.5 Immunostaining

2.5.1 Fluorescence labeling

The original solution (50 μg) was dissolved in 50 μl DMSO to make 1 μg/μl Calcein AM stock solution. 10 μl stock solutions were added into 9990 μl of PBS to make a 1:1000 working solution. Also, 1 μg/μl Hoechst 33342 stock solution was prepared and diluted into a 1:1000 working solution. Samples were put into new 96-well plates and washed twice with PBS solution for 5 minutes and then 1 ml of Calcein AM and Hoechst 33342 working solution was added. This was incubated for 30 minutes at 37 ℃ under standard culture conditions. The samples were then washed twice with PBS solution and tested with a fluorescence microscope using a 490 nm excitation filter and a 520 nm emission filter.

2.5.2 Neuron and glia cell labeling

Three different trackers, Calcein AM, propidium iodide and Hoechst 333425 were used to label dead and living cells. Samples were washed twice with PBS and incubated with labelling solution for 45 minutes at 37 ℃ and then washed twice with PBS again. The samples were observed under a laser scanning confocal microscope (Leica Microsystems, Manheim/Wetzlar, Germany).

Three different trackers, tubulin 3, GFAP antibody and Hoechst 33342 were used to

label neuron and glia cells. Samples were washed twice with PBS and treated with paraformaldehyde (PFA) for 30 minutes and then washed twice with PBS again. The samples were treated with 0.3% Triton X-100 for 20 minutes at room temperature and then washed three times with PBS. Next, 5% BSA was added and the samples were incubated for 1 hour. Afterwards, the samples were added to 1:200 rabbit anti-rat β-tubulin 3 and mouse anti-rat GFAP and then left overnight at 4 ℃. The samples were taken to the dark room and restored to 37 ℃ and then washed with PBS three times. Then, 1:100 FITC-labelled goat anti-rabbit and 1:70 TRITC-labelled goat anti-mouse were added. The samples were then incubated at 37 ℃ for 40 minutes and washed three times with PBS and once with deionized water. The samples were then observed under a laser scanning confocal microscope.

2.6 Morphology studies

2.6.1 Scanning electron microscopy

The surface of the membranes was examined with SEM (Jeol-high field). The samples were dried at room temperature overnight in a fume hood and cut into 10 mm x 10 mm squares and were then observed under a scanning electron microscope (JSM-6360LV) at an accelerating voltage of 20 KV after gold coating (JEOL JFC-1200 fine coater). The diameter of the electrospun fibres was analysed based on 150 randomly selected fibers from the SEM images using image analysis software (ImageJ) the measured

point was labeled with numbers as shown in Figure 2-9. Diameter measurement is shown in Figure 2-9. The scale bar on the SEM image was measured and converted to pixels then the software will calculate the actual distance per pixel. The diameter is measured by drawing cross the nanofiber with straight line tool shown with arrow in Figure 2-9 ,the software will mark how long the line is and convert it to real distance and lable it with numbers as shown in Figure 2-9.

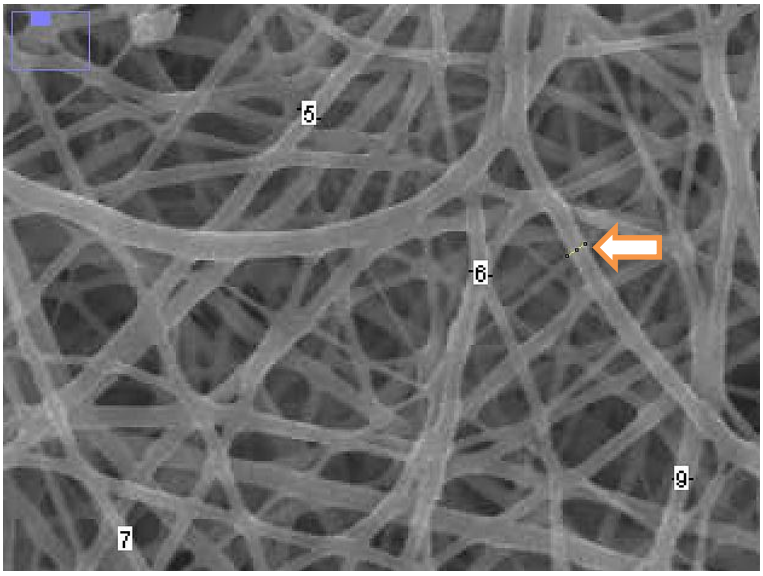

Figure 2-9 Diameter measurement with ImageJ (this is a zoom in image shown the details of the fiber diameter measurement)

2.6.2 Transmission electron microscope

The samples were specially electrospun on TEM copper 400 mesh for 30 seconds to obtain the required thickness for the TEM test. The meshes with different electrospun materials were dried in a fume hood for 8 hours and stored in a TEM sample box. The

samples were then observed under TEM to determine the distribution of CNTs inside the nanofiber. TEM mesh is shown in Figure 2-10.

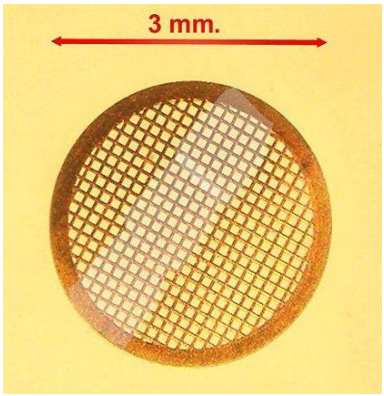

Figure 2-10 TEM mesh

2.7 Mechanical properties of electrospun materials

The mechanical properties of the composite electrospun scaffold were measured using a tensile tester (Instron 5948 universal testing systems). Test material was cut into 10 mm × 50 mm rectangles and then pulled at the speed of 10 mm/minute until broken. The thickness of each test sample was tested by micrometer and input into the tensile tester. Parameters including the Young's modulus, tensile strength and breaking strain were calculated. The experiment set up is shown in Figure 2-11.

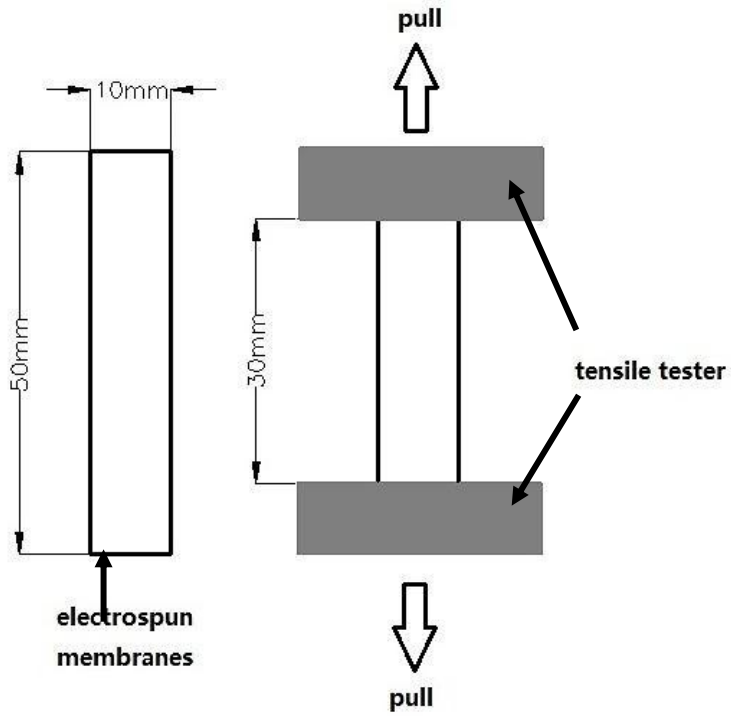

Figure 2-11 Schematic drawing of the tensile test of the electrospun membrane

Tensile testing, also known as tension testing, is a fundamental materials science test in which a sample is subjected to controlled tension until failure. The results of the analysis are commonly used to select a material for an application, for quality control and to predict how a material will react to other types of forces. Properties that are directly measured using a tensile test are ultimate tensile strength, maximum elongation and reduction in area. From these measurements, the following properties can also be determined: Young's modulus, Poisson's ratio, yield strength and strain-hardening characteristics. The most frequent testing machine used in tensile testing is the universal testing machine. This type of machine has two crossheads; one is adjusted for the length of the specimen, and the other is driven to apply tension to the test specimen.

The test process involves placing the test specimen in the testing machine and slowly extending it until it fractures. During this process, the elongation of the gauge section is recorded against the applied force. The data is manipulated so that it is not specific to the geometry of the test sample. The elongation measurement is used to calculate the engineering strain, ε, using the following equation:

$$\varepsilon = \frac{\Delta \mathrm{L}}{\mathrm{L}_0} = \frac{L - \mathrm{L}_0}{\mathrm{L}_0}$$

where ΔL is the change in gauge length, L_0 is the initial gauge length and L is the final length. The force measurement is used to calculate the engineering stress, σ, using the following equation:

$$\sigma = \frac{\mathrm{F}}{\mathrm{A}}$$

where F is the tensile force and A is the nominal cross-section of the specimen. The machine does these calculations as the force increases so that the data points can be graphed as a stress–strain curve.

2.8 Porosity

In this study, the method employed in the research of Abdullah and Khairurrii (Abdullah. M and Khairurrijal, 2009) was used. Origin Pro 8 software was used to calculate the surface porosity from SEM images. SEM images were inserted into Origin 8 and were converted to data using the built-in function. The images were converted to a two-dimensional matrix of grayscale. The elements of the matrix are grayscale value at certain locations (expressed in pixels). The dimension of the matrix is the same as the pixel dimension of the SEM image. The volume of the space beneath the sample's surface can be calculated using the instructions provided by Origin Pro. The surface porosity can then be calculated using equations. Consider that the most interaction between cells and membranes is on the surface level, and the thickness of the membranes is around 100 μm. In this study, the surface porosity is used as equal to the porosity of the whole material.

Porosity or void fraction is a measure of the void (i.e. 'empty') spaces in a material and is a fraction of the volume of voids over the total volume, between 0 and 1, or is a percentage between 0 and 100%. Generally, the surface of the material is not usually flat. It is considered to be flat when the roughness scale is negligibly small compared to a certain length criterion. For example, a porous surface is called flat if the roughness scale is negligibly small compared to porous dimension. In this study, the surface porosity is defined as follows. Consider a surface represented by a function f(x,

y), and this function represents the height of the surface at coordinates x and y measured from a certain base plane, as shown in Figure 2-12.

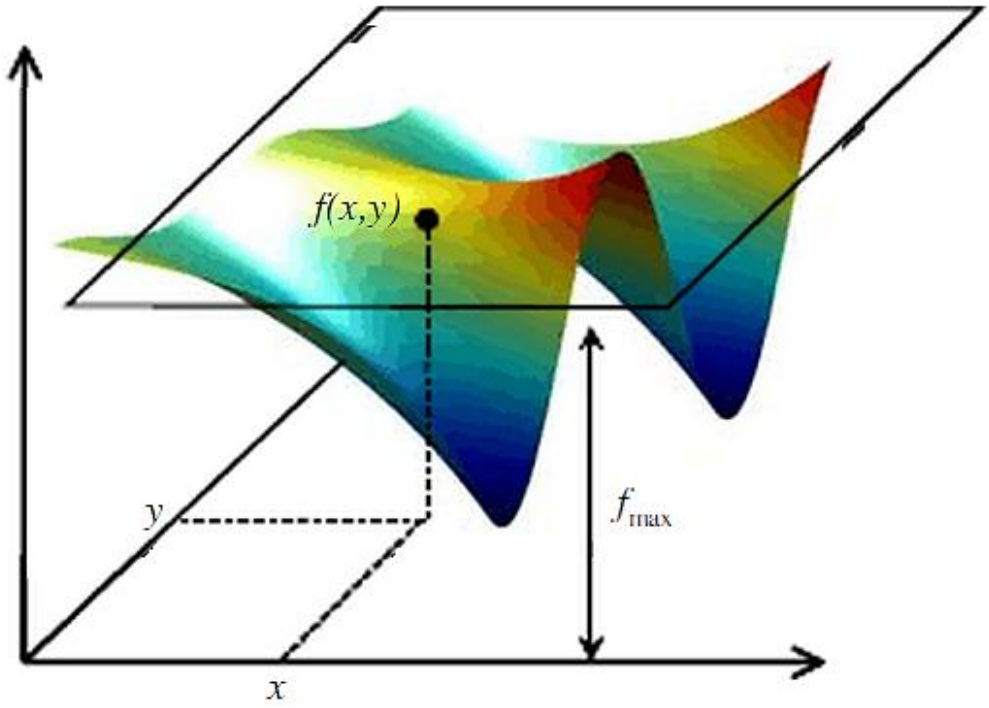

Figure 2-12 Example of the surface of a material and its coordinates

The space beneath the surface is solid material while the space above the surface is empty. The volume of solid material beneath the surface is calculated using the following equation:

$$Vs = \int_{x_{min}}^{x_{max}} \int_{y_{min}}^{y_{max}} f(x,y)\mathrm{dxdx}$$

where Vs is the volume of the solid material beneath the surface, x_{max} and x_{min} are the

boundaries of the surface at coordinate x and y_{max} and y_{min} are boundaries of the surface at coordinate y (the boundaries of the surface when projected at the base plane).

Suppose f_{max} is the maximum height of the surface measured from the base plane at coordinates x and y. A plane parallel was generated to the base plane, where the distance from the base plane is fmax. So the total volume of material when pore is absent from the volume of space beneath the flat surface of height fmax and bounded by min x, max x, min y and max y. The equation of the total volume is as follows:

$$V = f_{max}(x_{max} - x_{min})(y_{max} - y_{min})$$

where V is the total volume of the material's surface layer, and x_{max}, x_{min}, y_{max} and y_{min} are as described before.

The surface porosity is calculated as follows:

$$\emptyset = 1 - \frac{Vs}{V}$$

where $\emptyset$ is the surface porosity of the material, Vs is the volume of solid material beneath the surface and V is the total volume of the material's surface layer.

2.9 Hydrophobicity

The hydrophobicity of the materials was measured by calculating the static contact angles of the water drops on materials. Samples were fixed on the contact angle goniometer (SL200B). Next, 5 μl deionized water was dropped on each sample; the static contact angles were measured at 5 seconds and 30 seconds using the sessile drop method.

Contact angles are extremely sensitive to contamination; values reproducible to more than a few degrees are generally only obtained under laboratory conditions with purified liquids and very clean solid surfaces. If the liquid molecules are strongly attracted to the solid molecules, then the liquid drop will completely spread out on the solid surface, corresponding to a contact angle of 0°. This is often the case for water on bare metallic or ceramic surfaces. Generally, if the water contact angle is smaller than 90°, the solid surface is considered hydrophilic, and if the water contact angle is greater than 90°, the solid surface is seen as hydrophobic. Many polymers exhibit hydrophobic surfaces. Highly hydrophobic surfaces made of low surface energy (e.g. fluorinated) materials may have water contact angles as high as approximately 120°. Some materials with very rough surfaces may have a water contact angle even greater than 150° due to the presence of air pockets under the liquid drop. These are called superhydrophobic surfaces.

The contact angle goniometer uses an optical system to capture the image of pure liquid on a solid substrate. The angle formed between the liquid/solid interface and the liquid/vapour interface is the contact angle. The contact angle goniometer will gather the distance between the vertex and surface h and the cross range of the water drop on the surface 2r to calculate the contact angle θ. The measurement and equation are shown in Figure 2-13.

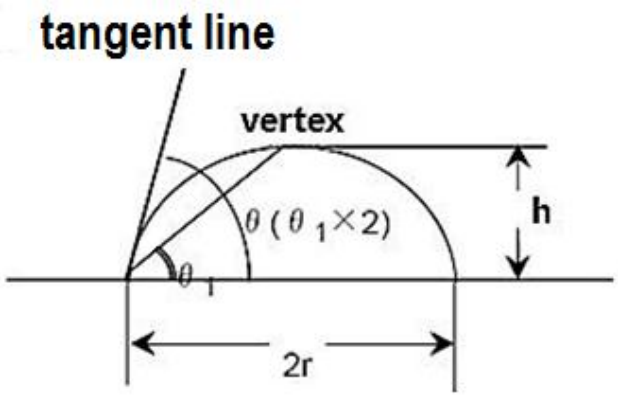

Figure 2-13 Schematic drawing of contact angle measurement

$$\tan\theta 1 = \frac{h}{r}$$

where θ is the contact angle. If the drop shape is part of a circle then mathematically θ=2×θ1, and h is the distance from the surface to the measured vertex. The contact angle can then be calculated using the following equation:

$$\theta = 2 \times \tan e^{-1} \frac{h}{r}$$

2.10 Statistical analysis

Data is presented as mean±SD obtained from independent experiments. Statistical analysis was performed using Origin 8 software and analysis of variance (ANOVA). Differences were considered statistically significant if $P<0.05$. The * sign is used in images represent that there is statistical difference between two groups. The ns sign is used to represent that there is no statistical significance.

3. Development and biocompatibility of crosslinked protein membranes

3.1 Introduction

The crosslinked membranes in microfluidic channel shows fascinating potential in tissue engineering research. This method could be widely used in various research applications such as cell culture, microbioreactor, biochemistry and molecular biology. Particularly, a microbioreactor with a suitable membrane could be an ideal device for neural tissue engineering study due to its micro size and highly controllable environment. Though, the mechanical and physical properties of the crosslinked membranes have been studied, the biocompatibility of the membranes are another important figure for tissue engineering study.

The aim of this study was to develop a technique to manufacture a suitable crosslinked protein membrane to fulfil the needs of cell culture experiments and to discover the potential biocompatibility of the crosslinked protein membranes. In this study, both sides of two kinds of crosslinked protein membranes were manufactured using a simplified method. The morphology of membranes was revealed with scanning electron microscope. PC12, ADSCs and primary cortical neurons from SD rats were cultured on the membranes. The biocompatibility of the membranes was evaluated by using Cell Counting Kit-8, and the OD value was measured at 490 nm.

3.2 Results

3.2.1 Different side of crosslink membrane has different morphology

A membrane has two sides. Based on the formation of the crosslinked membranes, the side that faces the BSA solution is called the organic side and the other side is called the chloride side due to the nature of the crosslinker. As shown in Figure 3-1, the organic sides and chloride sides of membranes have very different morphologies. The organic sides of membranes have rough and uneven surfaces, and the chloride sides have fairly flat surfaces. Between two different crosslinkers, the organic side of TCL membranes showed more porous structure and bigger bulge than the organic side of IDCl membranes. The chloride side of TCL membranes has more porous structure than the chloride side of IDCl membranes and seems to have smoother surface.

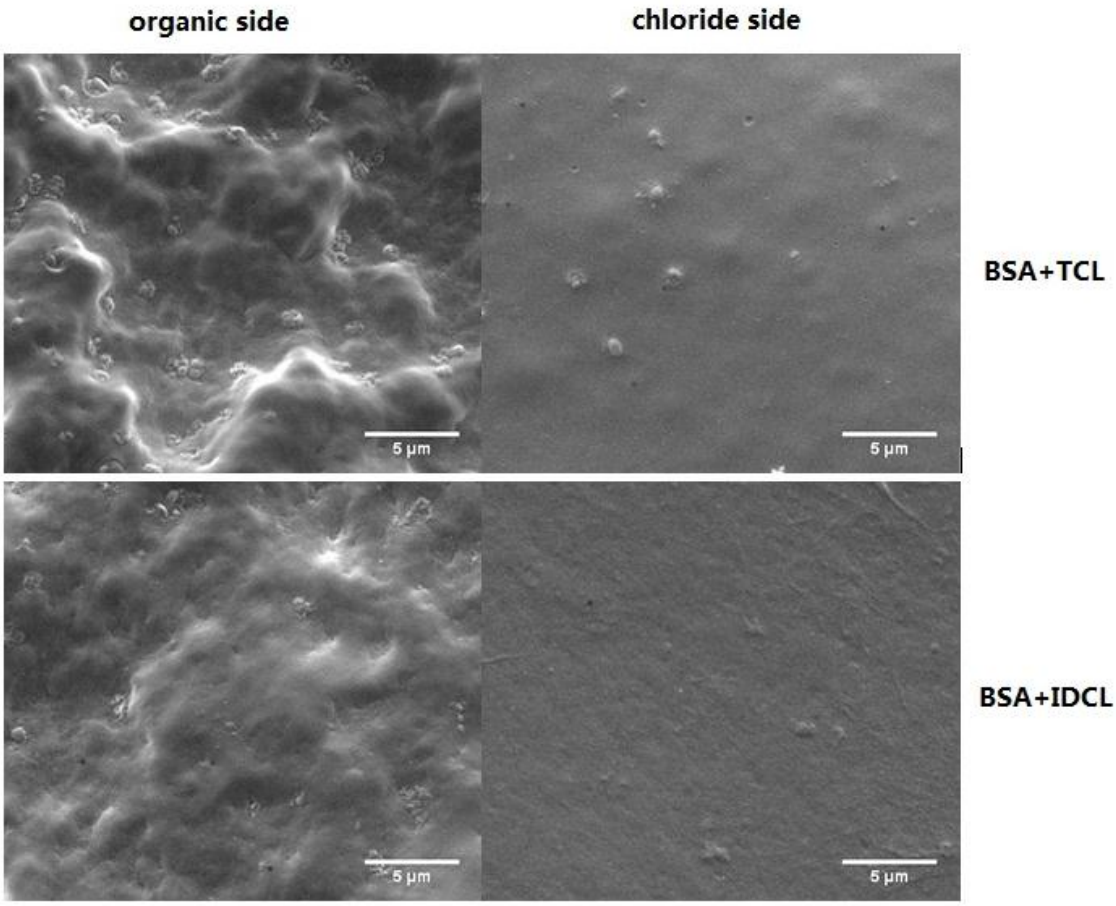

Figure 3-1 Different sides of crosslinked membranes under a SEM

3.2.2 The organic side shows better biocompatibilities than chloride side

PC12 and ADSCs were cultured on membranes for 8 days. As seen in Figure 3-2, the results show that at 8 hours, the control group had the highest cell viability and the two chloride sides had the lowest cell viability. Based on this result, after seeding, the control group had better cell attachment and a better survival rate than the membranes. In the first 4 days, PC12 grew faster in the control groups than on membranes. After 4

days of culturing, the growth of cells on membranes slowed down, but the cells in control groups grew rapidly. The cells in the control groups reached the maximum cell viability at day 4, which is much higher than the cell numbers on membranes. Between membranes, the two chloride sides reached the maximum cell viability at day 6, but cells on the two organic sides kept growing until day 8. Considering the previous results, the organic sides also have better cell survival rates than the chloride sides. According to the results of cell culture, the organic sides of the membranes showed better biocompatibility than the chloride sides. As shown in Figure 3-6, similar to PC12, at day 2 ADSCs in the control group had the highest cell viability compared to the two organic sides, and the two chloride sides had the lowest cell viability. However, cell growth on membranes reached maximum viability at day 4, two days earlier than the control group. However, the maximum cell viability in the control group almost doubled compared to the membranes. Also, between membranes, cells growing on the organic sides showed better survival rate and maximum cell viability.

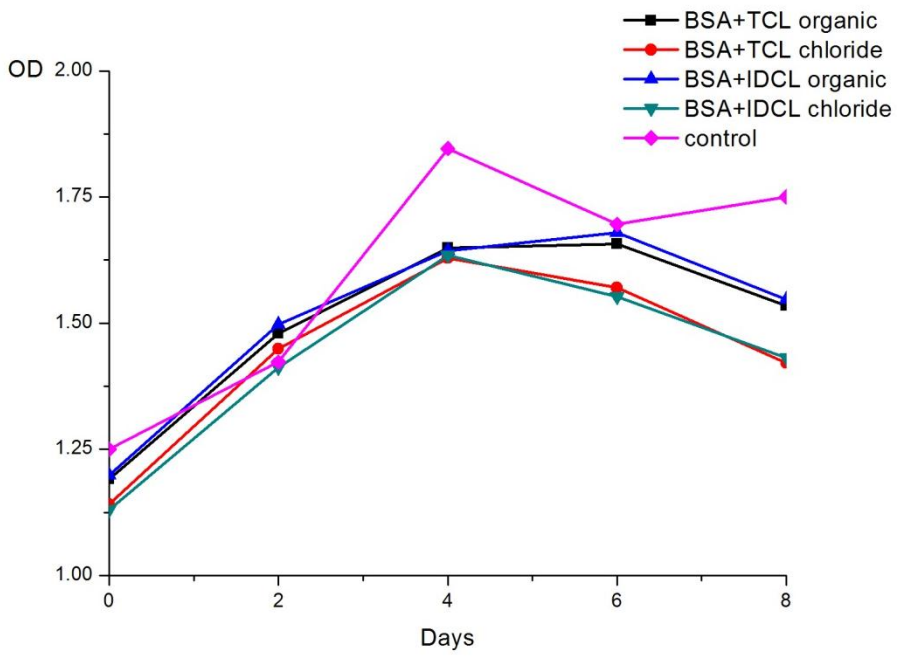

Figure 3-2 Cell growth curve of PC12 on different crosslinked protein membranes

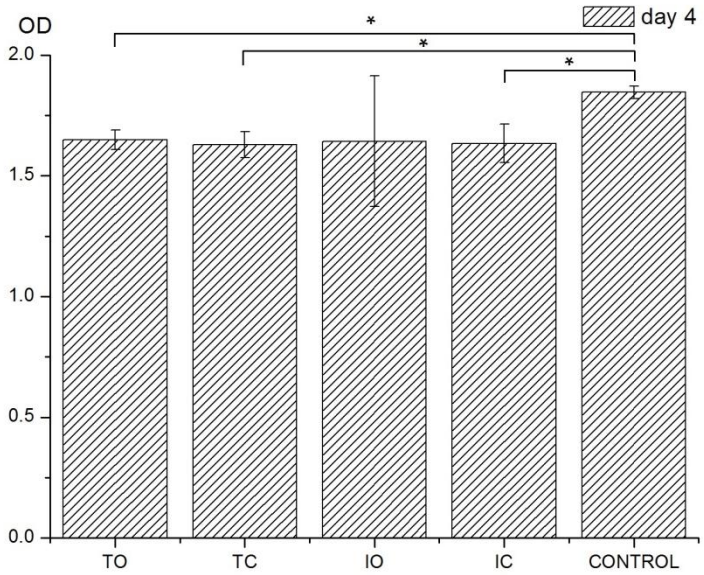

Figure 3-3 OD value of PC12 on membranes at day4 (TO: BAS with TCL organic side, TC: BAS with TCL chloride side, IO: BSA with IDCL organic side, IC: BSA with IDCL chloride side)

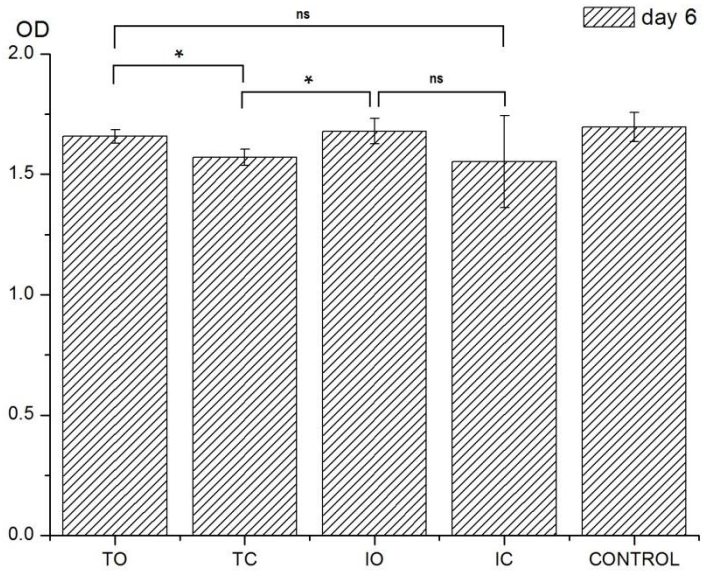

Figure 3-4 OD value of PC12 on membranes at day6 (TO: BAS with TCL organic side, TC: BAS with TCL chloride side, IO: BSA with IDCL organic side, IC: BSA with IDCL chloride side)

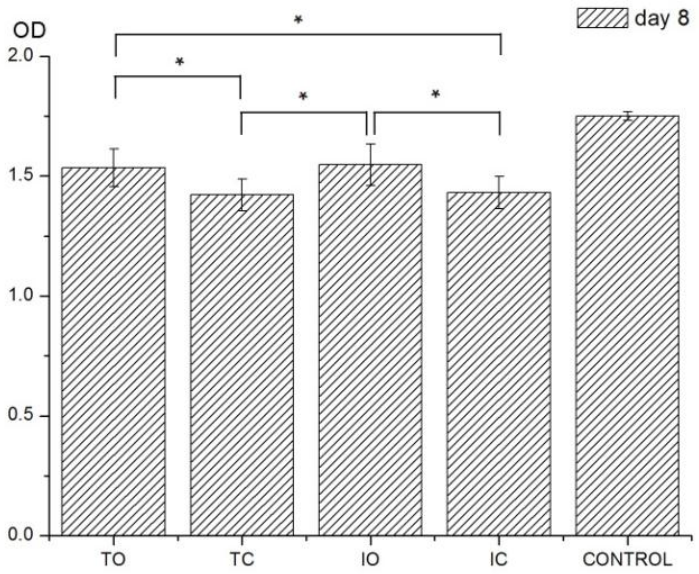

Figure 3-5 OD value of PC12 on membranes at day 8 (TO: BAS with TCL organic side, TC: BAS with TCL chloride side, IO: BSA with IDCL organic side, IC: BSA with IDCL chloride side)

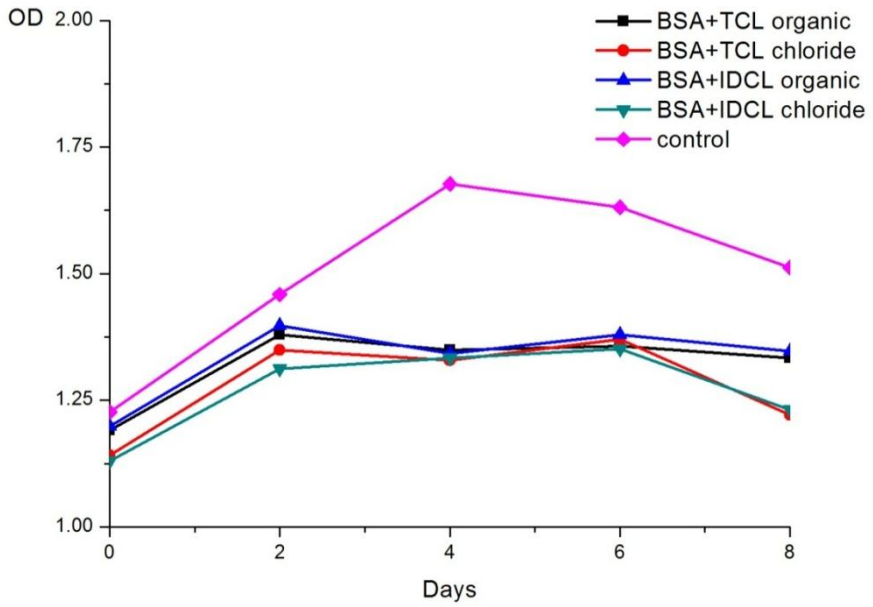

Figure 3-6 Cell growth curve of ADSCs on different crosslinked protein membranes

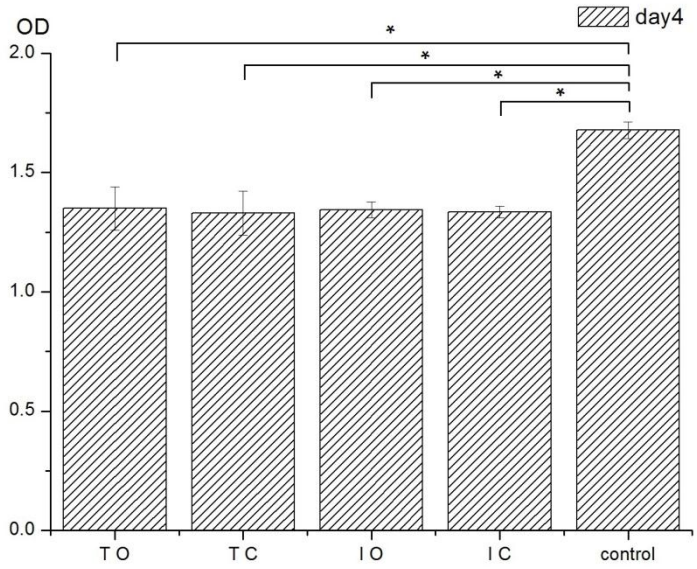

Figure 3-7 OD value of ADSCs on membranes at day4 (TO: BAS with TCL organic side, TC: BAS with TCL chloride side, IO: BSA with IDCL organic side, IC: BSA with IDCL chloride side)

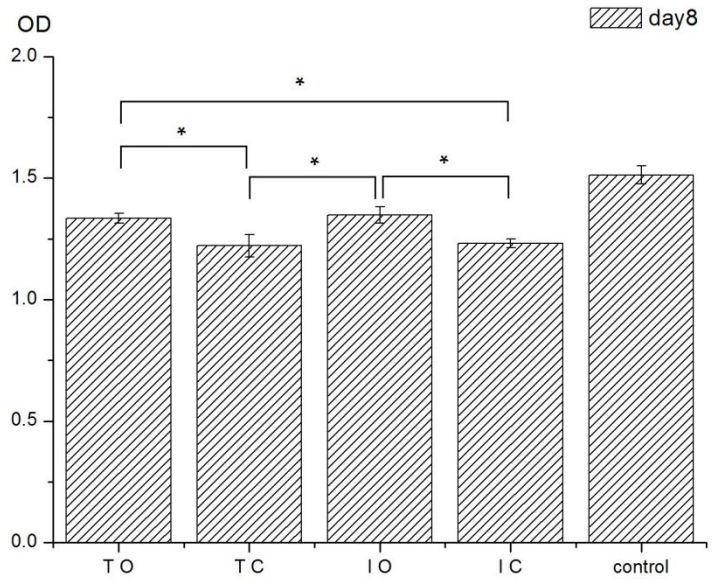

Figure 3-8 OD value of ADSCs on membranes at day 8 (TO: BAS with TCL organic side, TC: BAS with TCL chloride side, IO: BSA with IDCL organic side, IC: BSA with IDCL chloride side)

3.3 Discussion

3.3.1 The morphology difference of membranes

The organic and chloride sides of the membranes have different morphologies, as shown in Figure 3-1. This was consistent with previous findings of asymmetric membranes with interfacial formation and bulk structure. In bulk interfacial polymerization, a microporous support membrane is typically used to provide an interfacial barrier that allows the transport of monomers only by diffusion. The smooth surface is formed because of the smooth interface between the two flows due to the laminar flow. At the beginning of the protein and chloride crosslinking, the reaction is rapid and leads to a smooth surface. After the quick formation of a smooth membrane skin, during the initial reaction, a rate-limiting barrier for the transport of the chloride from the organic side into the protein solution was inhomogeneity, formed the random porosity and native membrane structure of this membrane, so possibly the solute diffused unevenly. Also, the morphology of the membrane becomes asymmetric, as shown in Figure 3-9. Moreover, the structure difference of the two crosslinkers may be due to their different chemical structure (Figure 1-4). The different angle of chemical bonds could lead to different chain structures according to the crosslinked reaction.

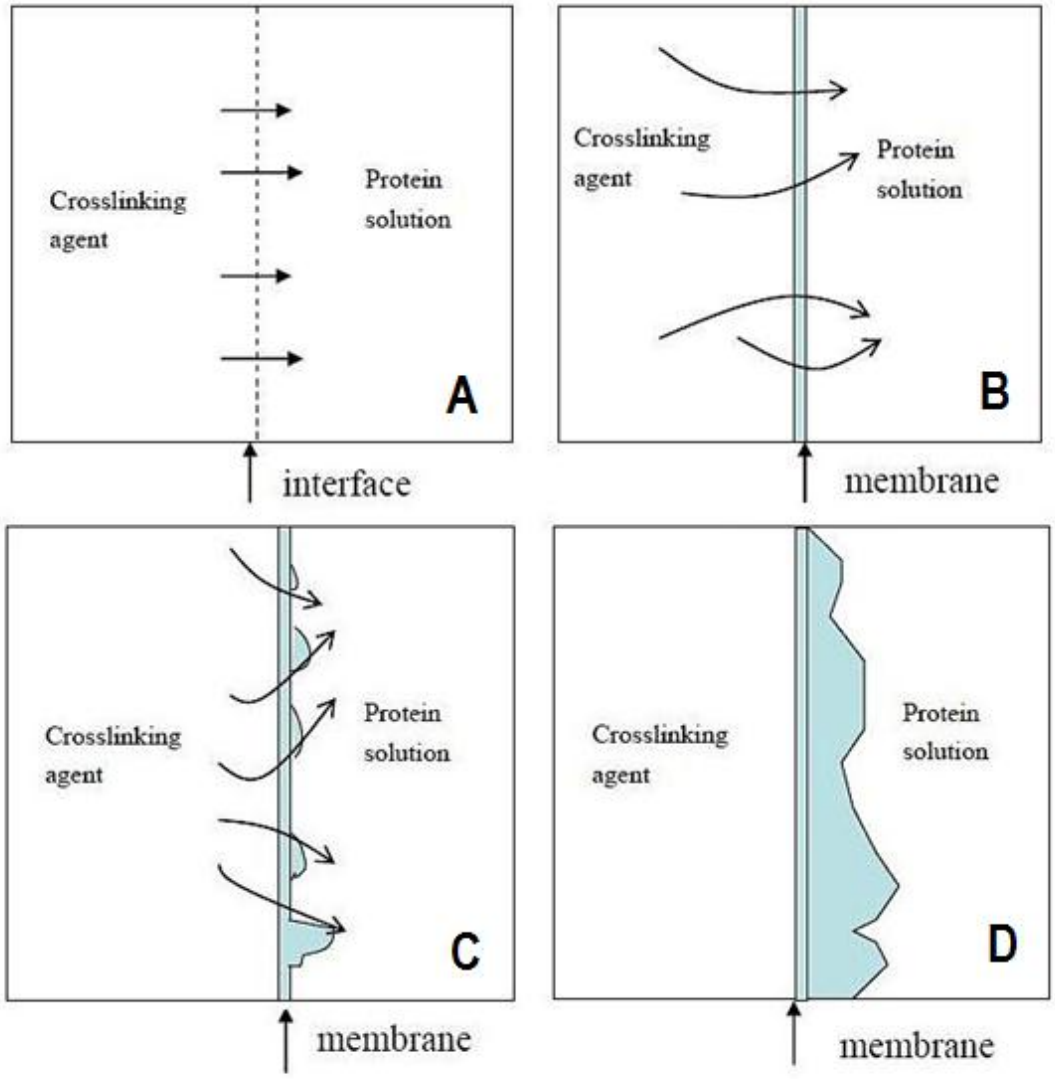

Figure 3-9 Schematic drawing of the progress of membrane formation (arrows show the flow direction of the crosslinking agent)

3.3.2 The biocompatibility difference of membranes

Research has indicated that the morphology of the scaffold material could significantly affect the proliferation, migration and even the differentiation of many kinds of cells. Some research shows that electrospun materials provide enhanced biocompatibility due to the similar structure of the extracellular matrix. Other studies report that micro-patterns on scaffold material could confine single cells, allowing cells to be manipulated in various ways, such as apoptosis, the control of cell–cell architecture, cell internal organization and cell division axis.

Based on the nature of the crosslinking reaction, the protein and crosslinker molecules re-establish new chemical bonds with each other and link one to another like a chain, so in a molecular view there should not be any chemical difference between two sides of membranes. Therefore, the biocompatibility difference could only be caused by the morphology of the membranes.

The 3D structure of the organic side could provide better cell attachment and more space for cell proliferation. Based on Figure 3-2 and Figure 3-6, the chloride sides had lower cell viability from the beginning and maintained the same trend as the organic sides. Therefore, the OD difference between the organic and chloride sides is not statistically significant. Combined with the former conjecture, the morphology of organic sides provides more cells at the beginning so the cells on the chloride sides

could not outgrow them. In addition, the organic sides have a little more space for cell growth, which explains the higher maximum cell viabilities.

Due to the fast evaporation of the xylene solvent, it is possible that residual TCL or IDCL crystals were left on the chloride side, which will induce cytotoxicity in the membranes. These residuals might not be washed off in the membrane preparation process because they could be buried inside the membranes during the crosslink reaction and would have negative effect with the culture medium.

As previously mentioned, the crosslinked membranes were made on glass cover slips and were moved into the 24-well plate later Therefore, the membranes have to be smaller than the well to become manoeuvrable during the process. Thus, during cell culture experiments there will be cells that grow outside the membranes. When the CCK-8 is used, the cell from outside will join in the reaction and contribute to the results. Considering the fact that the control group tended to have better biocompatibility than on the membranes, the actual cell numbers on full membranes should be a little lower than shown in the results.

3.3.3 Standard curves of CCK-8 experiments

In the biocompatibility research of PC12 and ADSCs, CCK-8 was used to indicate the cell viability on membranes. Instead of cell numbers, OD values were used because based on the principle of CCK-8, OD values were the properties that were actually measured and the only way to link OD value to cell numbers is to use a standard curve.

A standard curve is used to determine the relationship between cell numbers and OD values. Multiple samples with known cell numbers are measured and graphed, which then allows the unknown cell numbers to be determined by interpolating measured OD values on the graph. However, there are many aspects that could affect the measurement of OD values, for instance, different culture mediums, drugs and cell conditions.

Firstly, culture mediums or drugs that contain metal ions, such as lead chloride, ferric chloride and cupric sulfate, will suppress the chromogenic reaction, leading to decreased accuracy of the experiment. The culture medium used for PC12 cell culturing is Dulbecco's Modified Eagle Medium (DMEM), which contains 0.1 mg/L ferric nitrate hydrate. Therefore, the OD value will be slightly lower than it should be because of the suppression of the chromogenic reaction.

Secondly, because the OD value depends on light absorption, different culture mediums will have different blank absorption values. This means the culture medium itself will absorb a portion of light; for example, IMDM has blank absorption of about 1 and McCoy's medium has blank absorption of about 0.3. To get accurate cell numbers from OD values, blank absorption values is also a key feature that need to be considered.

Thirdly, reductants and oxidants will change the OD values; reductants will increase the OD value and oxidants will decrease the OD value. In this case, the membranes were not degradable but the residual of IDCL and TCL could have affected the result.

Lastly, the conditions of cells will also affect the measurement. Suspension cells tend to have lower OD values than the cells that already attached. Also, the cells in the logarithmic growth phase and the stationary phase will have different effects on OD value due to the different dehydrogenase activity in these stages. The dehydrogenase will react with CCK-8 and release formazan, which is source of light absorption.

Theoretically, there is a linear relationship between the OD values and cell numbers but in this case the standard curve isn't linear the result is affect by many aspects. In summary, the cell number data is obtained by combine the OD data and standard curve data together so it suffered the errors from both experiments, based on the reasons

mentioned before, OD values were used instead of cell numbers because otherwise there is no advantage but only an increase in errors. Furthermore, because of the crosslinked protein, membranes have difficulty fitting in 96-well plates and electrospun materials have difficulty fitting in 24-well plates. The comparison between the two kinds of materials with cell numbers is not necessary, even if all the materials can fit. Many different conditions of these two experiments are inevitable and will dramatically decrease the accuracy of the result.

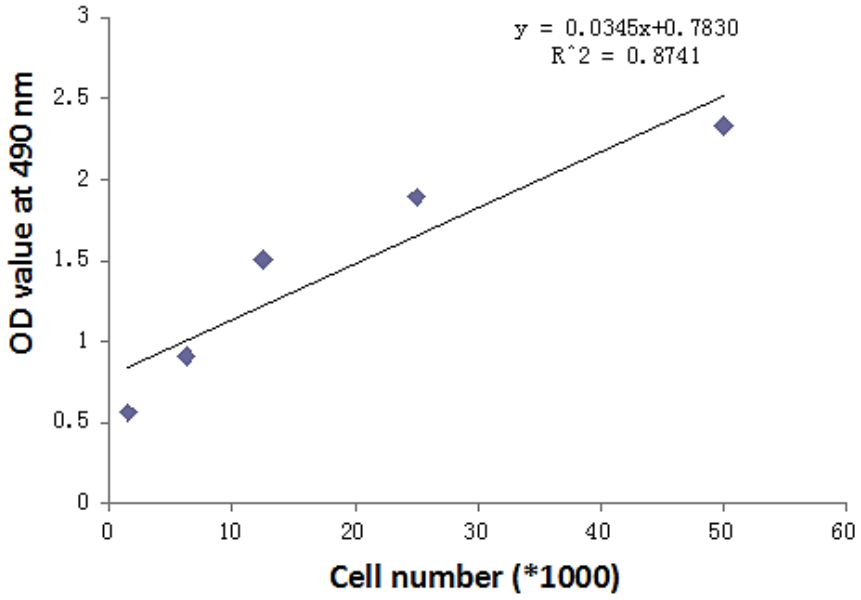

Figure 3-10 Standard curve of ADSCs

4. Effect of CNTs and silk fibroin on electrospun PLGA membranes

4.1 Introduction

PLGA is a popular material in tissue engineering applications due to its controllable and low toxic degradation ability. The electrospinning technology could provide PLGA materials better morphology that similar to the natural ECM environment which will lead to a better biocompatibility in cell culture applications. The PLGA electrospun materials could also be enhanced with many other materials, collagen for example, which has benefit on cartilage tissue engineering. Other materials like CNTs and silk materials are both reported to have advantages in neural tissue engineering study (G.H. Altman, 2003, Mottaghitalab, 2013). Therefor CNTs and silk could be a great add to the PLGA electrospun materials for neural tissue engineering research.

The aim of this study was to discover and develop the technology of manufacturing PLGA composite electrospun materials and to investigate the governing mechanisms and associated properties of these materials. In this study, electrospun PLGA membranes, PLGA, CNTs and SF composite membranes were manufactured. The

physiochemical properties and biocompatibility of the electrospun membranes were investigated.

4.2 Results

4.2.1 CNTs and silk fibroin change the morphology of electrospun PLGA membranes

As shown in Figure 4-1, all four kinds of materials have smooth and clean nanofiber structures. The introduction of SF increased the diameter of nanofibers.

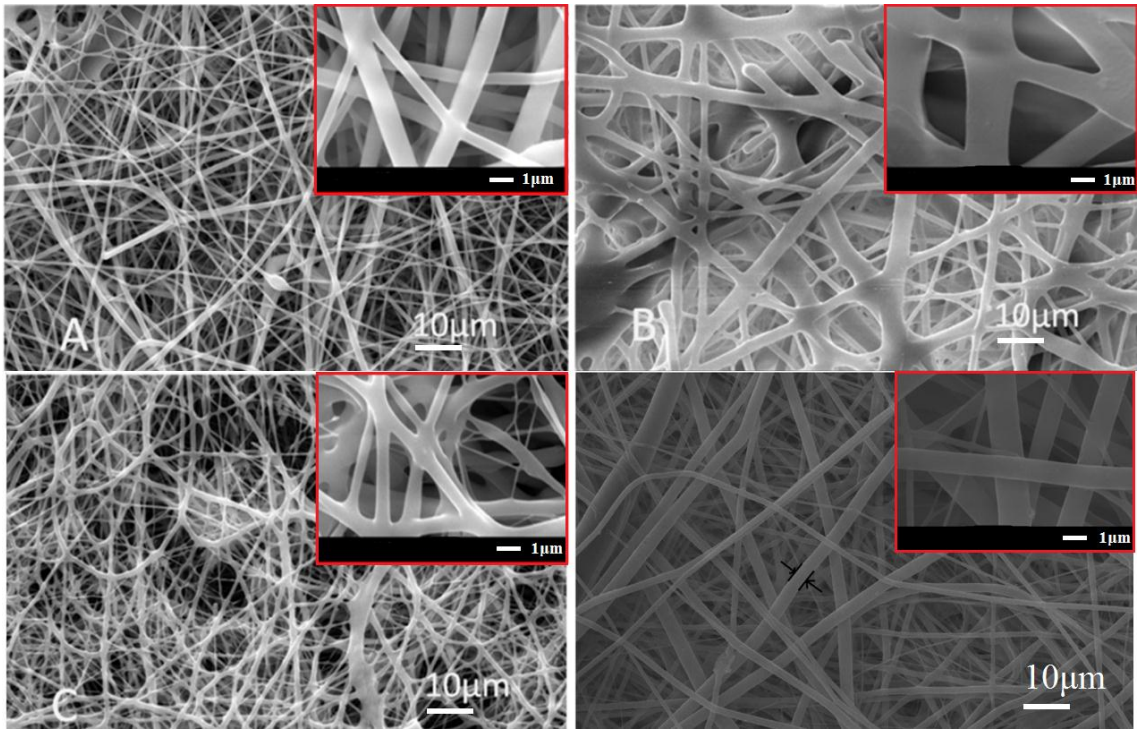

Figure 4-1 SEM images of different composite scaffolds (A: PLGA; B: PLGA and silk fibroin; C: PLGA and CNTs; D: PLGA and SF and CNTs)

4.2.2 CNTs and silk fibroin change the mechanical properties of electrospun

PLGA membranes

The Young's modulus for each electrospun material appears in Figure 4-2. With the introduction of CNTs, the Young's modulus of the material increased about 50 MPa, which is almost one-third of the original PLGA material. However, the Young's modulus of the material that was added with SF was significantly decreased, even though the material was enhanced with both CNTs and SF.

The tensile strength of the electrospun materials is shown in Figure 4-3. The tensile strength of the material enhanced with CNTs almost tripled compared to the PLGA material. The introduction of SF decreased the tensile strength of the materials.

The breaking strain of the materials is shown in Figure 4-4. This property shares the same trend as the Young's modulus and tensile strength. However, the breaking strain of the material that added with SF decreased dramatically, making the membranes extremely easy to break. In summary, adding CNTs to PLGA will increase the material's mechanical properties and adding SF will decrease the mechanical properties.

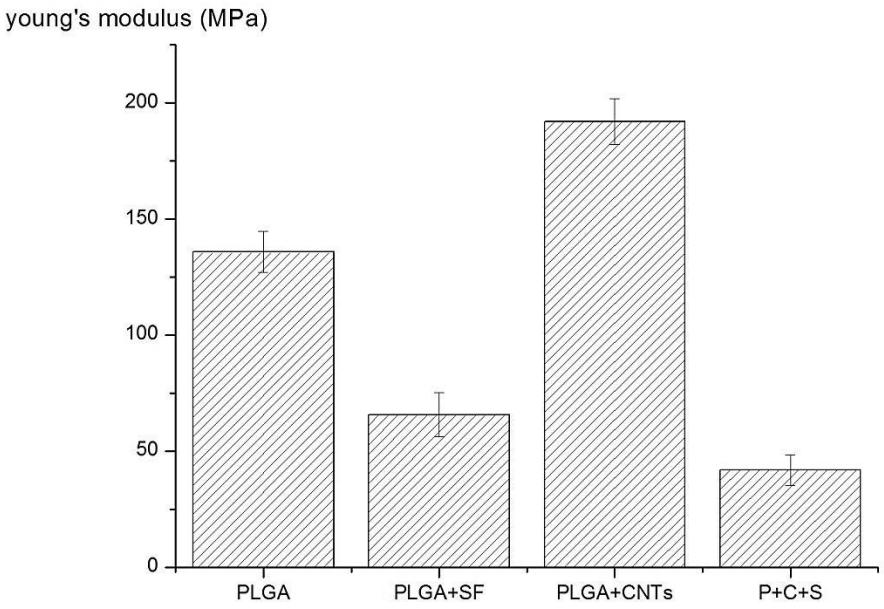

Figure 4-2 Young's modulus of different composite materials (P+S+C: PLGA and silk fibroin and CNTs)

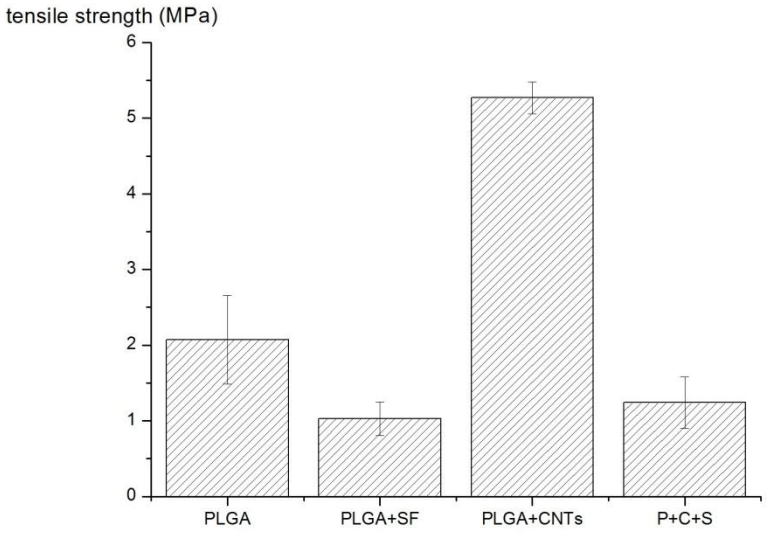

Figure 4-3 Tensile strength of different composite materials groups (P+S+C: PLGA and silk fibroin and CNTs)

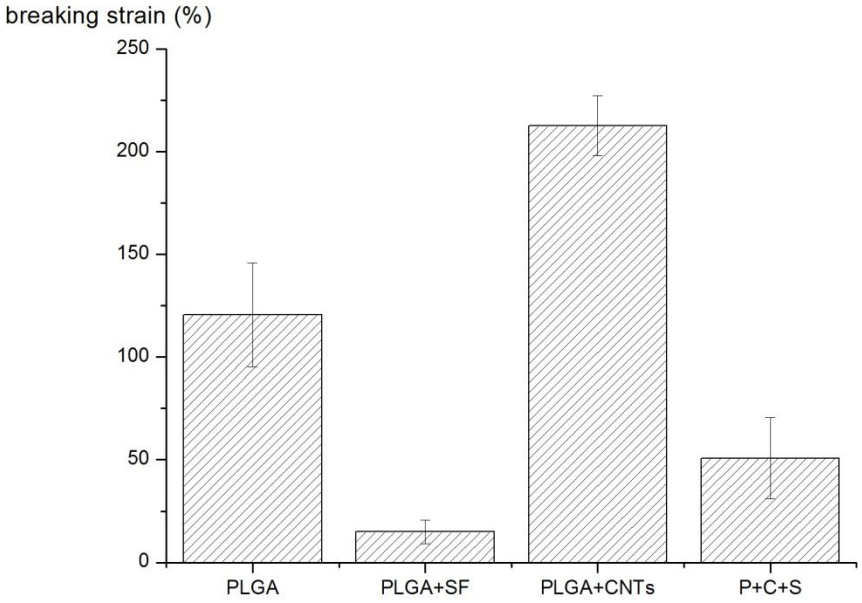

Figure 4-4 Breaking strain of different composite materials (P+S+C: PLGA and silk fibroin and CNTs)

4.2.3 CNTs and silk fibroin increase the hydrophilicity of electrospun PLGA membranes

The hydrophobicity of the material was measured by calculating the static contact angle of water on the electrospun materials. According to the results shown in Figure 4-5, the 120 ° contact angle at 5 seconds and the approximate 100 ° contact angle at 30 seconds indicate that PLGA electrospun material is fairly hydrophobic. According to the results, the addition of CNTs slightly decreased the contact angle to 80 °, increasing the hydrophilicity of the material. However, with the addition of SF, the contact angle at 5 seconds decreased substantially to about 20 °. Moreover, both materials with SF were able to absorb the water entirely within 30 seconds.

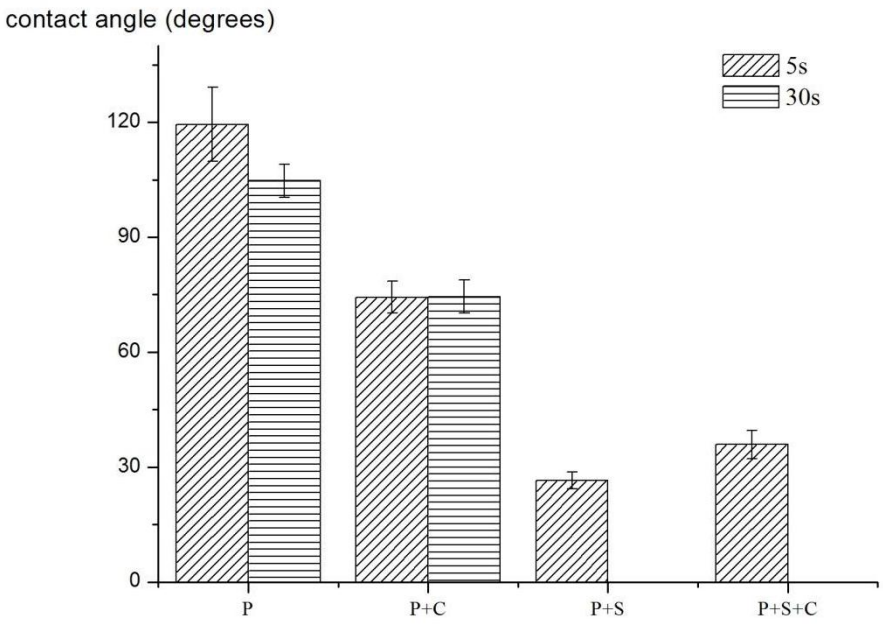

Figure 4-5 Hydrophobicity of different composite nanofibre scaffolds (P: PLGA C: PLGA and CNTs S: PLGA and SF PCS: PLGA and SF and CNTs)

4.2.4 CNTs and silk fibroin increase the biocompatibility of electrospun PLGA membranes

PC12 and ADSCs were cultured on electrospun material for 8 days. The PC12 cell growth curve is shown in Figure 4-6. The lag phase of PC12 is one day. Day 1 to day 3 is the log phase in which cells grow rapidly before entering the stationary phase in which the cells stay at a certain number. The result shows that the control group always had the highest cell numbers compared to the other four materials until day 7. The log phase of cell growth lasted about 3 days before reaching maximum cell viability at day 5. After day 5, the cell viability dropped rapidly, except for the two materials that were enhanced with SF. Based on this result, after seeding the control group shows better cell attachment and better survival rate compared to the electrospun materials; however

the materials that had SF added showed better biocompatibility in terms of maintaining cell proliferation. ADSCs were cultured on electrospun materials; the cell growth curve is shown in Figure 4-10. For ADSCs, the materials enhanced with SF showed even better biocompatibility from the beginning, but cell viability decreased significantly and stopped dropping on day 1 before the log phase. Similarly, ADSC viability in the control group started to fall from day 5; however, cells grown on electrospun material were able to maintain in the stationary phase.

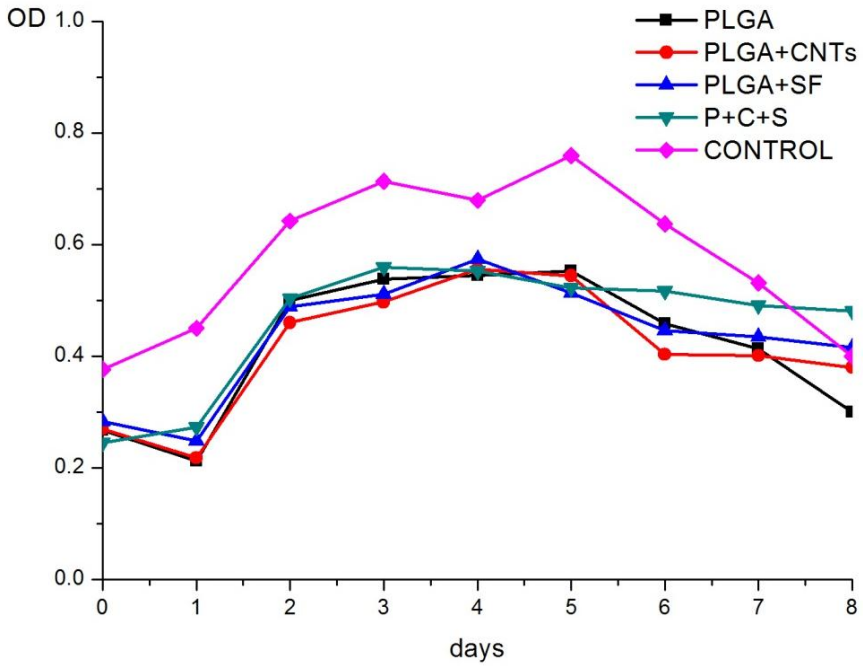

Figure 4-6 Cell growth curve of PC12 grown on different composite nanofibre scaffolds

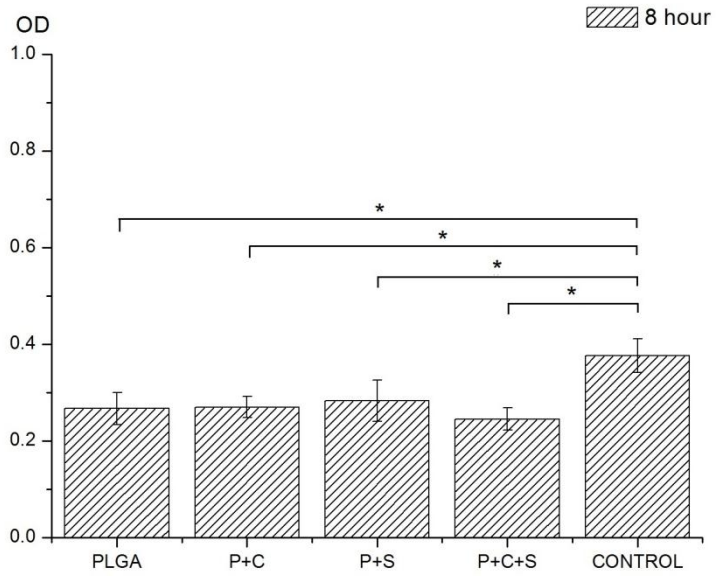

Figure 4-7 PC12 on different composite nanofiber scaffolds at 8 hours (P+C: PLGA and CNTs; P+S: PLGA and silk fibroin; P+S+C: PLGA and silk fibroin and CNTs)

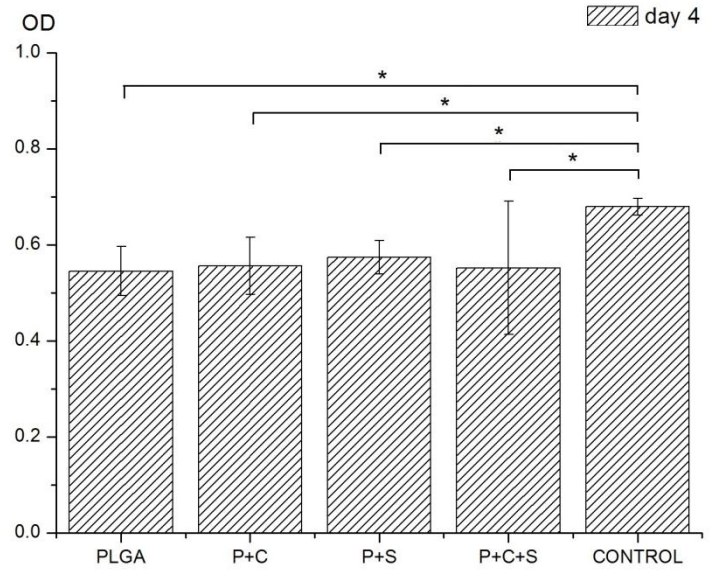

Figure 4-8 PC12 on different composite nanofiber scaffolds at day 4 (P+C: PLGA and CNTs; P+S: PLGA and silk fibroin; P+S+C: PLGA and silk fibroin and CNTs)

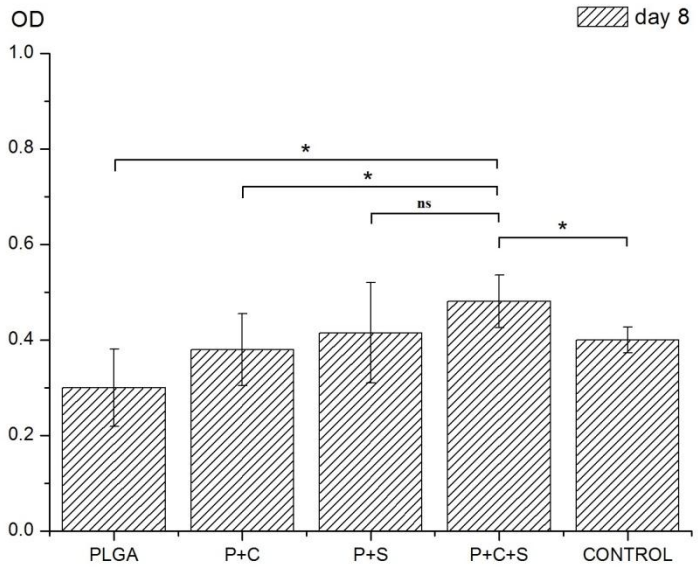

Figure 4-9 PC12 on different composite nanofiber scaffolds at day 8 (P+C: PLGA and CNTs; P+S: PLGA and silk fibroin; P+S+C: PLGA and silk fibroin and CNTs)

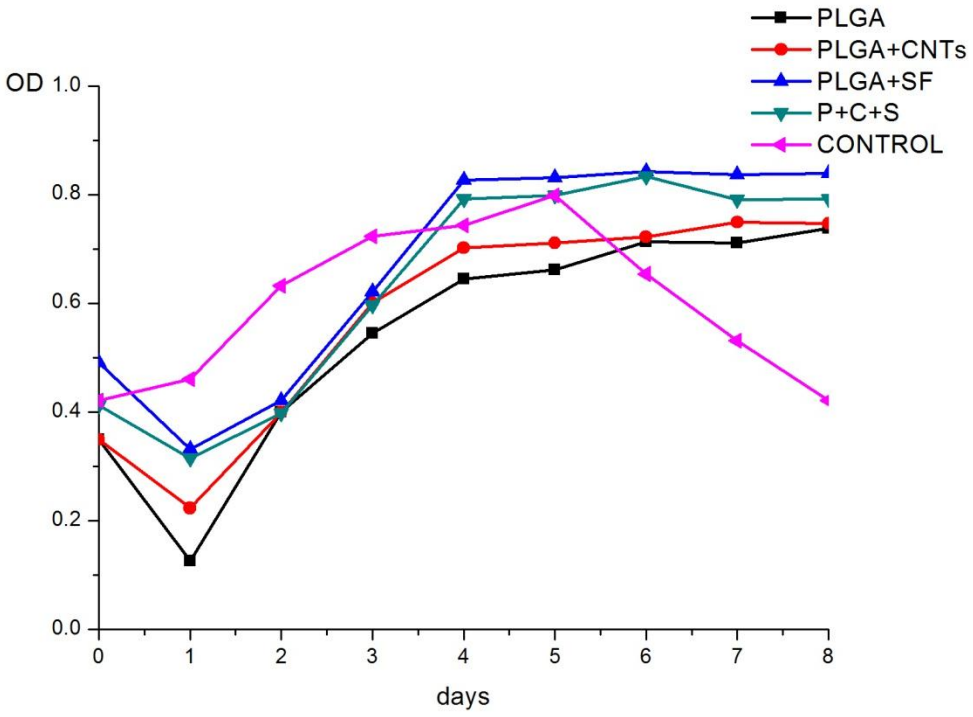

Figure 4-10 Cell growth curve of ADSCs grown on different composite nanofibre scaffolds

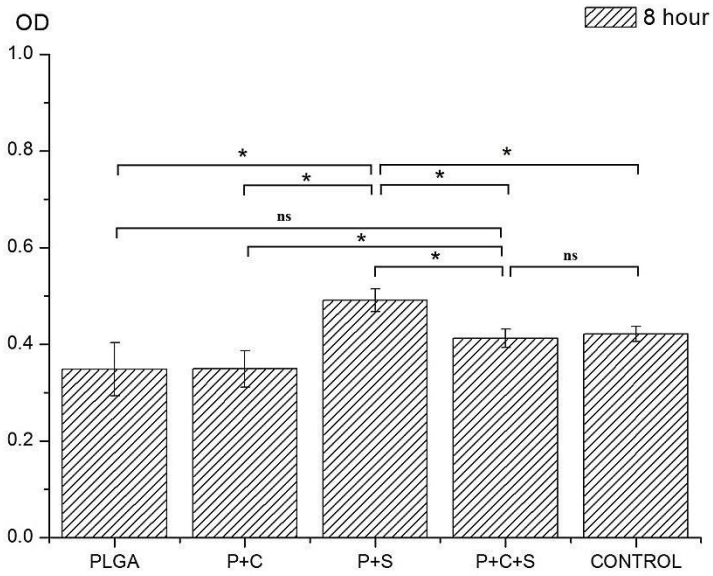

Figure 4-11 ADSCs grow on different composite nanofiber scaffolds at 8 hours (P+C: PLGA and CNTs; P+S: PLGA and silk fibroin; P+S+C: PLGA and silk fibroin and CNTs)

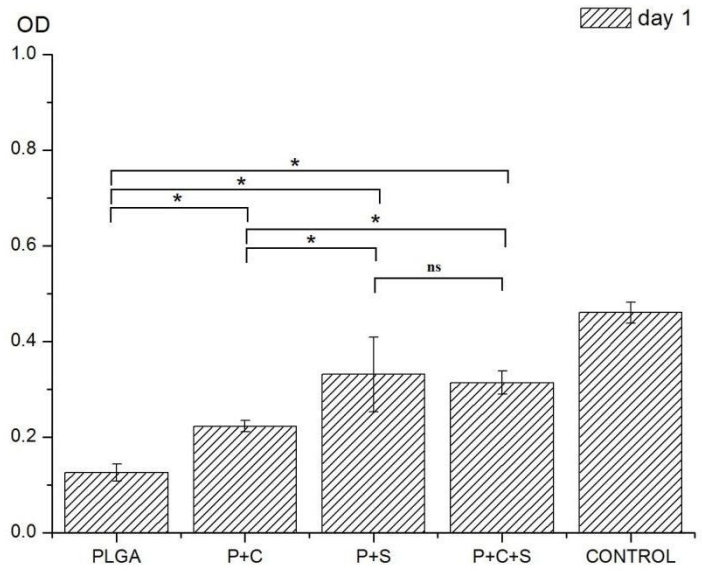

Figure 4-12 ADSCs grow on different composite nanofiber scaffolds at day 1 (P+C: PLGA and CNTs; P+S: PLGA and silk fibroin; P+S+C: PLGA and silk fibroin and CNTs)

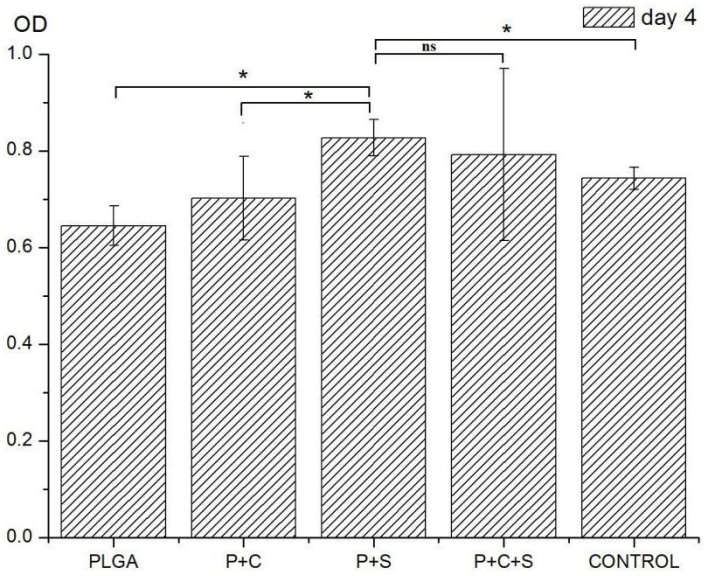

Figure 4-13 ADSCs grow on different composite nanofiber scaffolds at day 4 (P+C: PLGA and CNTs; P+S: PLGA and silk fibroin; P+S+C: PLGA and silk fibroin and CNTs)

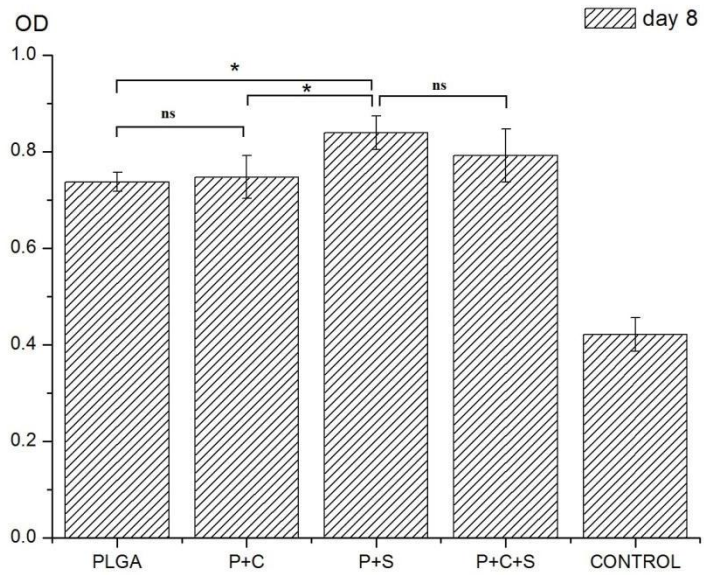

Figure 4-14 ADSCs grow on different composite nanofiber scaffolds at day 1 (P+C: PLGA and CNTs; P+S: PLGA and silk fibroin; P+S+C: PLGA and silk fibroin and CNTs)

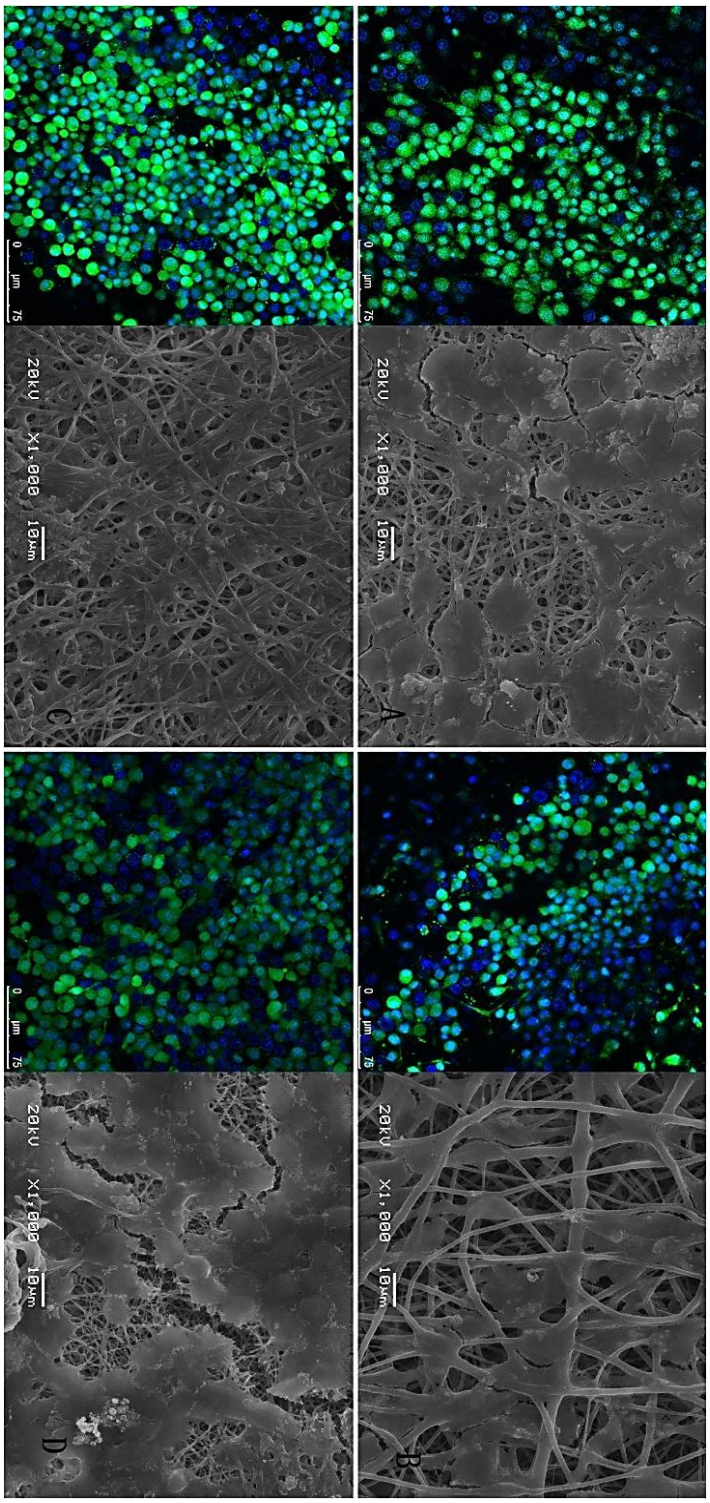

Figure 4-15 laser scanning confocal microscope images and SEM images of PC12 cells grow on scaffold at day 4. (A: PLGA; B: PLGA+CNTs; C: PLGA+ Silk; D: PLGA+CNTs+Silk)

4.3 Discussion

4.3.1 The effect of enhancing material on biocompatibility

Much of the research indicates that SF as a natural protein material has great biocompatibility and excellent hydrophilicity. Thus, materials enhanced with SF will give the composite material better cell attachment ability and biocompatibility.

The present study suggests that PLGA is a potential scaffold for nerve tissue engineering and predicts the orientation and growth of nerve stem cells on the scaffold (Bini et al., 2006).

CNT materials have been reported to have excellent biocompatibility for osteocyte cells due to their superior mechanical properties. Some research indicates that CNTs will benefit neuron cell cultures because the electro-conductivity will stimulate neuron growth and neural differentiation. Therefore, enhancing with CNTs will bring the composite materials better biocompatibility for neuron culturing.

4.3.2 The effect of materials' degradation on biocompatibility

As mentioned previously, the oxidizing agent will decrease the OD value during the CCK-8 test. Unfortunately, the main material used in electrospinning is PLGA, which is a degradable material. The degradation products lactic acid and glycolic acid are

oxidizing agents. According to the resultsFigure 5-8, the PH drop of the electrospun material is exceptionally fast in the first few days; however, the degradation progress will slow down significantly afterwards. Thus, with the change of culture medium the acid environment will adjust to normal. A benefit of degradation is that the pore size of the material will increase and provide more space for cell proliferation.

According to the results, the overall cell viability of PC12 on electrospun membranes was much lower than in the control group. However, the cell viability of ADSCs on electrospun membranes tells a different story and even showed better biocompatibility than in the control group during a later culture period. This is because PC12 is more sensitive to the acid environment, so the degradation of materials will affect PC12 more than ADSCs.

5. Effect of different CNT concentrations on electrospun PLGA membranes

5.1 Introduction

The previous study have revealed that the addition of CNTs to PLGA materials not only give the composite materials the ability to inhabit neurons but there also is a relationship between CNTs concentration in PLGA electrospun materials and the biocompatibility of composite materials for primary cortical neurons and neuroglia cells. Unlike silk material which is natural protein material that can provide good biocompatibility just by itself, the CNTs are single element nanotubes, the cellular responds of CNTs and neurons could be a great interested in neural tissue engineering study and the study of the mechanisms of this relationship could also help to develop more advance materials.

The aim of this study was to explore the potential of PLGA and CNT composite electrospun materials on supporting the proliferation of neurons and to investigate the effect of different CNT concentrations on electrospun composite nanofiber membranes. In this study, PLGA and CNT composite electrospun membranes with various CNT concentrations were manufactured, and the physiochemical properties and biocompatibility of the electrospun membranes were investigated.

5.2 Results

5.2.1 Effect of different CNT concentrations on the morphology of electrospun PLGA membranes

SEM images of the electrospun scaffolds are shown in Figure 5-1. The electrospun material with different CNT concentrations showed smooth and clean nanofiber structures. However, the electrospun scaffolds enhanced with CNTs were more likely to stick together and the diameters of nanofiber became uneven. The nanofiber diameters are shown in Figure 5-2. The diameters of the materials changed slightly when low concentrations of CNTs were added (0.001 g/ml–0.007 g/ml), but when the CNT concentration reached 0.01 g/ml, the nanofiber diameters increased significantly. The porosity of the scaffolds slightly increased with the increasing CNT concentrations, as shown in

Figure 5-3.

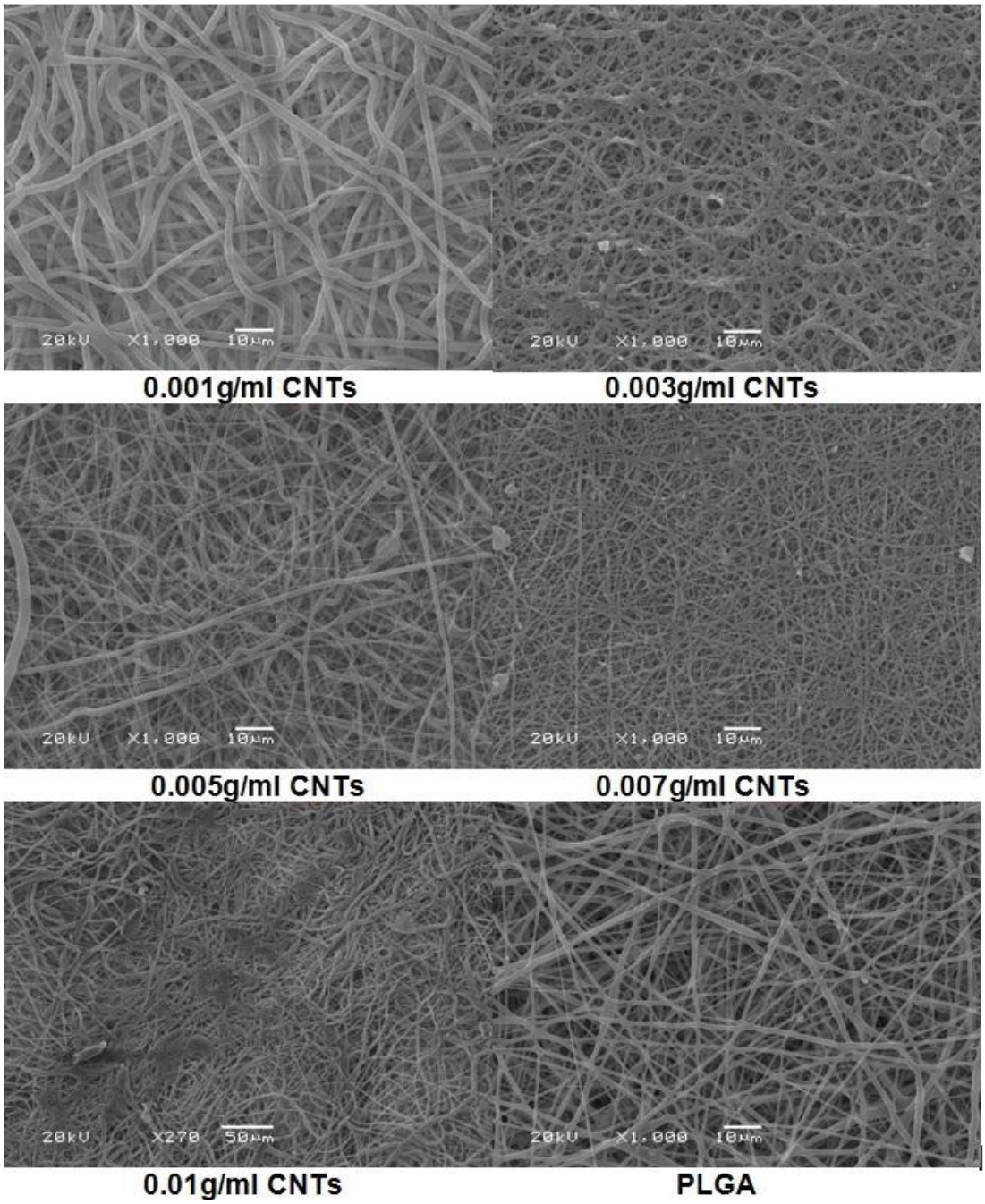

Figure 5-1 SEM images of scaffolds with different CNT concentrations

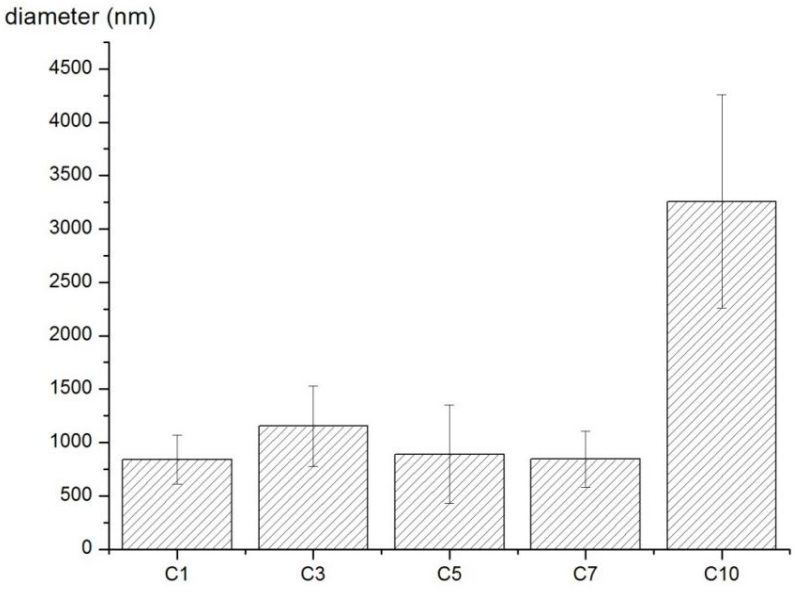

Figure 5-2 Average fibre diameter of scaffolds with different CNT concentrations

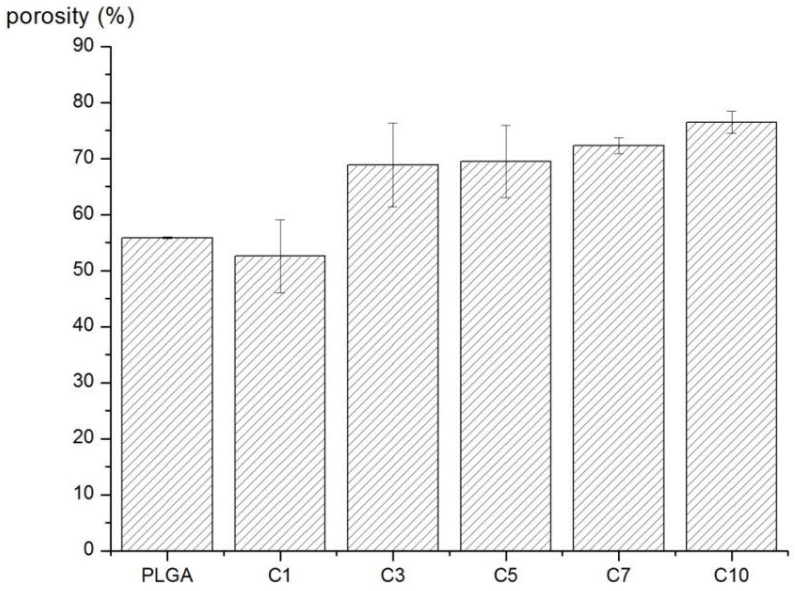

Figure 5-3 Porosity of scaffolds with different CNT concentrations

Distribution of carbon nanotubes in nanofibre materials

The distribution of CNTs in nanofibre materials was studied using TEM, as shown in Figure 5-4. There are generally three kinds of CNT distribution forms that exist in nanofibre materials. Large groups inside or outside nanofibres usually appear at the junction of multiple nanofibres (A, B), single CNTs appear inside the nanofibre (C) and CNTs appear partly outside the nanofibre (D).

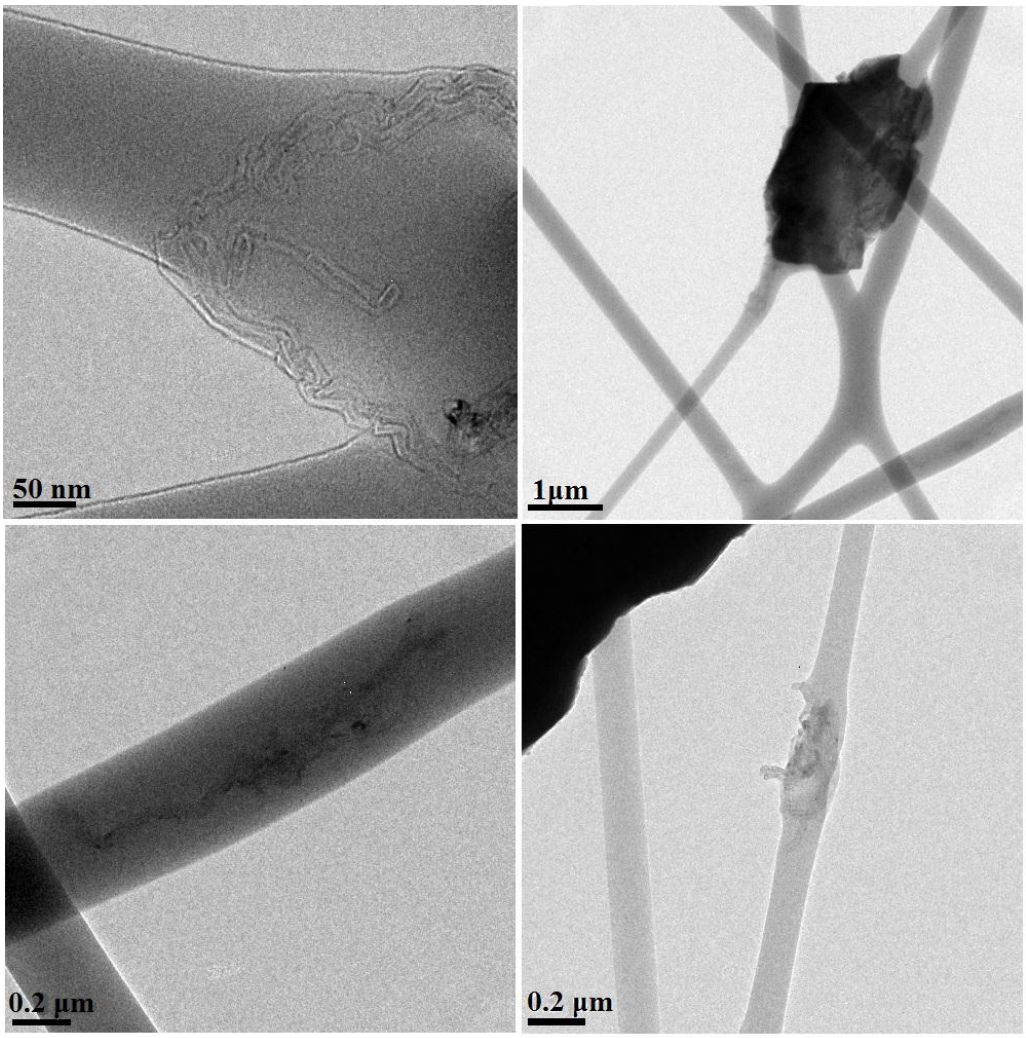

Figure 5-4 TEM images of CNTs inside nanofibers

5.2.2 Effect of different CNT concentrations on the physiochemical properties of electrospun PLGA membranes

Figure 5-5 shows the Young's modulus of the scaffolds. The Young's modulus did not change at 0.001 g/ml of CNTs compared with PLGA. However, with the increasing CNT concentration, the Young's modulus of the scaffolds dropped by different degrees. The breaking strain of the scaffolds with the 0.01 g/ml CNT concentration decreased to a very low level compared to the original PLGA material. Moreover, introducing CNTs to PLGA material improved the tensile strength, especially at the 0.001 g/ml CNT concentration.

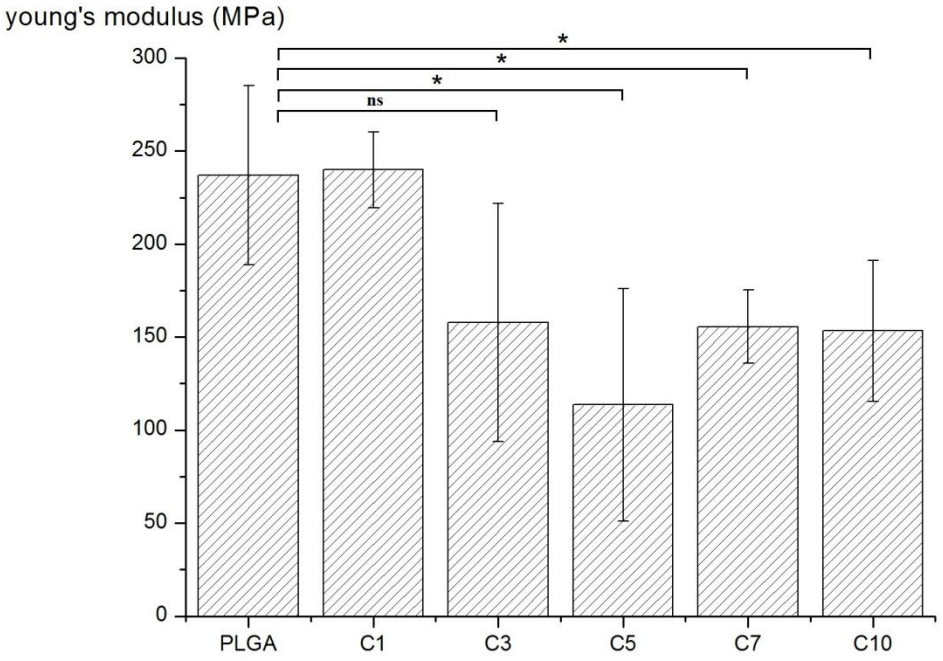

Figure 5-5 Young's modulus of scaffolds with different CNT concentrations

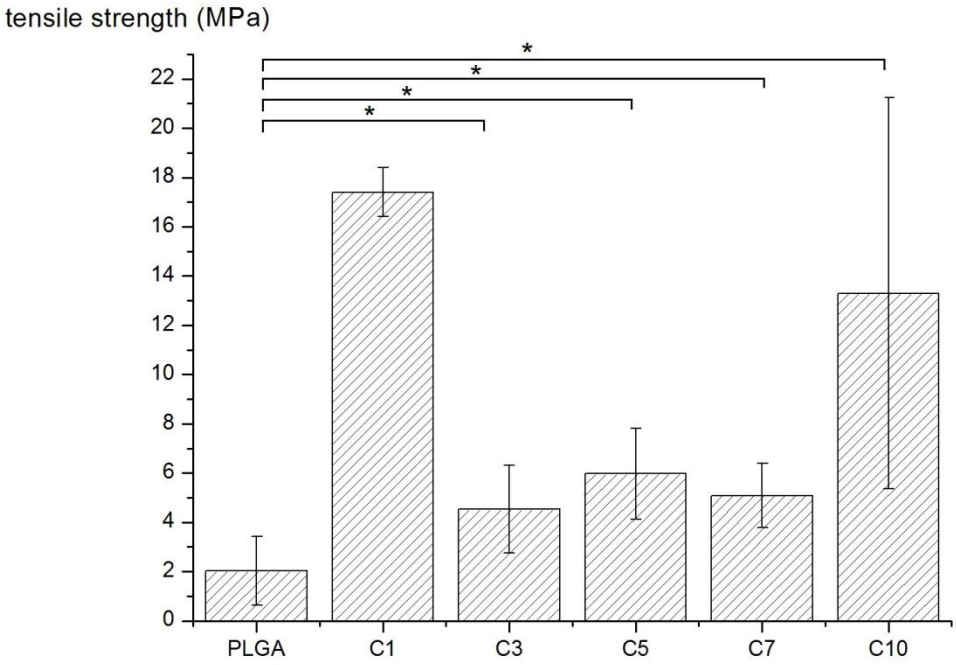

Figure 5-6 Tensile strength of scaffolds with different CNT concentrations

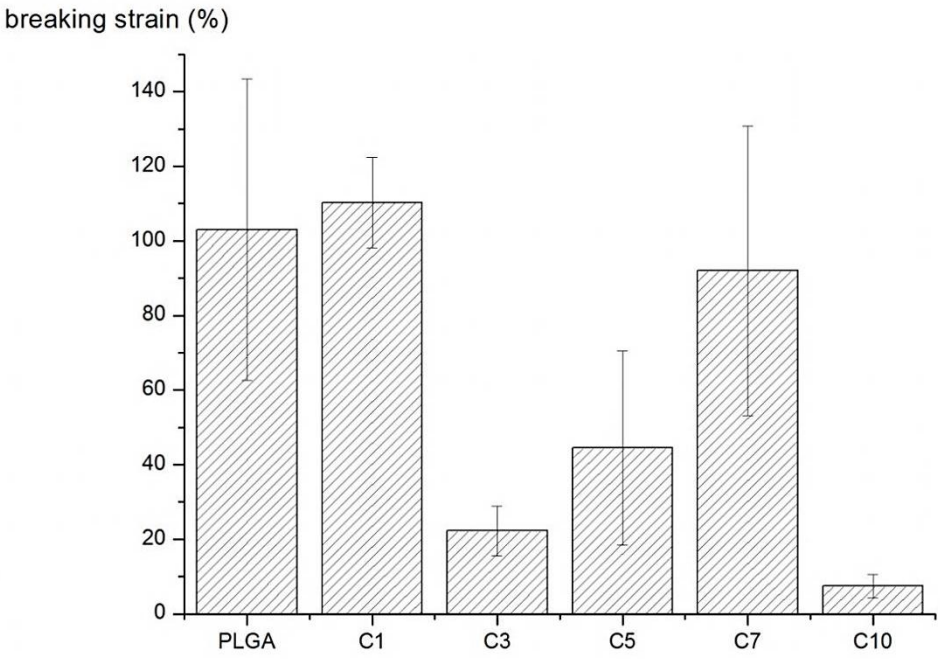

Figure 5-7 Breaking strain of scaffolds with different CNT concentrations

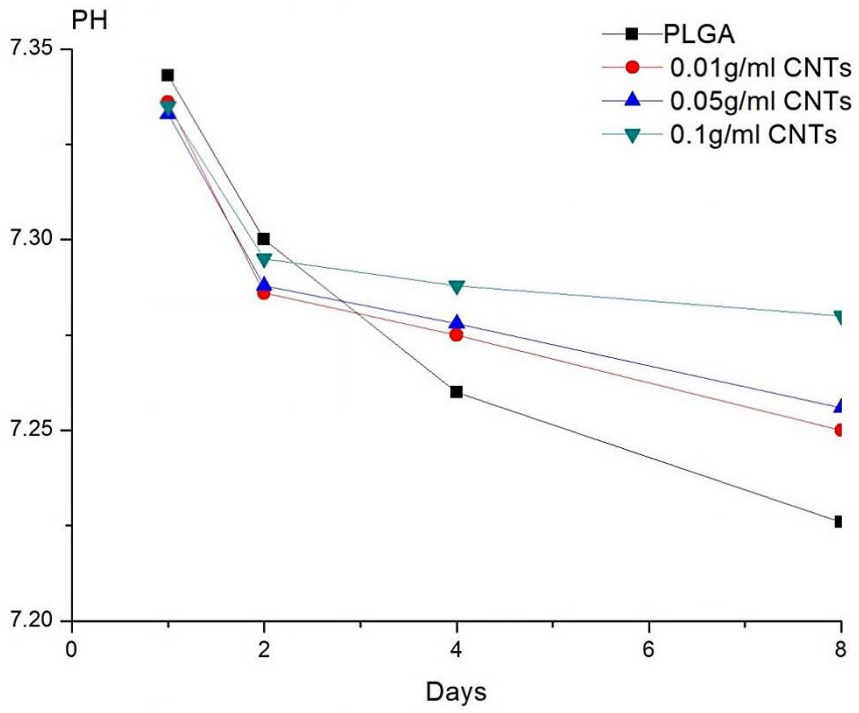

Figure 5-8 PH changes of different CNT concentrations at day 1,2,4 and 8

5.2.3 Effect of different CNT concentrations on the biocompatibility of electrospun PLGA membranes

Biocompatibility for neurons is determined by calculating neuron and glial cell numbers after 8 days of culturing on electrospun scaffolds. The cell survival ratio was calculated by counting the number of living cells and apoptotic cells. The neuron ratio was calculated by counting neuron numbers and glial cell numbers. The results indicated that neurons are not able to survive on pure PLGA electrospun scaffolds and only scaffolds with 0.01 g/ml of CNTs could maintain a high cell survival rate after 8 days of cell culturing. However, there was a significant drop in cell numbers at day 4. The cell survival rates of samples with other CNT concentrations were all below 50% after 8 days of culturing. After 4 days of

culturing, the neuron numbers on the scaffold did not change significantly with 0.01 g/ml of CNTs. Meanwhile, there was a boost in the cell survival rate, which means the change was caused by the overgrowth of glial cells. The fluorescence images from the laser scanning confocal microscope showed the growth of multiple elongations along with astrocytes, which is typical of neuronal cells.

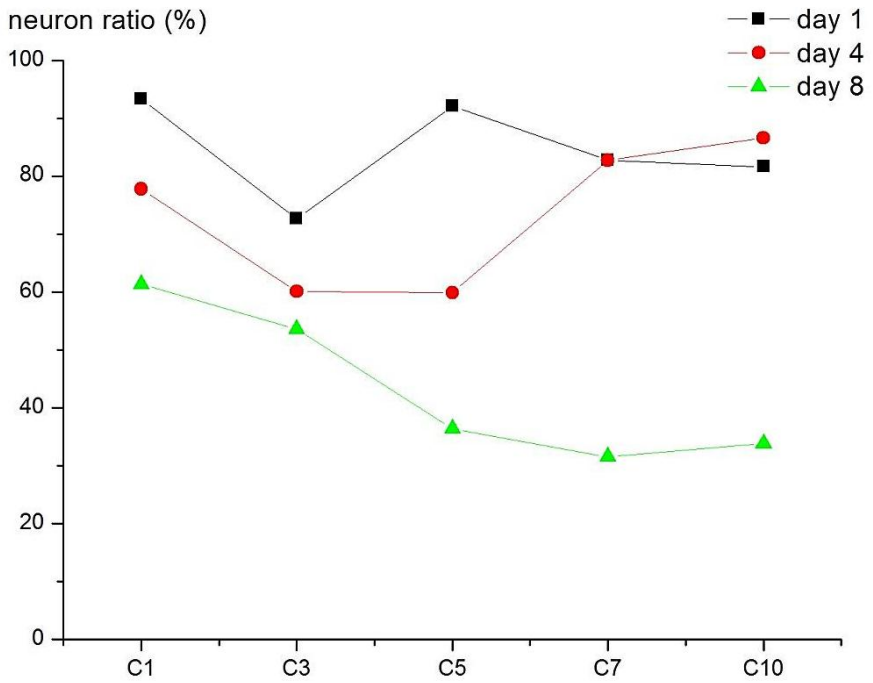

Figure 5-9 Neuron cell ratio on scaffolds with different CNT concentrations at day 1, day 4 and day 8

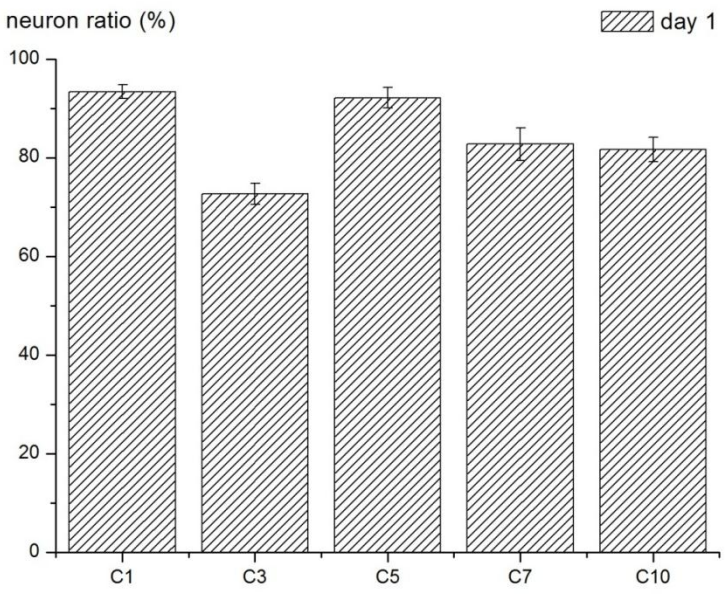

Figure 5-10 Neuron ratio on scaffolds with different CNT concentrations at day 1

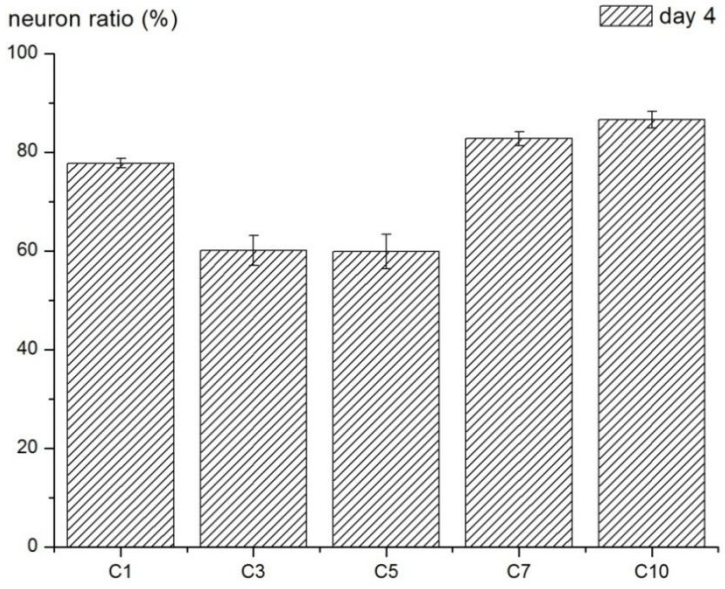

Figure 5-11 Neuron ratio on scaffolds with different CNT concentrations at day 4

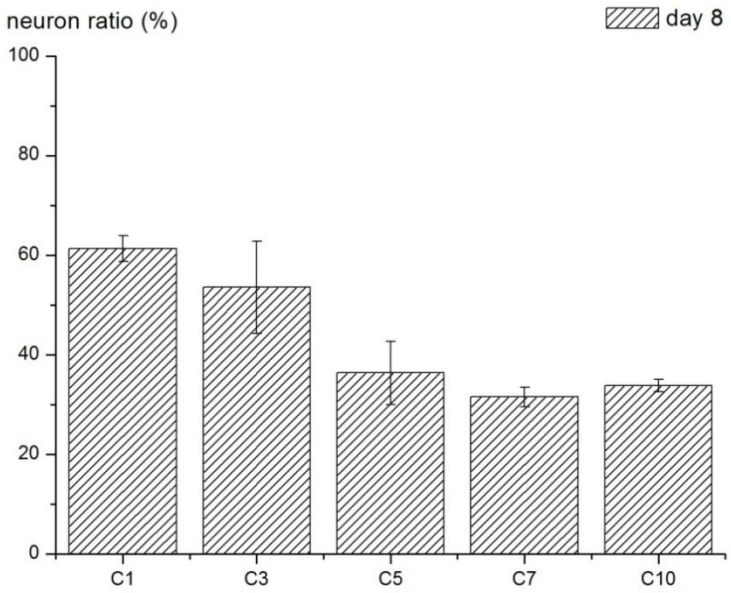

Figure 5-12 Neuron ratio on scaffolds with different CNT concentrations at day 8

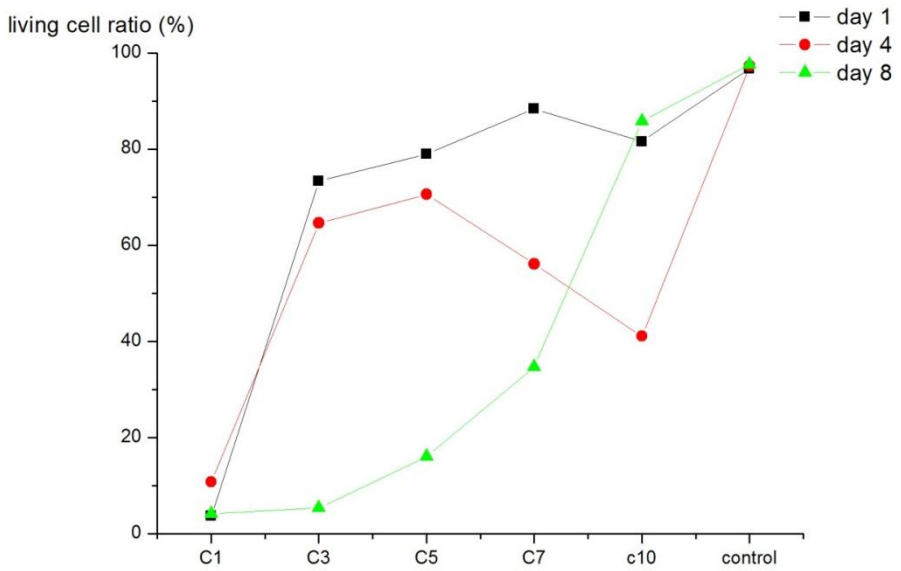

Figure 5-13 Living cell ratio on scaffolds with different CNT concentrations at day 1, day 4 and day 8

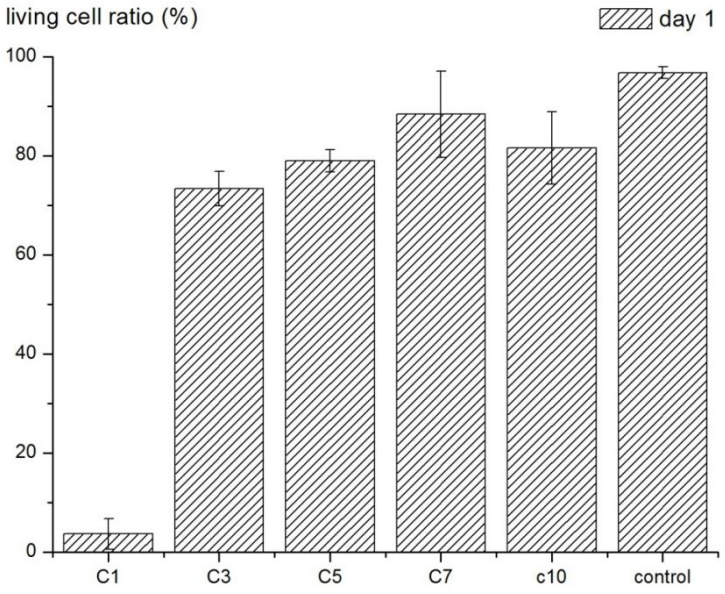

Figure 5-14 Living cell ratio on scaffolds with different CNT concentrations at day 1

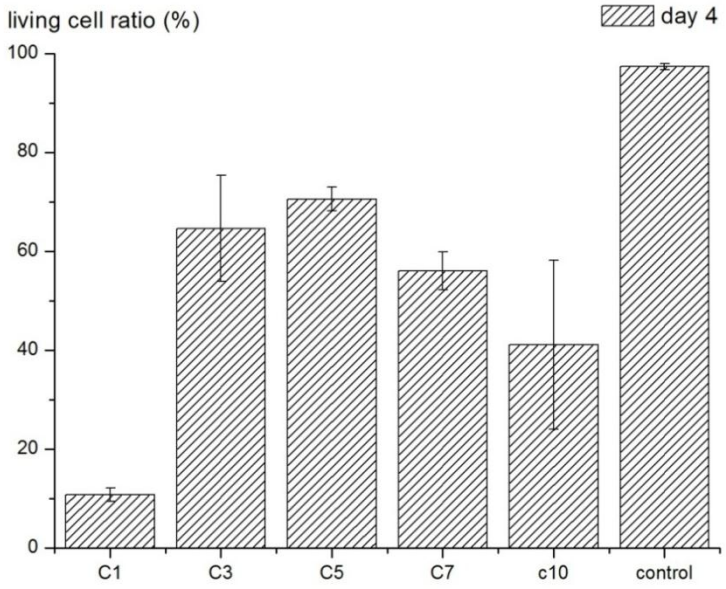

Figure 5-15 Living cell ratio on scaffolds with different CNT concentrations at day 4

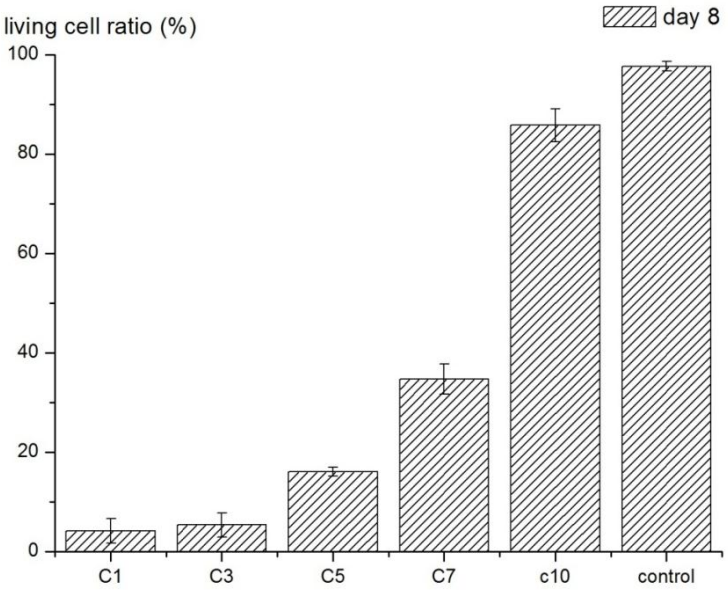

Figure 5-16 Living cell ratio on scaffolds with different CNT concentrations at day 8

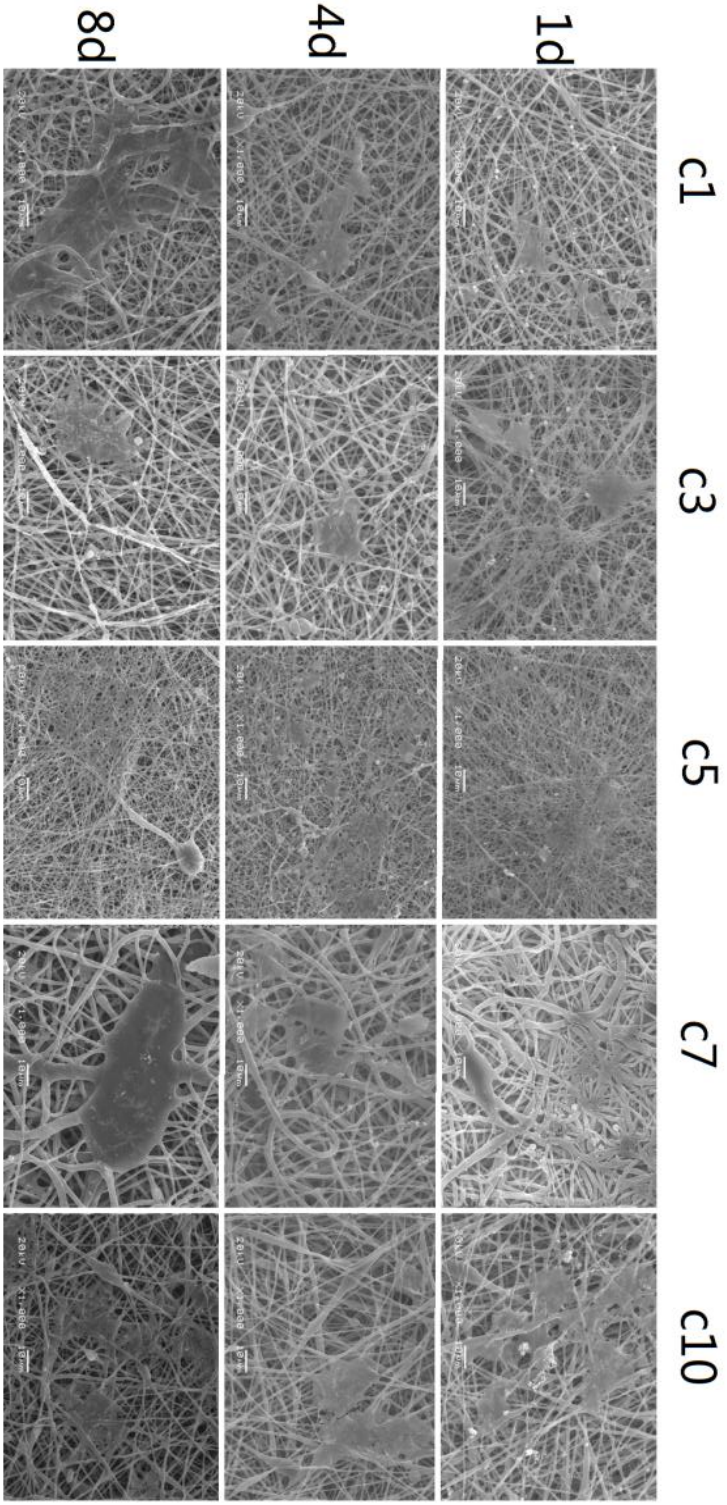

Figure 5-17 SEM images of scaffolds with different CNT concentrations; (C1) CNTs 0.01 g/ml, (C3) CNTs 0.03 g/ml, (C5) CNTs 0.05 g/ml, (C7) CNTs 0.07 g/ml and (C10) CNTs 0.1 g/ml.

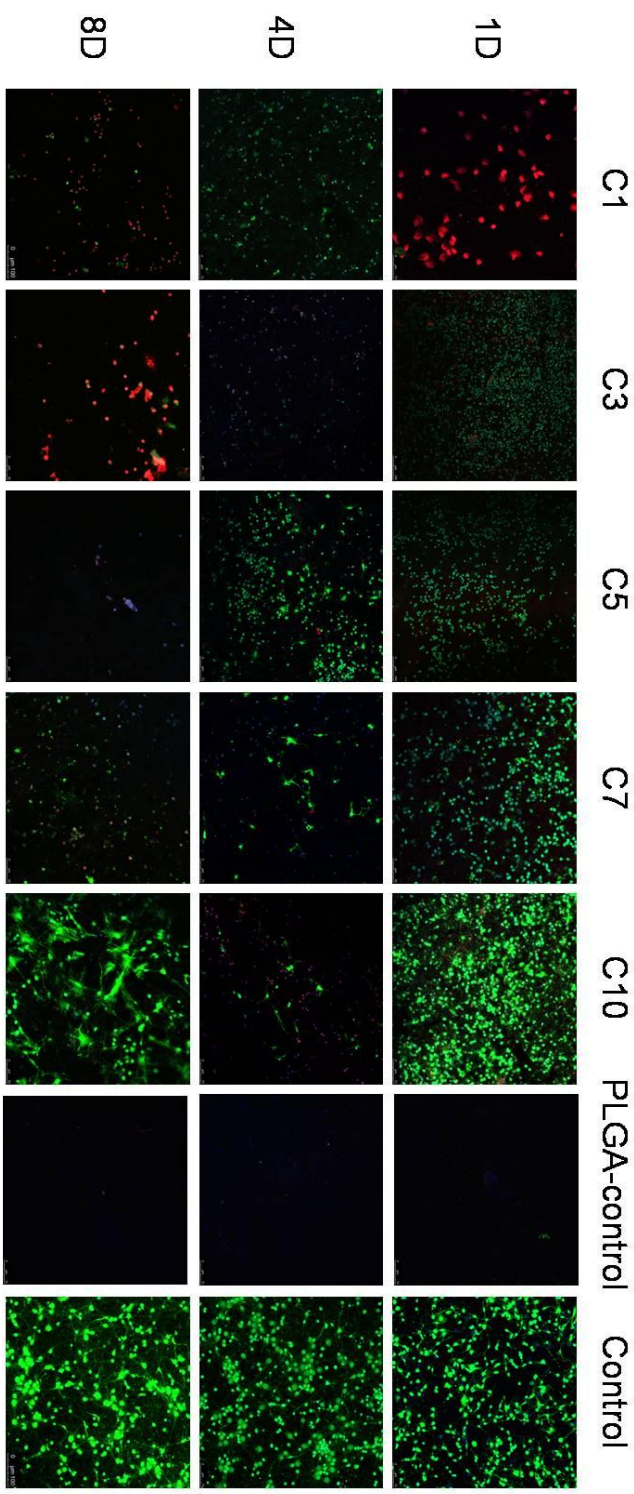

Figure 5-18 Laser scanning confocal microscope images of neuron cells grown on the scaffold (C1:0.001g/ml CNTs; C3:0.001g/ml CNTs; C5:0.001g/ml CNTs; C7:0.001g/ml CNTs; C10:0.01g/ml CNTs)

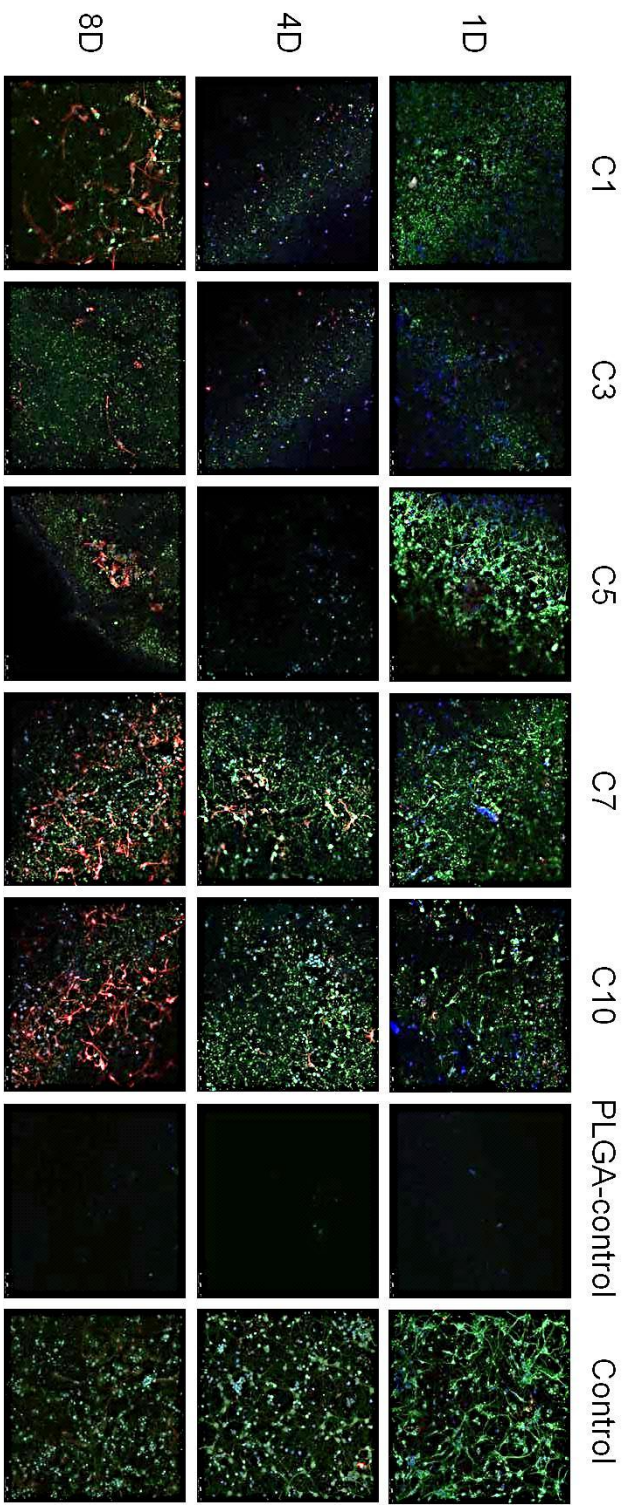

Figure 5-19 Laser scanning confocal microscope images of neuron cells grown on the scaffold (C1:0.001g/ml CNTs; C3:0.001g/ml CNTs; C5:0.001g/ml CNTs; C7:0.001g/ml CNTs; C10:0.01g/ml CNTs)

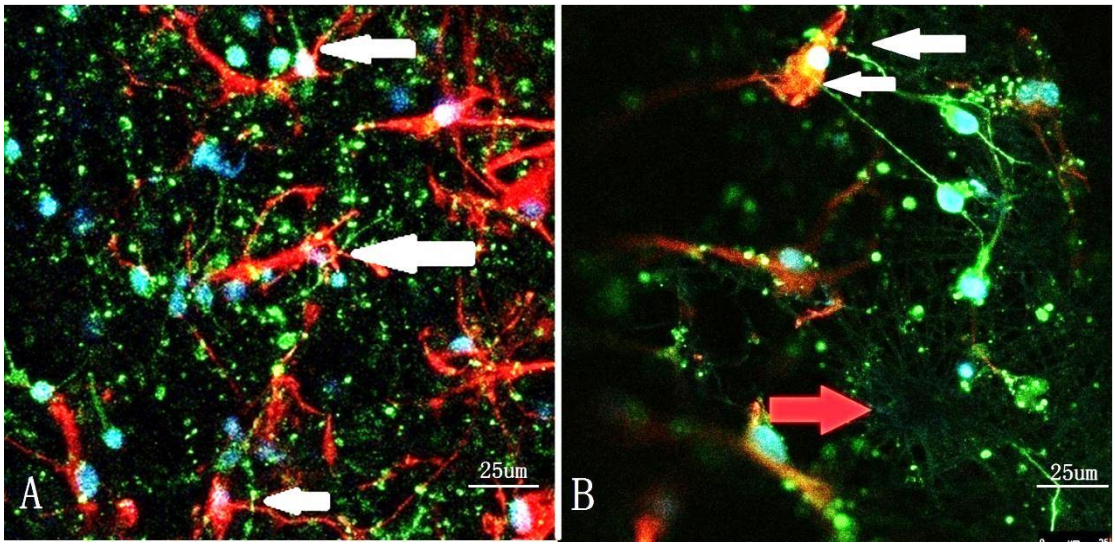

Figure 5-20 Laser scanning confocal microscope images of neuron cells grown on the scaffold. (A) Neuron cells on electrospun PLGA scaffold with 0.07 g/ml CNTs. (B) Neuron cells on electrospun PLGA scaffold with 0.1 g/ml CNTs

5.3 Discussion

The properties of the electrospun scaffolds are widely affected by the materials used for electrospinning and the controlling parameters of electrospinning, such as molecular weight and molecular distribution of the material, electrospinning solution properties (concentration, viscosity, conductivity and surface tension), voltage, collecting distance, environmental parameters, etc. In this research, The only change to the material is the change of CNT concentration, which could lead to the changes in viscosity and conductivity. The reduction in the mechanical properties is mainly because of the use of non-surface modified CNTs; therefore, there are no chemical bonds between PLGA molecules and CNTs and the addition of CNTs will compromise the structural integrity of nanofibers. Some studies have used surface-modified CNTs to provide various functions, such as increased mechanical properties, improved hydrophilicity, reduced toxicity or even support for specific cells (Mottaghitalab et al., 2013, Belyanskaya. et al., 2009, Pan. et al., 2012, Sharma et al., 2012, Ozden-Yenigun et al., 2012). As we are aiming for an implantable scaffold for neural regeneration, the requirements for surface modification could be varied, so in this study we use non-surface modified CNTs to leave this option open.

Based on the results, the scaffold with 0.01g/ml CNTs has the best biocompatibility for neuron growth among all the samples. Its cell survival rate dropped greatly between day 1 and day 4 and rebounded between day 4 and day 8. However, neuron cell viability did not change between day 4 and day 8, which means there was a massive proliferation of glia cells between day 4 and day 8 of culture. This may caused by the PH change. As previously mentioned, the culture medium was half renewed every 3 days after the first day of culturing. Therefore, the degradation of PLGA caused the PH in the culture medium to keep decreasing until the medium was changed. As we know, the neuron cells are very environmentally sensitive, and the continual drop in the PH will inhibit neuron proliferation. Moreover, the decrease in PH during PLGA degradation becomes slower with time, so the PH between day 4 and day 8 will be higher than the PH between day 1 and day 4, which may still not be suitable for neuron proliferation but may be enough for glia cell growth.

When PLGA was electrospun with suitable controlling parameters, the electrospun nanofiber were smooth and clean with similar fiber diameters (Zhang et al., 2011, Bianco et al., 2010). However, after CNTs were added to the electrospinning solution, the morphology of the electrospun scaffolds changed; the fiber diameters became uneven, and the fibers that came in contact with each other became stuck together.

6. Summary and future work

6.1 Summary

In this study, the potential of the crosslink protein membranes as scaffold material has been researched; ADSC, PC12, and rat primary neuron were cultured on the crosslink protein membranes. The previous research of the crosslink protein membranes are focus on physiochemical properties, this research further discovered the potential application of the crosslink membranes and fulfilled the biocompatibility profile of the membranes. During the research a set of special technique were created to provide fast produce large area crosslink protein membranes that are suitable for cell culture experiments. Include a dropping method that could produce large number of crosslinked protein membranes that fit in 24-well culture plate, and 3D printed ABS rings were used to immobilize the membranes in culture plates, metal rings and glass rings were also tested during the research but they all have contaminate issues so finally one time used 3D printed ABS rings were used in the experiment. The study also discovered that the organic side of the crosslink protein membranes have positive effect on long term culture for PC12 and ADSCs.

The mechanical properties of crosslink membranes were studied using nanoindentation tests (Chang, 2010). The modulus of elasticity of membranes made with BSA and TCL is 2.13 GPa. The modulus of elasticity of membranes made with BSA and IDCL is 1.56

GPa. Compared with the 135 MPa of the electrospun PLGA membrane and the 65 MPa of the PLGA+SF composite material, the electrospun material was found to be far 'softer' than the crosslink material. This means electrospun materials are easier to deform.

Regarding electrospun materials, the results show that adding CNTs will increase the composite material's mechanical properties and the addition of SF will decrease the composite material's mechanical properties, even if the material is added to both SF and CNTs. The results show the biocompatibility of the crosslink membrane for PC12 cells is better than for ADSCs. For electrospun materials, the result is opposite; the electrospun materials show better biocompatibility for ADSCs but lower biocompatibility for PC12 cells.

Regarding the crosslink membranes and electrospun membranes, except ADSCs on electrospun membranes, in all other situations the PC12 cells and ADSCs are not able to out grown the cells cultured in cell culture treated culture plates. The viability test of ADSCs cultured on electrospun materials was able to 'beat' the culture plates after 4 days of culturing.

The results of neuron culturing show that after 8 days of culturing with increasing CNT concentrations, the neuron ratio decreased. The addition of CNTs greatly increased the

PLGA electrospun material's biocompatibility with rat primary cortical neurons and neuroglia cells.

Comparing the manufacture and manoeuvrability of crosslink membranes and electrospun membranes, the reagents in the crosslink link membrane (TCL and IDCL) are toxic and react with water. The solvent xylene is flammable but of modest acute toxicity; the principal mechanism of detoxification is oxidation to methylbenzoic acid and hydroxylation to hydroxylene. The reagents in the electrospun membrane (PLGA and SF) are non-toxic and biodegradable. The cytotoxicity of CNTs is debatable. The solvent in the electrospun membrane (HFIP) is a volatile, corrosive liquid that can cause severe burns and respiratory problems; however, it evaporates quickly so can be easily eliminated in the fume hood. The production of crosslink membranes is done manually and is time consuming, and the production of electrospun membranes is automatic and more cost-efficient.

In terms of maneuverability, the crosslink membrane is very easy to fracture and hard to handle. The electrospun membrane can be easily cut with scissors and fixed using clips.

Although the crosslink membrane did not have excellent biocompatibility, the very unique properties of crosslink membranes can be fabricated in microfluidics and can

provide an opportunity to study the cell co-culturing of neurons and glia cells to reveal the interaction between them. Microfluidic membranes can also be used in drug testing if we can manage to control the pore size to only allow reagents with a certain molecule size to path through. To do so, a microfluidic-based micro bioreactor will need to be built and the exam technique of such equipment would also be required.

The CNTs increased the biocompatibility of the electrospun PLGA composite membrane. To understand the interaction between CNTs and cells, a tracker is needed to mark out the CNTs on fluoresce images if possible. There have already been successful attempts using quantum dot fluorescent markers to mark CNTs in nanofibers. Recent challenges include studying the toxicity of the marker and improving its reaction rate with CNTs and also reducing the interference of nanofiber on fluorescence images.

6.2 Future work

Due to the fast evaporation of the xylene solvent, it is possible that residual TCL or IDCL crystals were left on the chloride side, which will induce cytotoxicity in the membranes. These residuals might not be washed off in the membrane preparation process because they could be buried inside the membranes during the crosslink reaction and would have negative effect with the culture medium. So a new cleaning method is needed for the membranes fabrication process to make sure the membranes have as less residuals as possible.

To further test the biocompatibility of the crosslink and electrospun membranes, the ability to support PC12 cells and ADSC differentiation is needed. PC12 cells of embryological origin are easy to differentiate into neuron-like cells with similar properties. Differentiation ability is also a vital feature of ADSCs. The identification of ADSCs and the identification of neurons after the differentiation of ADSCs is also necessary.

The crosslink membranes could be a useful tool for research cell-cell interaction like the reaction between neurons and glia cells. A microfluidic based bioreactor system could be built as shown in Figure 6-1. The system include culture medium supply system that can support long term cell culture in the bioreactor, also the oxygen and pH level is monitored by light sensors the cell viability is monitored by analysis the

impedance signal that provided by the electrode in bioreactor. The crosslink membranes is fabricated in PDMS microfluidics channel and two kind of cells could be cultured in different side of the channel, due to the controllable pore size of the crosslink membranes，the material that allowed to join the cell-cell interaction is also selectable which could provide more flexibility and options to the research.

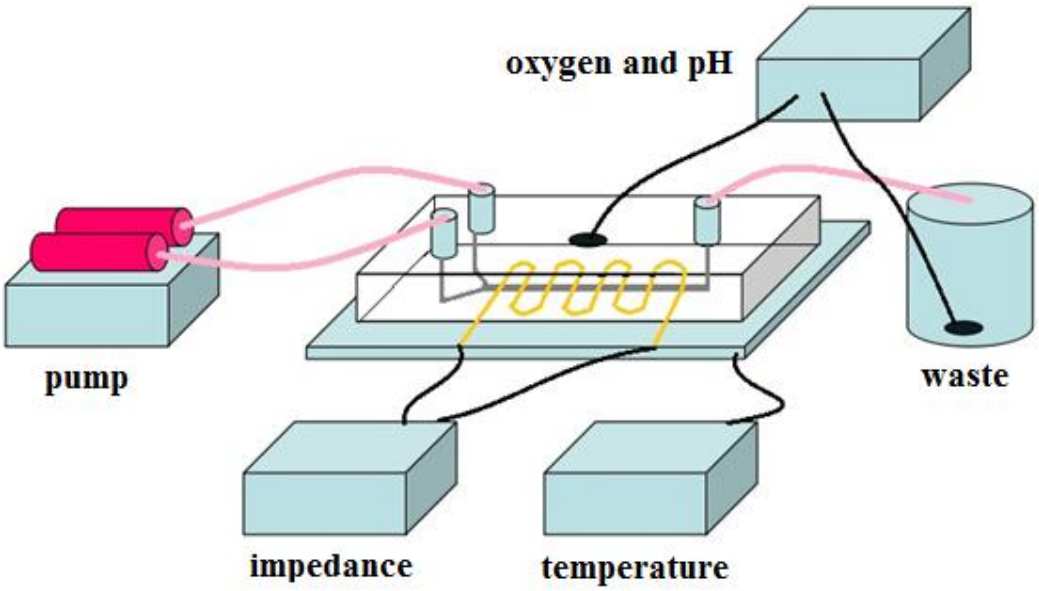

Figure 6-1 Schematic drawing of microfluidics bioreactor system

7. References

ABDULLAH. M & KHAIRURRIJAL 2009. A Simple Method for Determining Surface Porosity Based on SEM Images Using OriginPro Software. *Indonesian Journal of Physics,* 20**,** 37-40.

ARIS STERODIMAS, J. D. F., BEATRIZ NICARETTA, IVO PITANGUY 2010. Tissue engineering with adipose-derived stem cells (ADSCs): current and future applications. *Journal of Plastic, Reconstructive & Aesthetic Surgery,* 63**,** 1886-1892.

ARSHADY.R 1999. In the name of particle formation. *Colloids and surface a-physicochemical and engineering aspects,* 153**,** 325-333.

B. KUNDU & S.C. KUNDU 2010. Osteogenesis of human stem cells in silk biomaterial for regenerative therapy. *Progress in Polymer Science,* 35**,** 1116-1127.

BABAK ZIAIE, E. A. 2004 Hard and soft micromachining for BioMEMS: review of techniques and examples of applications in microfluidics and drug delivery *Advanced Drug Delivery Reviews,* 56**,** 145-172.

BALDI A, *E. A.* 2006 A microstructured silicon membrane with entrapped hydrogels for environmentally sensitive fluid gating *Sensors and actuators B: chemical* 114 9-18.

BEEBE D J, *E. A.* 2002 Physics and applications of microfluidics in biology *Annual*

Review of Biomedical Engineering, 4**,** 261-286.

BELLUCCI, S. 2009. Toxicological and Biological in Vitro and in Vivo Effects of Carbon Nanotubes Buckypaper. *Cas: 2009 International Semiconductor Conference, Vols 1 and 2, Proceedings.* Sinaia IEEE.

BELYANSKAYA., L., WEIGEL., S., *et al.* 2009. Effects of carbon nanotubes on primary neurons and glial cells. *NeuroToxicology*.

BERIS, A. E. A. 2007. End-to-side nerve repair in peripheral nerve injury. *Journal of Neurotrauma,* 24**,** 909-916.

BERNIER G M & PUTNAM 1964. Myeloma proteins and macroglobulins: hallmarks of disease and models of antibodies. *Progress in hematology,* 51**,** 209-211.

BIANCO, A., DEL GAUDIO, C., *et al.* 2010. Microstructure and cytocompatibility of electrospun nanocomposites based on poly(epsilon-caprolactone) and carbon nanostructures. *Int J Artif Organs,* 33**,** 271-82.

BINI, T. B., GAO, S. J., *et al.* 2006. Poly(l-lactide-co-glycolide) biodegradable microfibers and electrospun nanofibers for nerve tissue engineering: an in vitro study. *Journal of Materials Science,* 41**,** 6453-6459.

BRODY J P, E. A. 1996 Biotechnology at low Reynolds numbers. *Biophysical Journal,* 71**,** 3430-3441.

BROWN, J. 1975. *Structure of bovine serum-albumin,* surrey, Federation proceedings.

CAO, E. A. 2009. The application of nanofibrous scaffolds in neural tissue engineering. *Advanced Drug Delivery Reviews,* 61**,** 1055-1064.

CHANG, H. E. A. 2010. Study of albumin and fibrinogen membranes formed by interfacial crosslinking using microfluidic flow. *Biofabrication,* 2**,** 035002.

CHEN, E. A. 2012. Human stem cell neuronal differentiation on silkcarbon nanotube composite. *Nanoscale Research Letters,* 7**,** 126.

CHIEM N & J, H. D. 1997 Microchip-based capillary electrophoresis for immunoassays: Analysis of monoclonal antibodies and184 theophylline *Analytical Chemistry* 69**,** 373-378.

CHUNMEI LI, E. A. 2006. Electrospun silk-BMP-2 scaffolds for bone tissue engineering. *Biomaterials,* 27**,** 3115-3124.

COLYER C L, E. A. 1997 Clinical potential of microchip capillary electrophoresis systems *Electrophoresis* 18**,** 1733-1741.

CRISAN, E. A. 2008 A perivascular origin for mesenchymal stem cells in multiple human organs. *Cell Stem Cell,* 3 301-313.

CUILIN LIN, E. A. 2011. Incorporation of carboxylation multiwalled carbon nanotubes into biodegradable poly(lactic-co-glycolic acid) for bone tissue engineering. *Colloids and Surfaces B: Biointerfaces,* 83**,** 367-375.

CUILIN LINA, Y. W., YOUQUN LAI A, WEI YANGA, FEI JIAO A, HONGGANG ZHANGA, & SHEFANG YEA, QIQING ZHANGA, 2011. Incorporation of carboxylation multiwalled carbon nanotubes into biodegradable

poly(lactic-co-glycolic acid) for bone tissue engineering. *Colloids and Surfaces B: Biointerfaces*.

DAN LI, Y. X. 2004. Electrospinning of Nanofibers: Reinventing the Wheel? *Advanced Materials* 16**,** 14.

DE UGARTE, E. A. 2003. Comparison of multi-lineage cells from human adipose tissue and bone marrow. *Cells Tissues Organs* 174**,** 101-109.

DELLAVALLE, E. A. 2007. Pericytes of human skeletal muscle are myogenic precursors distinct from satellite cells. *Nature Cell Biology,* 9**,** 255-267.

DOLDVARIGROUP. *Drug-delivery* [Online]. university of waterloo. Available: https://uwaterloo.ca/foldvari-group/research-program/drug-delivery [Accessed].

ERICKSON D & D, L. 2004 Integrated microfluidic devices *Analytica Chimica Acta* 507**,** 11-26.

ERICKSON D, L. D. 2004 Integrated microfluidic devices *Analytica Chimica Acta* 11-26.

F.G. OMENETTO & KAPLAN, D. L. 2008. A new route for silk. *Nature Photonics,* 2**,** 641-643

F.G. OMENETTO & KAPLAN, D. L. 2010. New opportunities for an ancient material. *Science,* 329**,** 528-531.

G.H. ALTMAN, E. A. 2003. Silk-based biomaterials. *Biomaterials* 24**,** 401-416.

GIMBLE J. M., E. A. 2007. Adipose-derived stem cells for regenerative medicine. *Circulation Research,* 100**,** 1249-1260.

GONDA. K, E. A. 2008. Preserved proliferative capacity and multipotency of human

adipose-derived stem cells after long-term cryopreservation *Plastic and Reconstructive Surgery,* 121**,** 401-410.

GREENE LA, T. A. 1976. Establishment of a noradrenergic clonal line of rat adrenal pheochromocytoma cells which respond to nerve growth factor. *Proceedings of the National Academy of Sciences of the United States of America,* 73**,** 2424–2428.

GREINER, E. A. 2007. Electrospinning: A Fascinating Method for the Preparation of Ultrathin Fibers. *Angewandte Chemie International Edition,* 46**,** 5670-5703.

GUANGLIN WANG, E. A. 2010. Electrospun PLGA–silk fibroin–collagen nanofibrous scaffolds for nerve tissue engineering. *In Vitro Cellular & Developmental Biology - Animal,* 47**,** 234-240.

H. TAO, E. A. 2012. Silk Materials - a road to sustainable high technology. *Advanced Materials,* 24**,** 2824-2837.

HADD A G, E. A. 1997 Microchip device for performing enzyme assays *Analytical Chemistry,* 69**,** 3407-3412.

HISAMOTO H, E. A. 2003 Chemicofunctional membrane for integrated chemical processes on a microchip. *Analytical Chemistry,* 75**,** 350-354.

HUANG C J, E. A. 2006 Integrated micofluidic systems for automatic glucose sensing and insulin injection *Sensors and Actuators B: Chemical,* 122**,** 461-468.

HUANG, E. A. 2003. A review on polymer nanofibers by electrospinning and their applications in nanocomposites. *Composites Science and Technology,* 63**,**

2223-2253.

HUANG, Z.-M., ZHANG, Y. Z., *et al.* 2003. A review on polymer nanofibers by electrospinning and their applications in nanocomposites. *Composites Science and Technology,* 63**,** 2223-2253.

J. GARGIULIA, E. A. 2006. Microfluidic systems for in situ formation of nylon 6,6 membranes *Journal of Membrane Science,* 282**,** 257-265.

JONG J, L. R. G. H. A. W. M. 2006 Membranes and microfluidics: a review. *Lab on a Chip* 6**,** 1125-1139.

KAKUDO.N., E. A. 2008. Proliferation-promoting effect of platelet-rich plasma on human adiposederived stem cells and human dermal fibroblasts. *Plastic Reconstructive Surgery,* 122**,** 1352-1360.

KATZ, A. J., ET AL. 2005. Cell surface and transcriptional characterization of human adipose-derived adherent stromal (hADAS) cells. *Stem Cells* 23**,** 412-423.

KHALED AL-ARIBE, G. K. K., AMARJEET S. BASSI 2006 Reconfigurable microfluidic chip based on a light-sensitive hydrogel *Optomechatronic actuators, manipulation, and systems control* [Online], 6374.

KIRILL EFIMENKO, W. E. W., JAN GENZER, 2002 Surface Modification of Sylgard-184 Poly (dimethyl siloxane) Networks by Ultraviolet and Ultraviolet/Ozone *Treatment Journal of Colloid and Interface Science,* 254 306-315.

KONRAD R, E. A. 1998 Microreaction Technology. *In:* EHRFELD, W. E. (ed.)

Proceedings of the first internation conference on microreaction technology Springer-Verlag Berlin Heidelberg.

L.S. NAIR, C. T. L. 2007. Biodegradable polymers as biomaterials. *Prog. Polym. Sci. ,* 32**,** 762-798.

LIAO, H. H. E. A. 2011. Improved cellular response on multiwalled carbon nanotube-incorporated electrospun polyvinyl alcohol/chitosan nanofibrous scaffolds. *Colloids and Surfaces B-Biointerfaces,* 84**,** 528-535.

LIU CHANGCHUN, C. D., CAI HAOYUAN,ET AL. 2006. A rigid poly(dimethylsiloxane) sandwich electrophoresis microchip based on thin-casting method *Electrophoresis* 14**,** 2917-2923.

LIU CHANGCHUN, T. J. A., BAU HAIM H 2011 A membrane-based, high-efficiency, microfluidic debubbler *Lab on a chip* 11**,** 1688-1693.

LIU S, S. Y., JA W W 1999 Optimization of high-speed DNA sequencing on microfabricated capillary electrophoresis channels *Analytical Chemistry,* 71**,** 566-573.

LIU, Z. J., ZHUGE, Y., ET AL. 2009. Trafficking and differentiation of mesenchymal stem cells. *J Cell Biochem,* 106**,** 984-991.

M.K. HOTA, M. K. B., ET AL. 2012. A natural silk fibroin protein-based transparent bio-memristor. *Advanced Functional Materials,* 22**,** 4493-4499.

MCDONALD J C, D. D. C., ET AL. 2000 Fabrication of microfluidic systems in poly(dimethylsiloxane) *Electrophoresis* 21**,** 27-40.

MOORTHY J , B. D. J. 2003 In situ fabricated porous filters for Microsystems *Lab Chip* 3**,** 62-66.

MOTTAGHITALAB, F., FAROKHI, M., *et al.* 2013. A biosynthetic nerve guide conduit based on silk/SWNT/fibronectin nanocomposite for peripheral nerve regeneration. *PLoS One,* 8**,** e74417.

MOTTAGHITALAB, F. F., M. ET AL. 2013. A Biosynthetic Nerve Guide Conduit Based on Silk/SWNT/Fibronectin Nanocomposite for Peripheral Nerve Regeneration. *PLoS One,* 8.

N. KASOJU, U. B. 2012. Silk fibroin in tissue engineering. *Advanced Healthcare Materials,* 1**,** 393-412.

NAIR, G., GARGIULI, J. F., *et al.* 2006. In situ fabrication of cross-linked protein membranes by using microfluidics. *Chembiochem,* 7**,** 1683-1689.

NAIR G, G. J. F., ET AL. 2006 In situ fabrication of cross-linked protein membranes by using microfluidics *ChemBioChem* 7**,** 1683-1689.

NAIR LAKSHMI S, L. C. 2006. Polymers as biomaterials for tissue engineering and controlled drug delivery Advances in Biochemical. *Engineering-Biotechnology* 176**,** 47-90.

OZDEN-YENIGUN, E., MENCELOGLU, Y. Z., *et al.* 2012. MWCNTs/P(St-co-GMA) composite nanofibers of engineered interface chemistry for epoxy matrix nanocomposites. *ACS Appl Mater Interfaces,* 4**,** 777-84.

PAN., H., ZHANG., Y., *et al.* 2012. Significantly Reinforced Composite Fibers

Electrospun from Silk Fibroin/Carbon Nanotube Aqueous Solutions. *biomacromolecules*.

PATEL, E. A. 2008. Collagen-chitosan nerve guides for peripheral nerve repair: a histomorphometric study. *Journal of Biomaterials Applications,* 23**,** 101-21.

PAUL C. H. LI, D. J. H. 1997 Transport, manipulation and reaction of biological cells on-chip using electrokinetic effects *Analytical Chemistry,* 69**,** 1564-1568.

PETERSON D S 2005 Solid supports for micro analytical systems *Lab Chip,* 5**,** 132-9.

QIAO, B. E. A. 2011. Study on the Electrospun CNTs/Polyacrylonitrile-Based Nanofiber Composites. *Journal of Nanomaterials,* 2011.

R.H.S. WESTERINK, A. G. E. 2008. The PC12 cell as model for neurosecretion. *Acta Physiologica,* 192**,** 273-285.

ROMÁN A. PÉREZ , J.-E. W., ET AL. 2013. Naturally and synthetic smart composite biomaterials for tissue regeneration. *Advanced Drug Delivery Reviews,* 65**,** 471–496.

SABATA MARTINO , F. D. A., ET AL. 2012. Stem cell-biomaterial interactions for regenerative medicine. *Biotechnology Advances,* 30**,** 338-351.

SHARMA, Y., TIWARI, A., *et al.* 2012. Fabrication of conducting electrospun nanofibers scaffold for three-dimensional cells culture. *Int J Biol Macromol,* 51**,** 627-31.

SHARON L. EDWARDS, J. S. C., ET AL. 2009. Tubular micro-scale multiwalled carbon nanotube-based scaffolds for tissue engineering. *Biomaterials,* 30**,**

1725-1731.

SHAWGO G M, R. G. A. C., ET AL. 2002 Bio-MEMS for drug delivery. *Current Opinion in Solid State and Materials Science,* 6**,** 329-334.

TOMBRINK, D. S. 2014. *Microfluidic Chip fabricated in Glass* [Online]. iX-factory GmbH. Available: http://www.ix-factory.com/applications-en/lab-on-a-chip-en.html?lang=en [Accessed].

TRAVIS J. SILL, H. A. V. R. 2008. Electrospinning: applications in drug delivery and tissue engineering. *Biomaterials,* 29**,** 1989-2006.

TUCH BE 2006. Stem cells-a clinical update. *Australian Family Physician,* 35**,** 719-721.

VAN DEN BERY A, G. A., ET AL. 1993 On-wafer fabricated free-chlorine sensor with ppb detection limit for drinking-water monitoring *Sensors and Actuators B: Chemical* 13**,** 396-399.

WANG G, E. A. 2011. Electrospun PLGA-silk fibroin-collagen nanofibrous scaffolds for nerve tissue engineering. *In Vitro Cellular & Developmental Biology-Animal,* 47**,** 234-240.

WEI LI, E. A. 2009. Multiple modular microfluidic (M-3) reactors for the synthesis of polymer particles. *Lab on a Chip,* 9**,** 2715-2721.

WEI ZHOU, Y. F., JING YANG 2015. Electrospun scaffolds of silk fibron and poly（lactide-co-glycolide) for endothlia cell growth. *Journal of Materials Science:*

Materials in Medicine, 26.

WILLIAM R. BERTI, E. A. 2006. Hydrolytic Stability of Terephthaloyl Chloride and Isophthaloyl Chloride *Environmental Science and Technology,* 40**,** 6330-6335.

WOOLLEY A T , M. R. A. 1995 Ultra-high-speed DNA-sequencing using capillary electrophoresis chips. *Analytical Chemistry,* 67**,** 3676-3680.

WU Z, W. B., ET AL. 2009 Soft inertial microfluidics for high throughput separation of bacteria from human blood cells *Lab Chip* 1193-1199.

YANG F, E. A. 2004. Fabrication of nano-structured porous PLLAscaffold intended for nerve tissue engineering. *Biomaterials,* 25**,** 1891-1900.

YANG F., E. A. 2005. Electrospinning of nano/micro scale poly(L-lactic acid) aligned fibers and their potential in neural tissue engineering. *Biomaterials,* 26**,** 2603-10.

YOON SUN JUNG, E. A. 2008. Reduction of Inflammatory Reaction of Poly(D,L-Lactic-Co-Glycolic Acid) Using Demineralized Bone Particles. *Tissue Engineering Part A,* 14**,** 539-547.

ZHANG, K., CHOI, H. J., *et al.* 2011. Preparation and characteristics of electrospun multiwalled carbon nanotube/polyvinylpyrrolidone nanocomposite nanofiber. *J Nanosci Nanotechnol,* 11**,** 5446-9.

ZHANG Y. Z, E. A. 2007. Biomimetic and bioactive nanofibrous scaffolds from electrospun composite nanofibers. *International Journal of Nanomedicine,* 2**,** 623-638.

ZIABICKI A 1976. *Fundamentals of fiber formation,* London, John Wiley & Sons Ltd

(January 1, 1976).

ZIAIE, B., BALDI, A., *et al.* 2004. Hard and soft micromachining for BioMEMS: review of techniques and examples of applications in microfluidics and drug delivery. *Advanced Drug Delivery Reviews,* 56**,** 145-172.